



**Carlos Miguel
de Sousa Silveira**

**Modelação multiescala de qualidade do ar urbana
para cidades mais saudáveis**

**Multiscale urban air pollution modelling: towards
healthier cities**



**Carlos Miguel
de Sousa Silveira**

Modelação multiescala de qualidade do ar urbana para cidades mais saudáveis

Multiscale urban air pollution modelling: towards healthier cities

Tese apresentada à Universidade de Aveiro para cumprimento dos requisitos necessários à obtenção do grau de Doutor em Ciências e Engenharia do Ambiente, realizada sob a orientação científica da Doutora Ana Isabel Miranda, Professora Catedrática do Departamento de Ambiente e Ordenamento da Universidade de Aveiro e sob coorientação científica da Doutora Joana Ferreira, Investigadora Auxiliar do Departamento de Ambiente e Ordenamento da mesma Universidade.

São devidos agradecimentos à FCT/MCTES pelo apoio financeiro ao CESAM (UID/AMB/50017/2019) através de fundos nacionais e co-financiamento FEDER, dentro do Acordo de Parceria de programas PT2020 e Compete 2020. Às mesmas entidades, agradece-se também o apoio financeiro concedido no âmbito do Projeto FUTURAR (PTDC/AAG-MAA/2569/2014).

Apoio financeiro da FCT através do POPH-QREN e do Fundo Social Europeu (FSE) no âmbito do III Quadro Comunitário de Apoio pela Bolsa de Doutoramento com a referência SFRH/BD/112343/2015.



Dedico este trabalho à minha esposa e filha pelo incansável apoio.

o júri

Presidente

Prof. Doutor Victor Miguel Carneiro de Sousa Ferreira
Professor Catedrático, Universidade de Aveiro

Prof. Doutor Carlos Alberto Diogo Soares Borrego
Professor Catedrático Convidado, Universidade de Aveiro

Prof. Doutora Taciana Toledo de Almeida Albuquerque
Professora Adjunta, Universidade Federal de Minas Gerais

Doutor Oriol Jorba Casellas
Senior Researcher, Barcelona Supercomputing Center

Doutora Sofia Isabel Vieira de Sousa
Equiparada a Investigadora Auxiliar, Universidade do Porto

Prof. Doutora Ana Isabel Couto Neto da Silva Miranda
Professora Catedrática, Universidade de Aveiro (Orientadora)

agradecimentos

Findo este caminho, muitas vezes sinuoso e desgastante, é altura de agradecer a quem, direta ou indiretamente, contribuiu para que fosse possível atingir este importantíssimo marco pessoal e profissional.

Em primeiro lugar, um agradecimento especial à minha orientadora, a Professora Ana Isabel Miranda, pela oportunidade concedida e por acreditar que eu seria capaz de superar este desafio. Aqui, gostaria de incluir a Joana Ferreira, coorientadora da tese e colega de gabinete desde a minha vinda para o GEMAC. A ambas, agradeço os conhecimentos transmitidos e valiosas sugestões que contribuíram para o meu desenvolvimento científico e enriquecimento deste trabalho de investigação.

Ao DAO-GEMAC, que me acolheu já lá vão quase 10 anos, e que eu considero ser a “minha segunda casa”. O espírito integrador, a cooperação, e o empenho diário para fazermos mais e melhor, são alguns predicados que tornam este grupo ímpar. Na impossibilidade de nomear todos os gemaquianos que passaram ou que estão nesta casa, tenho que deixar algumas palavras de apreço para pessoas que me ajudaram nesta caminhada. Ao Professor Carlos Borrego, enquanto mentor deste grupo; ao Diogo, à Ana Ascenso, à Vera e à Alexandra, pelos valiosos contributos ao longo da tese; e à restante equipa, pela disponibilidade demonstrada e pela troca de ideias e de experiências, que me ajudaram a tomar opções.

Por fim, mas não menos importante, o suporte emocional da família e a Ajuda Divina nos momentos particularmente mais difíceis. Aos meus pais, pela pessoa que sou e pelo enorme esforço para que conseguisse estudar. À minha esposa e filha Beatriz, por serem o meu pilar no dia-a-dia, e pela compreensão da minha ausência em momentos que deveriam ser de família. À restante família, pelo apoio e incentivo ao longo destes anos.

A todos, MUITO OBRIGADO pelo vosso apoio incondicional!

palavras-chave

Qualidade do ar urbana, impactos na saúde pública, tráfego rodoviário, dióxido de azoto, sistema de modelação multiescala, estratégias melhoria qualidade do ar.

resumo

A poluição atmosférica é atualmente um sério problema mundial de saúde pública, especialmente em áreas urbanas, devido à elevada densidade populacional e intensa atividade antropogénica. O setor dos transportes rodoviários é uma das principais preocupações e o que mais contribui para concentrações de dióxido de azoto (NO_2) na atmosfera, embora as condições químicas de fundo regional devam também ser consideradas. Neste contexto, a utilização de ferramentas de modelação é crucial para compreender a dinâmica atmosférica e humana a diferentes escalas, e apoiar na definição das melhores estratégias para melhoria da qualidade do ar (EMQA).

Esta tese tem como objetivo principal o desenvolvimento e aplicação de um sistema de modelação multiescala que permita simular qualidade do ar e impactos na saúde em cidades. Para isso, foi desenvolvido e operacionalizado o sistema modair4health - *multiscale air quality and health risk modelling*. Este sistema inclui o modelo online WRF-Chem, que fornece campos meteorológicos e de qualidade do ar da escala regional à urbana, e o modelo CFD VADIS, que utiliza os resultados do WRF-Chem para calcular o impacto das emissões do tráfego rodoviário no escoamento e dispersão de poluentes em áreas urbanas. Para avaliar os impactos na saúde humana, foi também integrado um módulo baseado nas abordagens linear e não-linear da Organização Mundial de Saúde (OMS), e os custos são calculados com base em estudos económicos.

A aplicação e avaliação do sistema modair4health permitiram identificar as configurações e dados de entrada mais apropriados, que foram posteriormente utilizados para testar EMQA sobre o caso de estudo, que corresponde a uma das áreas de maior tráfego rodoviário da cidade de Coimbra (Avenida Fernão de Magalhães). O WRF-Chem foi configurado com 3 domínios aninhados (resoluções de 25, 5 e 1 km^2), simulados para o ano 2015; enquanto que para o VADIS, foi definido um quarto domínio (resolução de 4 m^2) sobre o caso de estudo para simular concentrações de NO_2 em dois períodos específicos: uma semana no inverno e outra no verão. Para quantificar os impactos na saúde, as duas abordagens da OMS foram aplicadas ao caso de estudo para avaliar efeitos a curto-prazo. A abordagem não-linear apresentou resultados de saúde mais baixos que aparentemente estão melhor ajustados à realidade local. Por fim, foram avaliadas as potencialidades do sistema no apoio à tomada de decisão, testando dois cenários de gestão do tráfego rodoviário: substituição de 50% da frota de veículos abaixo de EURO 4 por veículos elétricos (ELEC), e introdução de uma Zona de Emissões Reduzidas (LEZ). O cenário ELEC potencia melhorias mais significativas na qualidade do ar e saúde.

Este estudo representa um avanço científico na modelação multiescala da qualidade do ar e saúde. O sistema modair4health pode ser facilmente adaptado e aplicado a outros casos de estudo para avaliar a qualidade do ar urbana e impactos na saúde, bem como para testar medidas de controlo da poluição atmosférica.

keywords

Urban air pollution, health impacts, road traffic, nitrogen dioxide, multiscale modelling system, air quality improvement strategies.

abstract

Ambient air pollution is nowadays a serious public health problem worldwide, especially in urban areas due to high population density and intense anthropogenic activity. Among the main urban air pollution sources, the road traffic sector is one of the major concerns and the largest contributor to nitrogen dioxide (NO₂) concentrations, though regional background chemical conditions must also be considered. In this context, the use of modelling tools is crucial to understand atmospheric and social dynamics in multiple scales, as well as to support in defining the best air quality improvement strategies.

The main objective of this thesis is to develop and apply a multiscale modelling system able to simulate air quality and health impacts in cities. For this purpose, the modair4health multiscale air quality and health risk modelling system was developed and operationalized. It includes the online model WRF-Chem, which provides air quality and meteorological fields from regional to urban scales, and the Computational Fluid Dynamics (CFD) model VADIS, which uses the urban WRF-Chem outputs to calculate flows and dispersion of traffic emissions-related air pollutants in urban built-up areas. A health module, based on linear and non-linear World Health Organization approaches, was also integrated in modair4health to assess the health impacts resulting from air quality changes, and the overall health damage costs are calculated based on economic studies. The application and assessment of the modair4health system allowed to identify the most appropriate configurations and input data, which were used to apply the system over the case study testing air quality improvement scenarios. One of the busiest road traffic areas of the city of Coimbra (Fernão de Magalhães Avenue) in Portugal was selected as case study. The application considered a 4 domains setup: three nested domains (25, 5 and 1 km² resolutions) for the WRF-Chem, and the 4th domain (4 m² resolution) over the target local study area and NO₂ for the VADIS. WRF-Chem was applied along the year 2015 and VADIS was simulating two particular periods: one week in winter and another one in summer. Short-term health impacts were estimated and the non-linear approach led to lower health outcomes that seem better adjusted to the local reality. Finally, to assess the modair4health capabilities for decision-making support, two traffic management scenarios were tested over the case study: replacement of 50% of the vehicle fleet below EURO 4 by electric vehicles (ELEC), and introduction of a Low Emission Zone (LEZ). Air quality and health positive impacts were higher for the ELEC scenario.

This study represents a scientific advance in multiscale air quality and health modelling. The modair4health system can be easily adapted and applied to other simulation domains, providing urban air pollution levels and subsequent health impacts for different case studies and supporting the assessment of air pollution control policies.

TABLE OF CONTENTS

1. INTRODUCTION.....	3
1.1. Urban air quality and health impacts	3
1.2. Objectives and structure.....	7
2. STATE-OF-THE-ART ON MULTISCALE AIR QUALITY AND HEALTH MODELLING	13
2.1. The challenges of air quality modelling when crossing multiple spatial scales	13
2.1.1. Overview of multiscale air quality modelling applications.....	15
2.1.2. Current limitations	23
2.1.3. Guidelines for strengthening the synergy among scales.....	26
2.2. Health impact pathways related to air quality changes	29
2.2.1. Exposure assessment and health risks	29
2.2.2. Quantification of physical health impacts.....	32
2.2.3. Economic evaluation	37
2.2.4. Overview of epidemiological and economic studies.....	39
2.2.5. Uncertainties in health impact assessment.....	42
2.3. Summary	44
3. DEVELOPMENT OF AN INTEGRATED MULTISCALE MODELLING SYSTEM...49	49
3.1. Architecture of the modair4health system.....	49
3.2. Air quality modelling	52
3.2.1. WRF-Chem description and input data processing.....	52
3.2.2. VADIS description and input data processing.....	57
3.3. Health impacts modelling	59
3.4. Operationalizing the modair4health system	62
3.5. Summary	66
4. MODAIR4HEALTH SYSTEM APPLICATION AND ASSESSMENT	69
4.1. Case study characterization	69
4.2. Air quality modelling from regional to urban scales	72
4.2.1. WRF-Chem setup	73
4.2.2. Model evaluation	89

4.3. Air quality modelling at local scale	93
4.3.1. VADIS setup and input data	93
4.3.2. Model evaluation.....	96
4.4. Quantification of health impacts	100
4.4.1. Selected health input metrics	100
4.4.2. Comparative analysis of the health impact methodologies	102
4.5. Summary	106
5. AIR QUALITY AND HEALTH MANAGEMENT.....	109
5.1. Selected air pollution management strategies	109
5.2. Evaluation of the chain of impacts	110
5.2.1. Atmospheric emissions	112
5.2.2. Air quality	112
5.2.3. Human health.....	116
5.3. Summary	121
6. CONCLUSIONS.....	125
6.1. Main research findings.....	125
6.2. Future developments	128
REFERENCES	133
APPENDIXES:	
APPENDIX A - Reclassification scheme of the new land cover classification	I
APPENDIX B - User options for application of the modair4health system	III
APPENDIX C - Characterization of the Portuguese air quality monitoring network	VII
APPENDIX D - Estimation of road traffic-induced NO₂ emissions for the case study considering the reference and traffic management scenarios	XIII
APPENDIX E - Short-term health damage costs estimated for the reference scenario	XV

LIST OF FIGURES

Figure 1.1. Pollutant concentrations ($\mu\text{g}\cdot\text{m}^{-3}$) recorded at each monitoring station in 2017: (a) annual mean of PM _{2.5} ; (b) annual mean of PM ₁₀ ; (c) annual mean of NO ₂ ; and (d) 93.2 percentile of the O ₃ maximum daily 8-hour mean (source: EEA, 2019).	5
Figure 1.2. Overview of the thesis structure.	8
Figure 2.1. General structure of a multiscale air quality modelling system.	14
Figure 2.2. Graphical interface of the AirQ+ software.	33
Figure 2.3. Estimated mortality risk due to the short-term NO ₂ exposure using the two RR methods (linear RR and non-linear RR).	35
Figure 3.1. Flowchart of the modair4health system.	51
Figure 3.2. General structure of the WRF-Chem model.	53
Figure 3.3. Dominant LC categories mapped for a regional domain coverage over central Portugal, resulting from interpolation onto a 1 km ² resolution grid based on: (a) default USGS LC; and (b) new LC classification.	55
Figure 3.4. General structure of the VADIS model.	58
Figure 3.5. General structure of the health module.	60
Figure 3.6. Schematic representation of the operational chain of the modair4health system.	63
Figure 4.1. Geographic location of the case study area: a) framework, b) part of the Centre Region, c) case study, and d) part of the Fernão de Magalhães Avenue.	70
Figure 4.2. Altimetry (m) of the Coimbra region (source: OpenStreetMap - URL13).	71
Figure 4.3. Portuguese air quality monitoring network characterized by station typology: rural, suburban, urban and traffic.	73
Figure 4.4. Spatial representation of the nested WRF-Chem simulation domains.	74
Figure 4.5. Agreement between the WRF-Chem simulations, with and without aerosol feedback, for the analysed meteorological variables: (a) solar radiation; (b) air temperature; and (c) precipitation.	77
Figure 4.6. Monthly agreement between the WRF-Chem simulations, with and without aerosol feedback, for the analysed meteorological variables: (a) solar radiation; (b) air temperature; and (c) precipitation. Dark grey box represents the annual average distribution of agreement for the domain grid cells, while light grey boxes indicate the monthly distribution of agreement for the domain grid cells. Red dashed line shows the median of the annual agreement.	78

Figure 4.7. Spatial differences of solar radiation comparing both simulations (with feedback – without feedback): (a) annual average including all hourly values; and (b) annual average of daily maximum values.....	79
Figure 4.8. Spatial differences of air temperature comparing both simulations (with feedback – without feedback): (a) annual average including all hourly values; and (b) annual average of daily maximum values.....	80
Figure 4.9. LC databases for the domain 2, over Portugal: (a) USGS LC; and (b) new LC.	82
Figure 4.10. Spatial distribution of the modelled O ₃ concentrations (µg.m ⁻³) by season: (a) new LC-based average O ₃ concentration (dots represent O ₃ averages from background monitoring stations); and (b) average differences between USGS LC and the new LC.	83
Figure 4.11. (a) Average Leaf Area Index (m ² .m ⁻²) for the spring and summer seasons using both LC approaches; and (b) 2 m average air temperature (°C) for the spring and summer using the new LC approach.	84
Figure 4.12. (a) Correlation, (b) BIAS, and (c) RMSE between observations from background air quality stations and hourly modelled O ₃ concentrations (µg.m ⁻³) by season and station typology using both approaches USGS and new LC for Portugal.	85
Figure 4.13. Dominant LC categories mapped for the domain 3 coverage resulting from interpolation of the new LC: (a) 1 km ² grid spacing; and (b) 5 km ² grid spacing (D2 cut on D3 area).....	87
Figure 4.14. Map of the annual mean NO ₂ differences (µg.m ⁻³) between D3 and D2 results.	88
Figure 4.15. Annual mean NO ₂ differences (µg.m ⁻³) between D3 and D2 grouped by dominant LC category. For the legend of LC categories, see Figure 4.13.	89
Figure 4.16. Boxplot of the hourly NO ₂ concentrations (µg.m ⁻³) observed (Obs) and modelled in the D2 and D3 domains.	90
Figure 4.17. (a) Correlation, (b) BIAS and (c) RMSE between NO ₂ observations from the Portuguese air quality monitoring network and the modelled concentrations (µg.m ⁻³) for the D2 and D3 domains.	92
Figure 4.18. Spatial representation of the local case study's urban structure (buildings volumetry and streets configuration) considered for the VADIS simulations. The traffic influence monitoring station used to evaluate the model performance is also identified. ..	93
Figure 4.19. Wind roses that characterize the direction and speed wind simulated by WRF-Chem for the geographic location of the local case study and winter and summer simulation periods.....	94

Figure 4.20. Seasonal traffic emission profiles (winter and summer) designed for the influence area of the COI station.....	95
Figure 4.21. Time series of hourly observed and modelled NO ₂ concentrations (µg.m ⁻³) in (a) winter and (b) summer periods considering the two approaches used for temporal disaggregation of traffic emissions: REF_def and REF_adj.....	97
Figure 4.22. Daily NO ₂ profiles including observations and modelled NO ₂ concentrations (µg.m ⁻³) in (a) winter and (b) summer periods, considering the two approaches used for temporal disaggregation of traffic emissions: REF_def and REF_adj.....	98
Figure 4.23. Correlation between observations and hourly modelled NO ₂ concentrations (µg.m ⁻³) in (a) winter and (b) summer periods, considering the two approaches used for temporal disaggregation of traffic emissions: REF_def and REF_adj.....	99
Figure 4.24. Spatial distribution of the total resident population per grid cell (4 m ² horizontal resolution) for the local case study.....	101
Figure 4.25. Daily total health impacts, translated in number of cases and damage costs due to short-term NO ₂ exposure, for the (a) winter and (b) summer periods using the linear (lin) and non-linear (non-l) AirQ+ methodologies.....	103
Figure 4.26. Total number of cases estimated for the winter and summer periods comparing the linear and non-linear AirQ+ methodologies.	104
Figure 4.27. Spatial representation of the (a) daily maximum NO ₂ concentrations (µg.m ⁻³); and (b) short-term health cost differences (cents/day) between AirQ+ methodologies (linear – non-linear) for the local case study of 26 th January (on the left) and 15 th June (on the right).	105
Figure 5.1. Spatial representation of the Fernão de Magalhães Avenue LEZ.....	110
Figure 5.2. Diagram of the chain of impacts associated to the selected traffic management options, to be evaluated following a SAA.	111
Figure 5.3. Time series of hourly modelled NO ₂ concentrations (µg.m ⁻³) in (a) winter and (b) summer periods for the reference and traffic scenarios at the location of the air quality monitoring station COI.	113
Figure 5.4. Daily averaged profiles of NO ₂ concentrations (µg.m ⁻³) in (a) winter and (b) summer periods for the reference and traffic scenarios at the location of the air quality monitoring station COI.	114
Figure 5.5. Reduction of NO ₂ concentrations (µg.m ⁻³) (REF minus scenario) on 26 th January at 19:00 (on the left) and 17 th June at 7:00 (on the right) comparing each tested scenario with the reference: (a) ELEC; and (b) LEZ.	115

Figure 5.6. Short-term health benefits (cents/day) (REF minus scenario) resulting from the (a) ELEC and (b) LEZ scenarios for the winter period.....	117
Figure 5.7. Short-term health benefits (cents/day) (REF minus scenario) resulting from the (a) ELEC and (b) LEZ scenarios for the summer period.....	119
Figure 5.8. Daily total avoided health impacts for the (a) winter and (b) summer periods using the ELEC and LEZ scenarios.	120
Figure E.1. Short-term health damage costs (cents/day) estimated for the REF scenario in the winter period.	XV
Figure E.2. Short-term health damage costs (cents/day) estimated for the REF scenario in the summer period.....	XVI

LIST OF TABLES

Table 1.1. EU and WHO air quality guidelines for human health protection related to PM10, PM2.5, NO ₂ and O ₃	4
Table 2.1. Brief characterization of the reviewed air quality modelling applications commonly used involving regional, urban and local scales.	15
Table 2.2. Air pollutants and their health effects based on respiratory and cardiovascular diseases (source: EC, 2005; Hurley et al., 2005).	30
Table 2.3. Epidemiological data and economic evaluation of health effects related to the most common air pollutants (PM2.5, PM10, O ₃ , NO ₂ and SO ₂).	39
Table 4.1. Configurations used for designing the nested WRF-Chem simulation domains.	74
Table 4.2. Main physical and chemical parametrizations used in the numerical WRF-Chem simulations.....	75
Table 4.3. WRF-Chem tests to different configurations and input data.....	75
Table 4.4. Health input metrics used to assess health impacts from short-term human exposure to ambient NO ₂ concentrations.	101
Table 5.1. Total and daily averaged health impacts estimated in each scenario for the (a) winter and (b) summer periods considering the whole domain.	121

LIST OF ABBREVIATIONS AND ACRONYMS

AirQ+ - Software tool for health risk assessment of air pollution
AQ - Air Quality
AQG - Air Quality Guidelines
AQS - Air Quality Standards
CFD - Computational Fluid Dynamics
CI - Confidence Intervals
COI - Cost-Of-Illness methodology
CFD - Computational Fluid Dynamics
CLC - Corine Land Cover
cont - continuation
COS2010 - Land cover map of Mainland Portugal for 2010
CRF - Concentration-Response Functions
CTM - Chemical Transport Models
D - Simulation domain
DALY - Disability-Adjusted Life Years
ECMWF - European Centre for Medium-Range Weather Forecasts
EEA - European Environment Agency
EI - Emission Inventory
ELEC - Electric vehicles scenario
EMEP - European Monitoring and Evaluation Programme
EMIWRF - Anthropogenic emissions interface
Eq. - Equation
EU - European Union
EURO - European emission standards
EV - Electric vehicles
FCA - Friction Cost Approach
GIS - Geographic Information Systems
GNFR - Gridding Nomenclature For Reporting
HCA - Human Capital Approach
HIA - Health Impact Assessment
INE - Portuguese National Statistics Institute
IPA - Impact Pathway Approach
LAI - Leaf Area Index
LC - Land Cover

LES - Large Eddy Simulation
LEZ - Low Emission Zone scenario
LV - Limit Value
MEGAN - The Model of Gases and Aerosols from Nature
modair4health - multiscale air quality and health risk modelling
MOZART - Model for OZone And Related chemical Tracers
mozbc - WRF-Chem preprocessing tool to create initial and boundary chemical conditions
MS - Member States
QALY - Quality-Adjusted-Life-Year
RANS - Reynolds Averaged Navier-Stokes
REF - Reference scenario
REF_adj - Adjusted traffic profiles
REF_def - Seasonal traffic profiles
RMSE - Root Mean Square Error
RR - Relative Risk
 R^2 - Coefficient of determination
SAA - Scenario Analysis Approach
SNAP - Selected Nomenclature for Air Pollution
TREM - TRansport Emission Model for line sources
UC - Urban Canopy
UCM - Urban Canopy Model
UCP - Urban Canopy Parametrizations
USGS - United States Geological Survey
VADIS - CFD model of pollutant DISpersion in the atmosphere under VAriable wind conditions
WHO - World Health Organization
WMO - World Meteorological Organization
WPS - WRF Preprocessing System
WRF - Weather Research and Forecasting model
WRF-Chem - Weather Research and Forecasting model with Chemistry
WTA - Willingness-To-Accept
WTP - Willingness-To-Pay
YLD - Years Lost due to Disability
YLL - Years of Life Lost
3D - Three-dimensional

Chapter 1

Introduction

1.1. Urban air quality and health impacts

1.2. Objectives and structure

1. INTRODUCTION

The current ambient air quality levels and consequent implications for human health in Europe, in particular over urban areas where the majority of the population lives and/or works and the main anthropogenic air pollution sources are located, are a main concern nowadays (Section 1.1). To assess these air pollution levels and health impacts in a broad temporal and spatial horizon, the use of modelling tools for research and dissemination purposes is a common practice. However, in integrated multiscale modelling a deep knowledge of the relationship between air quality and health and the selection of the most appropriate models, parametrizations, resolutions and input data are key aspects that dictate the quality of the modelling results. In line with the urban air quality challenging research issues, the objectives and structure of the thesis are also presented (Section 1.2).

1.1. Urban air quality and health impacts

To date, air pollution is a global threat and the biggest environmental risk factor to the human health. According to the World Health Organization (WHO), about three million premature deaths each year, mainly from chronic diseases, are related to outdoor air pollution problems (WHO, 2016a). The exponential population growth throughout the last decades, and consequent non-sustainably intensification of the human activity have been contributing to these records (Likhvar et al., 2015). From the point of view of the main pollution hotspots, particular attention should be attributed to urban areas, because more than half of the world's population lives there, and normally a dense network of emission sources is present, namely transports, industry and households (Miranda et al., 2015). However, the causes of air pollution must be analysed beyond the urban/local scales, since air pollutants are often transported across continents and ocean basins (APPRAISAL, 2013a; Ramanathan and Feng, 2009; Thunis et al., 2016). Thereby, the use of emerging modelling tools is essential and encouraged through environmental regulations to cover multiple scales with different purposes:

- (i) to analyse the relative importance of the main emitting sources;
- (ii) to understand atmospheric and demographic dynamics that allow relating air concentrations with human exposure;
- (iii) to assess health impacts resulting from short and long-term exposure to air pollutants;

(iv) to accomplish legal impositions for air quality improvement at the European Union (EU) level, in particular those related to air pollution management strategies for the zones/agglomerations where air quality standards are exceeded.

Following this framework, the European Environment Agency (EEA) annually presents an updated analysis of air quality and its impacts, based on official data reported by the EU Member States (MS). According to the latest EEA report (EEA, 2019), estimates of the urban population exposure to air pollutants in Europe for a recent three-year period (2015-2017) indicate worrying numbers taking into account the exposed population percentage above the air quality standards (AQS) established in the EU Ambient Air Quality Directive 2008/50/EC, which are more alarming when confronted with the WHO air quality guidelines (AQG) (Table 1.1).

Table 1.1. EU and WHO air quality guidelines for human health protection related to PM10, PM2.5, NO₂ and O₃.

	Pollutant – reference value (µg.m ⁻³)			
	PM2.5	PM10	NO ₂	O ₃
Averaging period	year	year	year	maximum daily 8-hour mean
EU AQS	25	40	40	120
WHO AQG	10	20	40	100

Notes:

- EU AQS for protecting human health of particulate matter with an equivalent aerodynamic diameter less than 2.5 µm (PM2.5) and 10 µm (PM10) and nitrogen dioxide (NO₂) levels are referenced as limit values;
- EU threshold for the ozone (O₃) is defined as a target value, not to be exceeded on more than 25 days/year, averaged over a three-year period.

Figure 1.1 shows the spatial distribution of the measured concentrations of PM2.5, PM10, NO₂ and O₃ by the European air quality monitoring networks in 2017, in which many stations are in non-compliance of the regulated values. Exceedances of the EU AQS are marked in red.

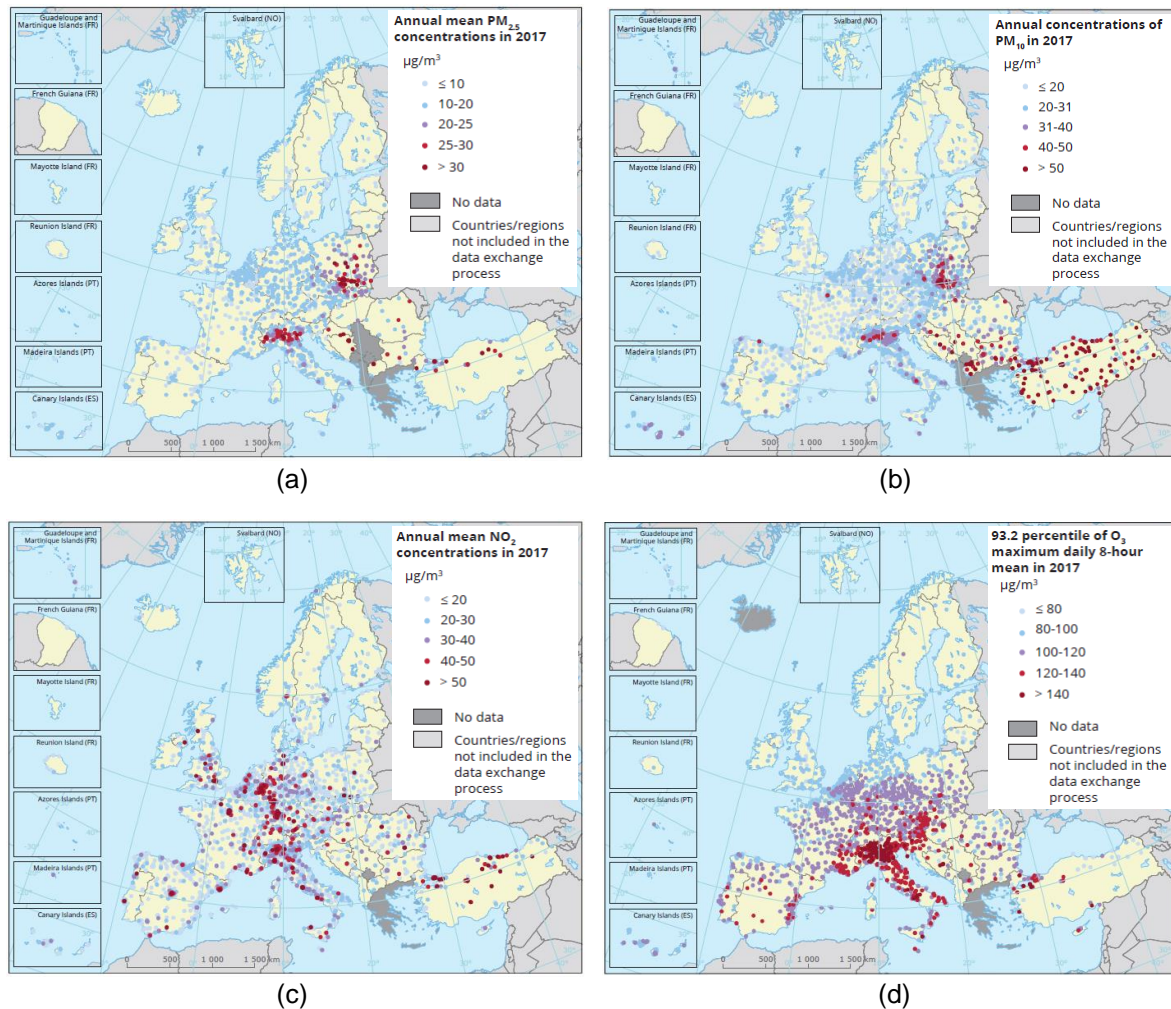


Figure 1.1. Pollutant concentrations ($\mu\text{g}\cdot\text{m}^{-3}$) recorded at each monitoring station in 2017: (a) annual mean of $\text{PM}_{2.5}$; (b) annual mean of PM_{10} ; (c) annual mean of NO_2 ; and (d) 93.2 percentile of the O_3 maximum daily 8-hour mean in 2017 (source: EEA, 2019).

$\text{PM}_{2.5}$ and PM_{10} concentrations were higher than the respective annual limit values (LV) in seven EU MS, representing 7 % of all the reporting stations, and occurred primarily in urban areas (83 %). Moreover, the stricter $\text{PM}_{2.5}$ value from the WHO AQG was exceeded at 69% of the stations, located in 30 of the 33 countries reporting $\text{PM}_{2.5}$ data. These indicators combined with high urban population exposure to $\text{PM}_{2.5}$ concentrations resulted in an estimation of 412000 premature deaths in Europe (of which 4900 occurred in Portugal) due to long-term exposure. In terms of annual mean of PM_{10} , the WHO reference value was exceeded in 51 % of the stations. It should also be noted that higher particulate matter (PM) concentrations in 2017 are also frequently associated to extreme natural events, as wildfires and natural dust, in particular over the Iberian Peninsula.

In urban areas, another critical air pollutant is NO₂, with the road traffic sector as the main emitting source. From all stations measuring NO₂, 10 % recorded concentrations above the EU annual LV, which are located, almost entirely (98 %), in urban or suburban areas. The highest concentrations, as well as 86 % of all data above the annual LV, were observed at traffic stations, to which intense road traffic activity is often associated. Translating these reported NO₂ concentrations in health impacts, 71000 premature deaths per year in Europe (610 deaths in Portugal) were estimated.

Regarding the O₃ concentrations, the EU target value was surpassed in 20 % of all stations reporting O₃, mostly corresponding to rural background stations (87 %). If the assessment value is based on the WHO AQG, only 2 % of the background stations were below this threshold. These high O₃ levels are strongly linked to extreme weather conditions, mainly due to the sharp rise of the air temperature that normally occurs in summer, and precursors emissions (nitrogen oxides, NO_x, and non-methane volatile organic compounds, NMVOC), favouring its production. In Europe, 15100 premature deaths (320 of them in Portugal) were estimated based on the O₃ concentration-human exposure relationship.

Notwithstanding the role of air quality monitoring networks in supporting air pollution control policies and health research, the way they are designed (i.e. spatial representativeness) may lead to an unbalanced checking of compliance with the AQS and biased population exposure assessments, given its restricted geographical and time coverage (Duyzer et al., 2015; WHO, 2016b). In this sense, the use of air quality models as a complement to monitoring data allows a more comprehensive air quality assessment, though the measurements are very important for validation of the modelling results. This assessment involves the application of different types of air quality models depending on the objectives, dimension of study domains and intended resolutions. For this purpose, mesoscale and microscale models have been developed and applied, although in most cases following distinct approaches.

In a typical urban atmosphere, the complexity of the urban structure (e.g. buildings volumetry, road network) has a relevant role in the physical and chemical processes governing the transport, dispersion, transformation and deposition of air pollutants (Chen et al., 2011; Russo and Soares, 2014; Srivastava and Rao, 2011; Tang and Wang, 2007; Vardoulakis et al., 2003). Thus, applying air quality models at local/urban scale requires that these small-scale processes be explicitly well resolved, but also to take into account the influence of a larger scale, since the dispersion and atmospheric chemistry contribute to variations in polluted air arriving to a region from other regions and/or countries (APPRAISAL, 2013a). However, the background and time-dependent boundary conditions

provided from mesoscale modelling (i.e. physical and chemical fields), are often greatly simplified mostly due to the nature of mesoscale-coupled urban schemes (Baklanov and Nuterman, 2009; Beevers et al., 2012; Kwak et al., 2015; Mensink et al., 2003). This is a key research area, since the proper link between mesoscale and local scale models, as well as the identification of the best parametrizations and input data, are essential requirements to decrease the uncertainties when analysing urban-to-local modelling results.

Another important challenge nowadays is to fully integrate in the air quality modelling system the health impacts, moving from air pollutant levels to health indicators, and thus getting closer to the society needs (Brandt et al., 2013; Pervin et al., 2008). The health impacts are highlighted by public health experts, aware of the link between air pollution and worsening morbidity (especially respiratory and cardiovascular diseases) and premature mortality (e.g. years of life lost). To quantify the extent of these adverse effects on different age groups, approaches combining air concentrations, population data and concentration/exposure-response functions (CRF) based on epidemiological studies have been used (Holland et al., 2005; WHO, 2013a). The resulting health impacts are often converted in monetary values, allowing a cost-benefit analysis of policy options considered for air quality management (Holland et al., 2005; Relvas et al., 2017).

Based on this air quality framework in Europe, the following research questions seeking to strengthen the knowledge and to bridge some gaps were formulated:

1. What are the most appropriate modelling tools for quantifying multiscale air quality and health impacts? How to connect them?
2. How do input data and model setup influence the modelling results?
3. What is the impact of the urban structure on the dispersion of air pollutants?
4. Will a modelling system be able to accurately estimate air concentrations and health impacts in urban areas?
5. How might the modelling system capabilities be useful to support decision-makers and stakeholders in selecting the best strategies for air quality and health management?

1.2. Objectives and structure

In order to answer these research questions, a set of objectives to be accomplished along the thesis were proposed. The main objective was to develop and apply a multiscale modelling system that integrates air quality and health impacts. To tackle this objective, the following specific goals were fulfilled:

- i. to develop an urban air pollution modelling system able to simulate atmospheric concentrations from urban to local scales. This modelling system should seek to bridge the gaps when crossing different scales;
- ii. to integrate quantifiable human health effects in the air pollution modelling system;
- iii. to apply and assess the system with high spatial and temporal resolutions for a particular local scale case study;
- iv. to provide recommendations based on the developed modelling system capabilities for local emission reduction or joint pollution control with neighbouring urban areas, supported by the analysis of different air quality management strategies and their potential health benefits.

The present document is organized in six main chapters, addressing: (i) a state-of-the-art review on air quality and health in Europe, and on available modelling tools commonly used to support assessments, (ii) the development and application of an integrated multiscale modelling system, (iii) the testing of air quality and health management strategies, and (iv) the main conclusions. This structure is schematically represented in Figure 1.2.

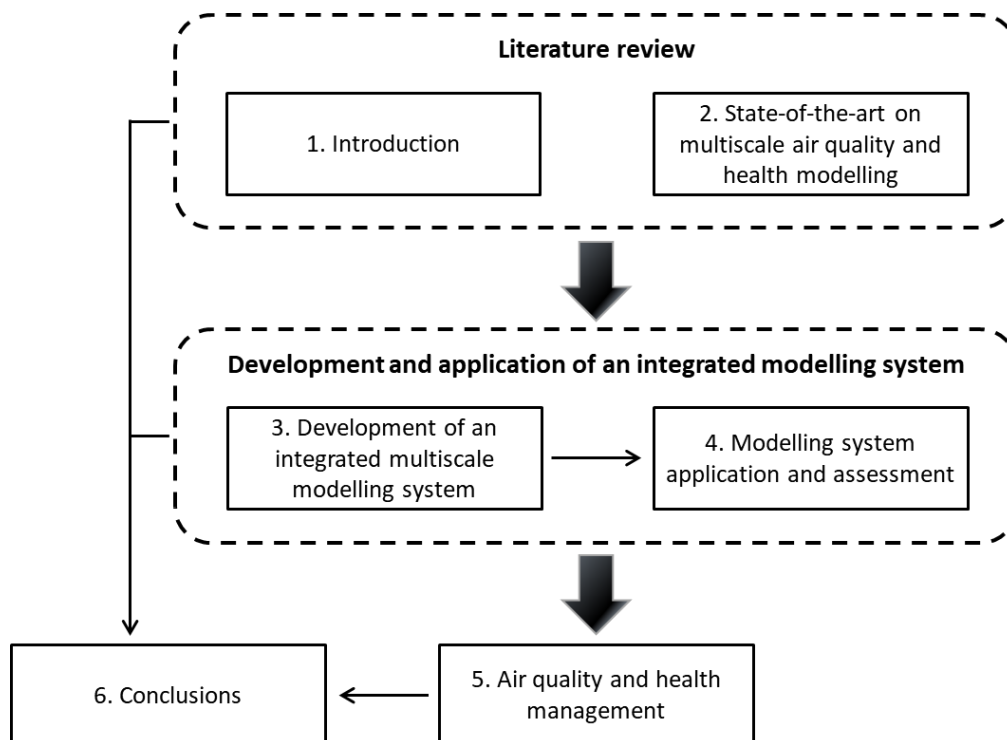


Figure 1.2. Overview of the thesis structure.

Chapter 1 provides an overview of the air quality in Europe and its effects on the human health, based on monitoring data and on the application of modelling tools at multiple scales. Large uncertainty sources are often associated to the selected models, their configurations and coupling, unsuitable input data to portray particular case studies, and to air quality-health relationships. These key aspects determine the quality of the modelling results, and thus represent some weaknesses of the current scientific knowledge, which allowed to identify gaps and challenges, and led to formulate research questions. The objectives and structure of the thesis are also presented.

Chapter 2 complements the introductory chapter of the thesis, focusing on the modelling approaches used for computing air quality and health impacts in a broad spatio-temporal spectrum. Taking as support the reviewed air quality modelling state-of-the-art, multiscale applications and their limitations are discussed, and a set of guidelines for strengthening the synergy among scales and harmonizing different types of models within a system is proposed. A summary of the health impacts related with air pollution exposure is also presented. For quantifying the extent of these impacts, translated into number of unfavourable cases and external costs (i.e. total health costs), recommended methodologies, information derived from epidemiological and economic studies, and associated uncertainties are described and analysed.

The main conclusions of Chapter 2 are very useful to give response to the research question 1, namely in selecting the most appropriate modelling tools and how to integrate them into a single system. Thus, in **Chapter 3**, the conceptual framework of the adopted models/methodologies and their input data processing configurations for designing a new integrated multiscale modelling system is described. Simultaneously, the modelling chain setup was operationalized for research and end-user purposes.

The application and the assessment of the developed modelling system are presented in **Chapter 4**, giving emphasis to a local case study. In order to identify the most suitable parametrizations and input data for the simulation domains, a few tests involving the selected models were performed. This exercise intends to assess the influence of input data and models setup, in particular of the urban structure, on modelling results (research questions 2 and 3); hence different configurations and some improvements in terms of key input data, as land cover classification and emission profiles, have been implemented and tested. For the evaluation of the multiscale air quality modelling results, measured data from the Portuguese air quality monitoring network are used. Health outcomes are quantified and evaluated for the local case study, considering two simulation periods (one week in winter

and another one in summer) and short-term air pollution exposure. In view of this system evaluation, it will be possible to understand the reliability of these estimates at urban scale (research question 4).

After the validation and consolidation of the modelling system regarding models, configurations and input data to be used, two air pollution management strategies focused on the road traffic sector and NO₂, are selected and tested in **Chapter 5**. The objective of these emission abatement scenarios is twofold: (i) assessing the system capabilities to support decision-makers and stakeholders in selecting the best strategies (research question 5), and (ii) providing some recommendations for both local pollution control and reduction of adverse health effects. The entire chain of impacts, from atmospheric emissions to air quality and health effects is evaluated. These impacts reflect the expected benefits with the implementation of the traffic scenarios.

Finally, the main findings of this thesis are presented in **Chapter 6**, discussing the identified scientific advances and limitations as a response to the formulated research questions. Based on the methodological limitations and proposed guidelines for strengthening the synergy among models and scales, some developments are also delineated as future work.

Chapter 2

State-of-the-art on multiscale air quality and health modelling

2.1. The challenges of air quality modelling when crossing multiple spatial scales

2.1.1. Overview of multiscale air quality modelling applications

2.1.2. Current limitations

2.1.3. Guidelines for strengthening the synergy among scales

2.2. Health impact pathways related to air quality changes

2.2.1. Exposure assessment and health risks

2.2.2. Quantification of physical health impacts

2.2.3. Economic evaluation

2.2.4. Overview of epidemiological and economic studies

2.2.5. Uncertainties in health impact assessment

2.3. Summary

2. STATE-OF-THE-ART ON MULTISCALE AIR QUALITY AND HEALTH MODELLING

In this chapter, a state-of-the-art on multiscale air quality and health modelling, including an analysis of uncertainties/limitations and guidelines for the development of an integrated multiscale modelling system, is presented. The contents are divided in two sections:

- Section 2.1 describes the challenges of air quality modelling when crossing multiple spatial scales (Silveira et al., 2019), and it was published as:

Silveira C., Ferreira J., Miranda A.I., 2019. The challenges of air quality modelling when crossing multiple spatial scales. *Air Quality, Atmosphere & Health*, 12(9), 1003–1017.

- Section 2.2 discusses health impacts based on the assessment of air quality, and is part of the following publication:

Silveira C., Roebeling P., Lopes M., Ferreira J., Costa S., Teixeira J.P., Borrego C., Miranda A.I., 2016. Assessment of health benefits related to air quality improvement strategies in urban areas: An Impact Pathway Approach. *Journal Of Environmental Management*, 183, 694-702.

2.1. The challenges of air quality modelling when crossing multiple spatial scales

Multiscale air quality assessment implies understanding the interaction among atmospheric processes and scales. In this perspective, the use of air quality models has a fundamental role and the way they address these interactions is very important for the quality of results. However, in multiscale air quality modelling, the relationship between models, simulation domains and resolutions remains a challenging research issue. This section presents a state-of-the-art review on multiscale air quality modelling applications from the regional to the street level, identifying which models are used, the methodological principles and the required input datasets. Based on the findings, an analysis of the current limitations associated with the integration of different models and multiple spatial scales in a single modelling system is presented and discussed. Lastly, taking as support the reviewed contents, a set of guidelines for strengthening the synergy among scales and harmonizing different types of models within a system is proposed.

Figure 2.1 shows the basic requirements involving a typical multiscale air quality modelling system, namely the information flow needed to interactively combine models at different scales and applications.

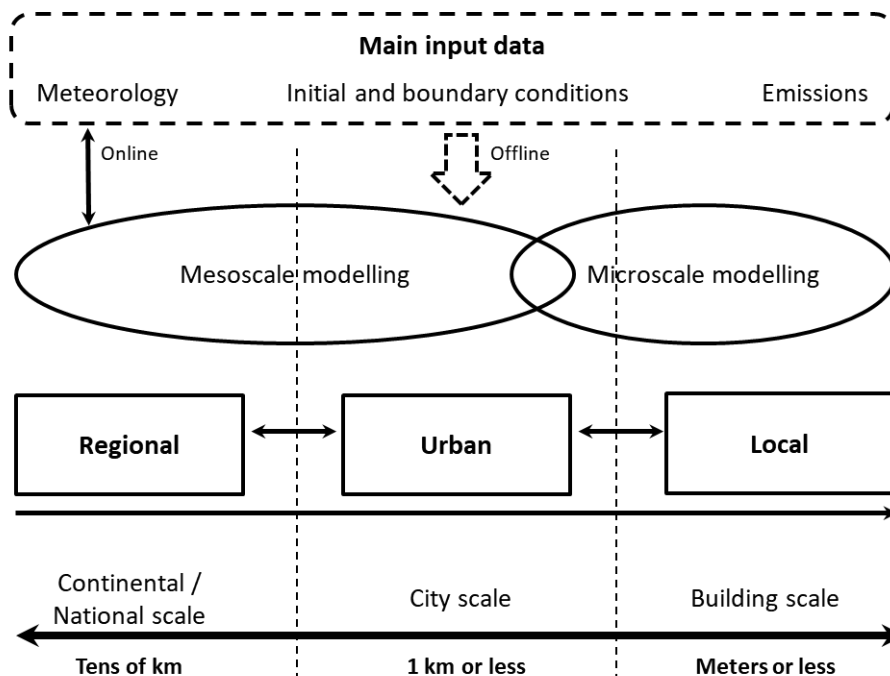


Figure 2.1. General structure of a multiscale air quality modelling system.

The air quality modelling is divided into mesoscale and microscale taking into account the suitable spatial coverage and resolutions for application of the involved models, seeking, in a multiscale perspective, to ensure the harmonious link among them. To feed offline air quality models, three main input datasets are used: meteorology, initial and boundary conditions and atmospheric emissions. In the case of online models, the calculation of meteorology and chemistry is done in parallel, allowing the assessment of potential feedbacks including, for example, direct aerosol effects on the radiation scattering and the influence of local weather patterns on chemical reactions. Two main types of coupling techniques for the down- and/or upscaling can be chosen: (i) one-way, when effects of the local/microscale on a larger scale are not considered, and (ii) two-way, whose scale effects are felt in both directions (regional to local and local to regional). The two-way option is mainly used in mesoscale modelling, favouring the feedback between simulation domains.

2.1.1. Overview of multiscale air quality modelling applications

Multiscale modelling systems for air quality assessment have often been applied using nesting approaches aimed at simulating urban areas. Based on a literature review addressing multiscale features and assumptions, a summary of the reviewed applications is presented in Table 2.1 including information about the model type, scales of application, domains, resolutions and other configurations. This review focuses on manuscripts from 2000 to 2019 available from the Web of Science, JSTOR and Scopus databases, giving preference to the most cited ones. The keywords/terms used for the search were “air quality”, “multiscale modelling” and “nesting”. The analysis of Table 2.1 is oriented towards urban/local areas, where the main air pollution problems are found.

Table 2.1. Brief characterization of the reviewed air quality modelling applications commonly used involving regional, urban and local scales.

Modelling system / Reference	Model	Type	Application scales	Domains / Spatial resolution	Other configurations / Comments
CALIOPE-Urban (Benavides et al., 2019)	The Community Multiscale Air Quality (CMAQ) model	Eulerian CTM	Regional to Urban	3 nested domains over Europe, Iberian Peninsula and Catalonia (12, 4 and 1 km ²)	<ul style="list-style-type: none"> - WRF meteorology - CMAQ emission sources: EMEP for Europe, and bottom-up/top-down approaches by SNAP for Spain - Traffic counting data and fleet composition to estimate emissions for the R-LINE model were used - CMAQ provides background concentrations for the R-LINE - There is no double counting of traffic emissions between models - R-LINE was adapted to street canyons using urban geometry data, and it has a simplified NO-NO₂ chemistry
	Research LINE source dispersion model (R-LINE)	Gaussian model	Urban to Local	Barcelona (Roadside)	
GEM-MACH (Russell et al., 2019)	Global Environmental Multiscale – Modelling Air-quality and Chemistry (GEM-MACH)	Online model (meteorology and chemistry are handled within a single model)	Regional to Urban	4 nested domains from two-thirds of the operational GEM-MACH domain to the Canadian provinces of Alberta and Saskatchewan (10, 10, 2.5, 1 km ²)	<ul style="list-style-type: none"> - Meteorological boundary conditions from operational GEM forecasts (outermost domain) and data assimilation for the inner domains - Emission sources: stack monitoring, regional and national EI - Chemistry is embedded within the GEM physics module - It represents the particles distribution by sizes (12 and 2-bin) - Two-way nesting

Table 2.1. Brief characterization of the reviewed air quality modelling applications commonly used involving regional, urban and local scales (cont).

Modelling system / Reference	Model	Type	Application scales	Domains / Spatial resolution	Other configurations / Comments
Street-in-Grid model (Kim et al., 2018)	Polair3D	Eulerian CTM	Regional to Urban	4 nested domains over western Europe, northern-central France, Île-de-France region, eastern Paris suburbs (0.5, 0.15, 0.04, 0.01 ^o)	<ul style="list-style-type: none"> - WRF meteorology (1.5 km²) - Polair3D emission sources: EMEP for domains 1 and 2, and Airparif EI for domains 3 and 4 - MOZART BC - At street level, detailed traffic emissions, geographic data, and meteorological and chemical background conditions provided from Polair3D were used
	Model of Urban Network of Intersecting Canyons and Highways (MUNICH)	Street-network model	Local	577 street segments within the domain 4	<ul style="list-style-type: none"> - MUNICH is composed by two main components: street-canyon and street-intersection - CB05 chemical mechanism was implemented in both models - There is no double counting of emissions - Feedback between models
EMEP4UK – ADMS-Urban (Hood et al., 2018)	EMEP regional version focused on air quality in the UK (EMEP4UK)	Eulerian CTM	Regional to Urban	2 nested domains over Europe and UK (50 and 5 km ²)	<ul style="list-style-type: none"> - WRF meteorology (10 km²) - EMEP4UK emission sources: UK National EI (5 km) and EMEP (50 km²) outside the UK - ADMS-Urban used a detailed EI by SNAP sector for London (1 km² grid resolution), and measured background concentrations as BC
	Atmospheric Dispersion Modelling System (ADMS-Urban)	Gaussian model	Urban to Local	Greater London region	<ul style="list-style-type: none"> - It has an “urban-canopy” module calculating wind speed and turbulence as a function of the surface roughness (enters with a buildings volumetry and roads network)
The THOR Integrated System (Jensen et al., 2017)	Danish Eulerian Hemispheric Model (DEHM)	Eulerian CTM	Regional	3 nested domains - Europe, Northern Europe and Denmark (50 x 16.7 and 5.6 km ²)	<ul style="list-style-type: none"> - MM5 meteorology - DEHM-UBM emission sources: EMEP for Europe, and Danish EI from all sectors on a 1 x 1 km² grid - DEHM was run in two-way nesting, using Northern Hemisphere results (150 km² resolution) from Brandt et al. (2012) as IC and BC conditions
	Urban Background Model (UBM)	Urban background pollution model	Urban	A few Danish cities (1 km ²)	<ul style="list-style-type: none"> - At street level, geometry urban data, traffic volume and emissions, meteorological parameters and background concentrations provided from the UBM were used
	Operational Street Pollution Model (OSPM)	Street canyon model	Local	98 selected streets in Copenhagen and 31 streets in Aalborg	

Table 2.1. Brief characterization of the reviewed air quality modelling applications commonly used involving regional, urban and local scales (cont).

Modelling system / Reference	Model	Type	Application scales	Domains / Spatial resolution	Other configurations / Comments
Integrated Urban Air Quality Modelling System (Kwak et al., 2015)	CMAQ	Eulerian CTM	Regional to Urban	3 nested domains over Seoul, Republic of Korea (9, 3 and 1 km ²)	<ul style="list-style-type: none"> - WRF meteorology - Mobile emissions are spatially allocated on roads of the CFD domain - CMAQ and WRF provide initial and time-dependent boundary conditions for the CFD - The same chemical mechanism used in the CMAQ was implemented in the CFD model
	CFD	CFD model	Local / microscale	High-rise building area of Seoul (1600 x 1600 x 997 m ³)	
Polair3D – SIREAM (Kim et al., 2015)	Polair3D	Eulerian CTM	Regional to Urban	Part of Europe (0.5°), France (0.125°), Greater Paris (0.02°)	<ul style="list-style-type: none"> - WRF meteorology - EMEP emissions (0.5°x0.5°) - INCA-LMDz IC and BC - Test different PBL schemes, with/without UCM
	Size REsolved Aerosol Model (SIREAM)	Implemented aerosol model			
CMAQ – CALPUFF (Zhang et al., 2015)	CMAQ	Eulerian CTM	Regional to Urban	Hong Kong Administrative Region (3 km ²)	<ul style="list-style-type: none"> - WRF meteorology for the CMAQ and CALMET. The latter produces finer-scale meteorological fields for the CALPUFF - Emission sources: CMAQ used a bottom-up EI for some sources (3 km² resolution), while CALPUFF used local emission data - CMAQ provide IC and BC for the CALPUFF - User-friendly system interface currently prepared for Hong Kong and Pearl River Delta region, but could be transferable to study other regions, providing a proper data set
	CALifornia PUFF (CALPUFF)	Multilayer non-steady state puff dispersion model	Urban to Local	Centered at Hong Kong (0.5 km ²)	
AURORA – IFDM – OSPM (Hofman et al., 2014)	Air quality modelling in Urban Regions using an Optimal Resolution Approach (AURORA)	Eulerian CTM	Regional to Urban	Antwerp city to street level	<ul style="list-style-type: none"> - Emission sources: industry, traffic, households - Local traffic emissions provided by the MIMOSA model - AURORA and IFDM were coupled using a method to avoid the double counting of the local emissions - IFDM and OSPM results were combined in order to get high resolution concentrations
	Immission Frequency Distribution Model (IFDM)	Bi-Gaussian plume model	Urban to Local		
	Operational Street Pollution Model (OSPM)	Street canyon model	Local		

Table 2.1. Brief characterization of the reviewed air quality modelling applications commonly used involving regional, urban and local scales (cont).

Modelling system / Reference	Model	Type	Application scales	Domains / Spatial resolution	Other configurations / Comments
Source-Oriented WRF/Chem with High Resolution (SOWC-HR) (Joe et al., 2014)	WRF/Chem	Online model (fully coupled-meteorology and chemistry)	Regional to Urban	3 nested domains over the Oakland region, California (12, 4 and 1 km ²)	<ul style="list-style-type: none"> - Higher resolution EI for the domains 3 and 4 were developed - LES is coupled in WRF/Chem - Changes on the PBL schemes were made to allow the nesting of the LES within the multiscale parent domains - Requires very small time intervals to keep the numerical stability in the advection scheme - Street canyon and building effects are not resolved - Two-way nesting - Online coupling
	Large Eddy Simulation (LES)	Subgrid-scale turbulence model	Urban to Local	Domain 4 focused on the Port of Oakland (250 m ²)	
The UK Integrated Assessment Model (UKIAM) (Oxley et al., 2013)	EMEP	Eulerian CTM	Regional	Europe (50 km ²)	<ul style="list-style-type: none"> - Emission sources: EMEP for non-UK areas; national and local EI for UK - Gaussian PPM only includes small derivations for NO₂ concentrations - Source-apportionment assessment from local and distant sources
	FRAME	Lagrangian CTM	Regional to Urban	UK (5 km ²)	
	Primary Particulates Model (PPM)	Gaussian model	Urban	UK (1 km ²)	
	BRUTAL	Street canyon model	Local	Roadside	
CHIMERE – “Stretching” method (Siour et al., 2013)	CHIMERE	Eulerian CTM	Regional	Europe (0.5°) to Belgium-Netherlands-Luxembourg (0.1°)	<ul style="list-style-type: none"> - WRF meteorology - EMEP emissions (0.5°x0.5°) - Zooming approach provides a simple and immediate way to better represent scale interactions within the CTM - One-way nesting
	“Stretching” method	Also called “Zooming”	Regional to Urban	Belgium-Netherlands-Luxembourg (300 m ²)	
The THOR Integrated System (Brandt et al., 2012)	DEHM	Eulerian CTM	Regional	Northern Hemisphere (NH – 150 km ²); 2 nested domains: Europe and North America (NA – 50 km ²)	<ul style="list-style-type: none"> - MM5 meteorology - Emission sources: RCP for NH and NA, EMEP for Europe (both EI with 0.5° x 0.5°) - DEHM was run in two-way nesting - UBM includes a simple scheme for dispersion and transport, as well as a simple chemical model including NO_x and O₃ reactions - OSPM used UBM outputs and emissions provided from a traffic model for simulating NO₂ dispersion and chemistry at the street scale
	UBM	Urban background pollution model	Urban	A few cities (1 km ²)	
	OSPM	Street canyon model	Local	Roadside	

Table 2.1. Brief characterization of the reviewed air quality modelling applications commonly used involving regional, urban and local scales (cont).

Modelling system / Reference	Model	Type	Application scales	Domains / Spatial resolution	Other configurations / Comments
CMAQ – ADMS-Roads (Beevers et al., 2012)	CMAQ	Eulerian CTM	Regional to Urban	London (3 km ²)	<ul style="list-style-type: none"> - WRF meteorology - Emission sources: EMEP (0.5°x0.5°), E-PRTR and London EI (1km² resolution) - STOCHEM IC and BC - CMAQ predictions were downscaled for a 20 m² grid using the bilinear interpolation method - ADMS represents the dispersion from road traffic (NO_x-NO₂-O₃)
	Atmospheric Dispersion Modeling System (ADMS-Roads)	Gaussian model	Urban to Local	Roadside (20 m ²)	
CCAM – TAPM (Thatcher and Hurley, 2010)	Conformal Cubic Atmospheric Model (CCAM)	Semi-Lagrangian atmospheric model	Regional	Australia (60 km ²)	<ul style="list-style-type: none"> - CCAM requires only global IC (1° resolution GFS) - It provides BC for the TAPM - TAPM was selected due to its combined prognostic meteorological and air pollution modelling capability
	The Air Pollution Model (TAPM)	Eulerian CTM	Urban	Urban regions centred on Melbourne (dynamic downscaling of 30, 10 and 3 km ²)	
CMAQ – AERMOD (Isakov et al., 2009)	CMAQ	Eulerian CTM	Regional to Urban	USA region (nesting from 36 to 12 km ²)	<ul style="list-style-type: none"> - MM5 meteorology - 1999 National EI - CMAQ was run for one year in nested mode - It provides regional background concentrations for the AERMOD - AERMOD is designed to capture local gradients from nearby sources, using highly simplified atmospheric chemical reactions. It uses “bottom-up” EI from mobile and stationary sources
	AERMOD	Gaussian model	Urban	New Haven (mobile and stationary sources network)	
Enviro-HIRLAM – M2UE (Baklanov and Nuterman, 2009)	Environment-High Resolution Limited Area Model (Enviro-HIRLAM)	Online model (fully coupled-meteorology and chemistry)	Regional to Urban	Copenhagen (nesting from 3 to 0.5 km ²)	<ul style="list-style-type: none"> - Enviro-HIRLAM provides IC and BC for the M2UE - It was run in one-way nesting - It uses urban parameterizations: at regional level are based on the roughness and flux corrections approach (EMS-FUMAPEX), while BEP is considered at the urban scale - M2UE calculates obstacle-resolved flows and dispersion based on the RANS approach and two-equation turbulence closure
	Obstacle-resolved Microscale Model for Urban Environment (M2UE)	CFD model	Local / microscale	Selected area of Copenhagen (from 50 to 3 m ²)	

Table 2.1. Brief characterization of the reviewed air quality modelling applications commonly used involving regional, urban and local scales (cont).

Modelling system / Reference	Model	Type	Application scales	Domains / Spatial resolution	Other configurations / Comments
CMAQ – HYSPLIT – AERMOD (Stein et al., 2007)	CMAQ	Eulerian CTM	Regional to Urban	Houston, Texas (1 km ²)	- CMAQ provides regional background concentrations and urban-scale photochemistry - A simulated HYSPLIT concentrations ensemble is used to assess the variability/dispersion from point sources, assuming non-reactive chemistry on sub-grid scales (useful to model the uncertainty) - AERMOD simulates the plume dispersion from mobile sources
	HYbrid Single-Particle Lagrangian Integrated Trajectory (HYSPLIT)	Lagrangian CTM	Urban to Local	Stationary sources	
	AERMOD	Gaussian model	Urban to Local	Selected roads network	
ECHAM5/MESSy – CMAQ (Jiménez et al., 2006)	Fifth-generation atmospheric GCM / Modular Earth Submodel System (ECHAM5/MESSy)	Atmospheric chemistry GCM	Global	Global (1.8° x 1.8°)	- The ECHAM5/MESSy coupling allows to simulate large-scale chemistry-climate - Emission sources: EDGAR3.2 EI for ECHAM5/MESSy; and EMEP (coarser domains) and high resolution emissions (1 h and 1 km ² – inner domain) for CMAQ
	CMAQ	Eulerian CTM	Regional to Urban	4 nested domains from Europe, Iberian Peninsula to a Catalonia area (72, 24, 6 and 2 km ²)	
MATCH (Gidhagen et al., 2005)	Multi-scale Atmospheric Transport and CHemistry (MATCH)	Eulerian CTM	Regional to Urban	Stockholm (5 km ² down to 0.5 km ²)	- HIRLAM meteorology (22 km ² resolution) - The flat topography allows the downscaling to the urban grid (500 m ²) and also interpolation in time to yield hourly data, involving higher vertical resolutions (4 layers below 15 m) and a recalculation of the turbulence over the city - Street canopies and buildings are not resolved in the model
Integrated system AURORA (Mensink et al., 2003)	AURORA	Eulerian CTM	Regional to Urban	Flemish region, Antwerp (1 km ²)	- ARPS meteorology (100 m ² resolution) - Detailed EI, described as a function of space, time and temperature - AURORA system integrates the OPS and the SBM
	Operational Priority Substances (OPS)	Lagrangian CTM	Regional to Urban	Flemish region, Antwerp (1 km ²)	- OPS calculates concentrations, and dry and wet depositions for primary and secondary components
	Street Box Module (SBM)	Street canyon model	Local	11 selected streets	- SBM assumes an uniform concentration distribution over the street with the box dimensioned by the length and width of the street and the height of the surrounding built-up area

Acronyms: ARPS - Advanced Regional Prediction System; BC - Boundary Conditions; BEP - Building Effects Parameterization; CALMET - CALifornia METeorological model; CB - Carbon Bond; EI - Emission Inventory; EMEP - The European Monitoring and Evaluation Programme; E-PRTR - The European Pollutant Release and Transfer Register; GCM - General Circulation Model; GFS - Global Forecast System; IC - Initial Conditions; INCA - INteraction with Chemistry and Aerosols model; LMDz - Laboratoire de Meteorology Dynamique zoomed; MM5 - Fifth-Generation Penn State/NCAR Mesoscale Model; MOZART - Model for OZone And Related chemical Tracers; PBL - Planetary Boundary Layer; RCP - Representative Concentration Pathways; SNAP - Selected Nomenclature for Air Pollution; UCM - Urban Canopy Model; WRF - The Weather Research and Forecasting model.

The large majority of the reviewed multiscale modelling applications only consider atmospheric feedbacks from larger simulation domains to the inner ones (i.e. one-way coupling), mainly when different types of air quality models are used. It means, therefore, that the influence of microscale processes on the regional/urban air quality is usually neglected. Some coarser resolution models have been adapted to include urban canopy parametrizations (UCP) (e.g. WRF, Enviro-HIRLAM) with the primary goal of representing the subgrid effects of urban surfaces, by means of averaged input parameters (e.g. urban fraction, building height, albedo, roughness), on air flows and air pollution processes taking place in the urban canopy (i.e. atmospheric layer between the surface and the highest building height). However, the UCP's numerical and empirical methods triggered to model the urban/local air quality are simple approximations to describe fluid's turbulent flows, heat transfer mechanisms and associated phenomena occurring in urban environment, since these are mostly based on the assumptions of horizontal homogeneities (Baklanov and Nuterman, 2009; Chen et al., 2011; Kim et al., 2015). Moreover, once the air quality models that integrate the respective modelling systems were run independently, the input data and physical and chemical processes underlying each model are treated separately taking into account their application scales and study domains.

Looking at the regional and urban scales, Eulerian offline chemical transport models (CTM) with UCP have been the most used to provide background and boundary chemical conditions for higher resolution models. However, the option for offline applications (i.e. meteorology is only provided to the CTM as an input) is gradually being replaced by using online modelling tools that allow a full integration and parallel computing of both meteorology and chemistry components, sharing the same simulation grids (horizontal and vertical levels), physical parametrizations, transport schemes and vertical mixing (Grell et al., 2005). In some studies, Lagrangian and Gaussian models are used to make the connection with mesoscale CTM (Hofman et al., 2014; Mensink et al., 2003; Oxley et al., 2013), and some Gaussian models were specifically configured for assessing the pollution dispersion in street canyons (Beevers et al., 2012; Benavides et al., 2019; Isakov et al.,

2009; Stein et al., 2007). Lagrangian trajectory models are computationally simpler and allow an easy determination of transboundary flows. In addition, they could be especially suitable for assessing the dispersion from individual emission sources, and their application over urban areas could be grounded in the longer reaction time scale of many chemical species than the travel time across the study area (Kukkonen et al., 2012; Stein et al., 2007). To analyse the intraurban spatial variability, ensemble modelling techniques with dispersion models (e.g. ADMS, OSPM, AERMOD, HYSPLIT) focused on the main emitting sources have been applied; in the case of HYSPLIT, it is through a trajectory analysis allowing the determination of the origin of air masses and establishing source-receptor relationships (Stein et al., 2007). In terms of atmospheric chemistry, in Lagrangian and Gaussian models, local pollutant concentrations (e.g. NO_x/NO₂ at traffic locations) are also derived from simplified chemical reactions (Brandt et al., 2012; Jensen et al., 2017), or through empirically tested quadratic relationships for rural, urban and roadside sites (Oxley et al., 2013).

The downscaling to the local/microscale is done through modelled meteorological and chemical data from the upper domain, and requires a more detailed characterization of the study case, especially regarding the buildings volumetry and streets configuration, so that street emissions and dispersion around these urban structures can be simulated (Brandt et al., 2012; Hofman et al., 2014). For this purpose, Computational Fluid Dynamics (CFD) models have been used, given their capability to deal with complex features and accurately evaluate their effects, solving the Navier-Stokes equations over small domains (few hundreds of meters) and in very high resolutions (meters or less) (APPRAISAL, 2013a; Schlünzen et al., 2011; Vardoulakis et al., 2003). The different CFD modelling-based experiments over densely built areas show that the urban geometry results in lower wind speeds leading to a less intense vertical mixing in contrast to suburban or rural areas (Baklanov et al., 2009; Beevers et al., 2012; Borrego et al., 2003; Tang and Wang, 2007; Vardoulakis et al., 2003). On the other hand, these street canyon experiments have also been used for computing UCP which take into account building effects on the local weather (e.g. wind speed, air temperature, turbulence), in order to provide spatially-averaged characteristics for the mesoscale models (Brown, 2000; Masson, 2006; Santiago and Martilli, 2010). Furthermore, in order to keep the numerical stability in the advection scheme, much smaller time steps linearly interpolated from mesoscale outputs and increasing horizontal and vertical resolutions (a few meters by a grid cell) are defined (Joe et al., 2014; Kwak et al., 2015).

For each modelling system, when results from the models combination were compared with the high resolution nested Eulerian CTM results and the available air quality measurements, a better statistical performance was achieved using the cascade of models. The coupling of models over different scales allows accounting for contributions from nearby and distant emission sources to the air quality at a specific location (e.g. in an industrial area, in rural areas or even in a street canyon) (Brandt et al., 2012; Isakov et al., 2009; Kim et al., 2018; Stein et al., 2007). However, the way the atmospheric emissions are included within the system requires particular attention, because the same emission sources may be considered by the different types of models, and adding as a background the modelled concentrations from upper domains could result in double counting the impact of these sources.

2.1.2. Current limitations

As discussed in the previous section, combining air quality results within multiscale models is not straightforward. In general, the inconsistencies found are related with the modelling assumptions and the nature of the available input data.

Mesoscale CTM are particularly useful to simulate chemically reactive species and address their long-range transport (Srivastava and Rao, 2011; Stein et al., 2007), but they fail in the realistic representation of atmospheric flows at lower spatial levels (e.g. city scale). This inaccuracy of the mesoscale modelling results over urban areas is associated with many factors, which should be highlighted:

(i) *No urban parametrization or unsuitability to characterize the three-dimensional (3D) urban structure*

The urban canopy (UC), a region where people live and human activities take place, has been a subject of much investigation (Baklanov et al., 2009; Schlünzen et al., 2011) given its highly complex atmospheric circulations, primarily due to the presence of multiple obstacles strongly modifying the air flows and the thermal land-atmosphere exchanges. In these circumstances, the use of CFD models to evaluate small-scale atmospheric dynamics is recommended; however, the common practice in multiscale modelling is to apply mesoscale models with increased resolution over urban areas without the adequate parametrizations or Gaussian models that despite the new developments to simulate urban areas are still limited (Baklanov and Nuterman, 2009; Thunis et al., 2016). Taking as example the urban canopy model (UCM)-coupled WRF-Chem modelling system, high uncertainties are related to the required urban parameters and selection of

the most representative values, especially due to the limited number of urban land use classes and value projection on a single layer (Kim et al., 2015). Notwithstanding all efforts to decrease the regional-to-urban modelling uncertainties, currently most of the operational mesoscale models do not consider the urban effects.

(ii) Limited grid resolution

Grid models are the best suited tools to deal with regional features. Nevertheless, when the goal is to estimate concentration fields very close to individual sources, the use of regional scale grid-based models is discouraged, since all emissions located within each cell are evenly distributed, not allowing the accurate simulation of the effects of these sources, either in the grid cell itself or in any of the nearby cells (APPRAISAL, 2013a; Stein et al., 2007). Furthermore, due to limitations in the mesoscale formulations, the highest typical grid resolution using these modelling tools (about 1 km²) is inadequate to capture the urban morphology (obstacles) and thermal characteristics inducing dispersion of air flows and pollutants within the UC, primarily close to densely urbanized areas and with many pollution sources (Baklanov and Nuterman, 2009; Kwak et al., 2015; Pay et al., 2014; Talbot et al., 2012; Thunis et al., 2016).

(iii) Local scale impacts on larger domains are often neglected

In air quality modelling, multiscale interactions can be represented through two-way nesting using a single CTM and/or large and small-scale coupled models. However, the coupling of models assumes that only the inner domain outputs resulting from large-scale simulations are passed to microscale models as initial and boundary conditions (i.e. offline coupling). Not considering microscale effects over upper simulation domains can be critical in areas exposed to air mass recirculation (sea breeze cells) or around regions with high pollutant emission gradients (large cities) (Siour et al., 2013).

In turn, at microscale applications to resolve fine-scale pollutant variations, current limitations could be accounted as follows:

(i) Limited pollutant dispersion modelling in the presence of obstacles using Gaussian approaches

As mentioned in Section 2.1.1, Gaussian models are often used to depict the pollutant dispersion around obstacles. However, the Gaussian formulation has been successfully employed in simplified flow configurations (under steady-state conditions) and for flat

and unobstructed landscapes. In the presence of complex surfaces, pattern observed in most cities, the plume dispersion modelling, depending on the urban geometry, turbulence and distance from the pollution sources, results probably in an oversimplification due to the use of empirical input parameters (i.e. all variables are ensemble averaged), and so, the validity of these models needs to be carefully evaluated (APPRAISAL, 2013a; Lateb et al., 2016).

(ii) Lack of proper input data

The use of local-scale atmospheric models is often hampered by a lack of adequate lateral boundary conditions to drive the flow in the finer domain, because, typically, these boundaries are extracted from regional/urban-scale results to produce time-varying local solutions, and they are often skewed due to the local meteorological dynamics, especially on complex terrain (APPRAISAL, 2013a; Borrego et al., 2003; Talbot et al., 2012). The desired resolution of the emission inventory is another concern in microscale air quality applications, since the spatial detail is frequently inadequate to fully characterize individual sources at the street-to-building scales (Likhvar et al., 2015; Thunis et al., 2016).

(iii) Simplified photochemistry

Local-scale dispersion models have been improved to provide a detailed description of the concentration patterns, but they are not properly treating the complex photochemical reactions and their effects, due to the longer reaction time of many chemical species than the travel time across an urban area (Stein et al., 2007). Thus, local-scale models are considering pollutants as passive compounds or are using a simplified chemical kinetic mechanism. This could be considered an advantage because it simplifies the simulation and it is computationally cheap, but it has to be carefully assessed to be sure that important (fast) chemical reactions are represented. For instance, if VOC emissions are larger than NO_x emissions, simplified photochemistry is not a valid approach. Moreover, the dimension of the domain has to be taken into account to understand how far the simplification of the chemistry can go.

The integration of complex chemistry mechanisms at the local scale is an important but also a challenging issue for the air quality modelling community, which must be duly weighed.

(iv) Timeframe analysis of CFD modelling

Analysing the evolution of modelled concentrations using CFD at the local/street level for long time periods is a challenge that still needs to be worked, due to the high complexity of the urban structure and computational requirements for processing information at very fine resolutions. When overcoming this issue, it will be possible to assess the influence of the main emission sources throughout a particular year and to evaluate the seasonality and dispersion and accumulation patterns in a wide range of weather conditions (Thunis et al., 2016).

2.1.3. Guidelines for strengthening the synergy among scales

In view of the current limitations and identified scientific developments in multiscale air quality modelling, additional efforts are needed to reduce uncertainties and differences among modelled atmospheric concentrations by comparing results from different scales and models. In this sense, the following set of guidelines to flexibly integrate regional-to-local-scale models and input data within a single system is proposed:

(i) Linking different types of air quality models

For a reliable representation of multiscale air quality, different types of air quality models need to be carefully coupled within the modelling system, and the relevant variables from the mesoscale (time-dependent boundary and background meteorological and chemical conditions) should be properly assimilated by a microscale model (Brandt et al., 2012; Hofman et al., 2014; Mensink et al., 2003; Oxley et al., 2013). Given the complexity of the involved atmospheric processes in the mixing layer, the option for online mesoscale models may allow a better characterization of the time-resolved dispersion of air pollutants and it has the advantage of integrating meteorology-chemistry feedbacks (Grell et al., 2004). Even the simplest urban canyon model requires a background concentration value as input, to account for the pollutant fraction that is not emitted within the simulated street (Vardoulakis et al., 2003). Obstacle-resolved simulations together with a canopy layer-based mesoscale approach are likely the simplest and the most promising way to include obstacle effects using structured grids in two-way nesting (Schlünzen et al., 2011). Another possibility to design a multiscale modelling system, though more complex to implement but with advantages, at least in terms of computational efficiency, is the integration of a local/microscale model within the mesoscale CTM. Thus, as a starting point for successful multiscale simulations, the urban characteristics should be well indicated, namely the urban canopy structure, shape

of the obstacles (e.g. building blocks and their distribution) and influence of the underlying surface (e.g. orography, land use type, roughness, thermal properties and energy consumption sources) over the urban atmospheric dynamics (Baklanov et al., 2007). At the microscale, using combined plume and box models is feasible to numerically and accurately examine the intraurban spatial variability and dispersion of air flows associated with building geometry and street configuration (Kwak et al., 2015; Mensink et al., 2003; Oxley et al., 2013). When dispersion models are used in a knowledgeable way, they can be very useful to improve the understanding of the physical and chemical processes that govern the transport mediated by the advection scheme and chemical transformation of atmospheric pollutants (Vardoulakis et al., 2003). Hence, to suitably represent atmospheric phenomena at different spatial and temporal scales, the base equations have to be treated and integrated in joint meso-to-microscale modelling approaches, ensuring the consistency of processes, essentially due to the need of time-dependent boundary conditions for various pollutants (Baklanov and Nuterman, 2009; Kwak et al., 2015).

(ii) Detailing emission inventories

Nowadays, emission inventories are recognized as one of the main uncertainty sources in air quality modelling applications. To improve the performance of the air quality models, a detailed knowledge of the pollutants emitted with high spatial and temporal resolutions is required. In the case of multiscale modelling systems, the emission inventory should be prepared to give response at multiple scales and disaggregated in time based on activity profiles by macrosector (Russo et al., 2019). Nevertheless, the dynamical downscaling involving different models should be conducted carefully, because the background conditions used to drive the microscale simulations could result in double counting the impact of emission sources, mainly if local sources are included in mesoscale/urban modelling. In order to accurately assess the impact from local emission sources, two air quality simulations using a multiscale model system could be performed: one for the base case in which local emissions are included in both CTM and small-scale model (double counting) and another simulation in which local emissions are only included in the small-scale model. The absolute difference in the air concentrations between the two simulations provides an indication of the magnitude of these impacts (Isakov et al., 2009). This analysis is very useful for deciding whether local emission sources should be included or not in mesoscale simulations and thus avoiding the double counting issue to use the resulting modelled concentrations as a background of microscale tools.

(iii) Using techniques of data assimilation and inverse modelling

Data assimilation can be a way to improve results from multiscale modelling, and inverse modelling can help in identifying the most relevant emitting sources for the different scales. Data assimilation techniques within atmospheric models employ observations with the purpose of improving air quality estimates, whereas the inverse modelling uses these predictions and measured data to estimate pollutant emissions. Thus, the use of these two types of techniques under the multiscale modelling framework could be an added value. It is not a common practice yet to use these two types of techniques in multiscale modelling; they are used in single-model applications. A step forward would be to assess their application within the entire multiscale modelling system, as a whole. However, a balance between improved results and computational efforts has to be done, as well as the analysis of the scales to be focused.

(iv) Increasing the spatial resolution of mesoscale models

This issue is a priority research area, mainly for multiscale urban air quality assessment, since the high-resolution mesoscale CTM outputs are needed to be compared with finer scale modelling results and measured data, but also to allow an accurate assessment of urban air pollution events. On the other hand, to provide the best air quality estimates, mesoscale models should jointly include local-scale features, long-range transport and photochemical transformations (Isakov et al., 2009; Siour et al., 2013; Stein et al., 2007). One way to increase the spatial resolution of mesoscale CTM (finer than 1 km²) is to use fully embedded large eddy simulation (LES) approaches, which allow the dynamic downscaling for grid resolutions around 200 m².

(v) Applying the modelling system with nesting capabilities

Nested atmospheric simulations arise as an appealing approach to get high-resolution outputs. Most studies involving multiscale modelling systems consider nesting using mesoscale models with a spatial ratio between simulation grids that should not exceed 3–5, since this ratio is primordial to keep the numerical stability, suitable approximation and accuracy of the models (Baklanov and Nuterman, 2009; Gidhagen et al., 2005; Stein et al., 2007; Thunis et al., 2016). The link to the local scale or microscale should be ensured with specific microscale tools (e.g. CFD models), merging the different types of models, preferentially in two-way nesting mode.

(vi) *Evaluating atmospheric feedbacks between simulation domains*

Combining modelled results from the different simulation domains is the most computationally efficient way to provide pollutant concentrations from nearby and distant sources (Isakov et al., 2009). The option for two-way nesting capability is *a priori* recommended, making possible to incorporate the influence of small-scale features on broader domains, as well as assessing the opposite effect (i.e. larger scale to microscale), though it requires more computational power (Brandt et al., 2012; Siour et al., 2013; Soriano et al., 2004). For a comprehensive assessment of air quality problems in a specific area, it is advisable to analyse potential feedbacks from the microscale to larger scale processes and vice-versa. The comparison of overlapping areas will be another test to take into account, in order to avoid mass inconsistency and generation of numerical noise (Baklanov and Nuterman, 2009).

2.2. Health impact pathways related to air quality changes

Health impacts of air pollution have been estimated using information from epidemiological studies and methods that describe how health can be integrated in air quality assessments. This section summarizes some research advances, starting with the exposure assessment and the identification of the main impacts, and then, the recommended methodologies for quantifying physical health impacts and monetary valuation of these damages are succinctly described. Thereafter, an overview of research studies underpinning these methodologies is presented, in particular with respect to the key impact functions and associated external costs, and finally, the inherent uncertainties of health impact assessment are analysed.

2.2.1. Exposure assessment and health risks

Human exposure to air pollution may result in a variety of physical health impacts, depending on the types of air pollutants, atmospheric concentration levels, duration and frequency of exposure, and stratification of the exposed population (e.g., age, current health status) (Baklanov et al., 2007; Burnett et al., 2018; WHO, 2016a). These physical impacts can occur in a short time period after exposure (short-term exposure) and result in acute effects, or are a consequence of the cumulative exposure over time (long-term exposure) resulting in chronic effects. They are often expressed through morbidity and mortality indicators, mostly related with respiratory and cardiovascular diseases. Focusing on these disease groups, the main effects derived from exposure to the most common air pollutants (PM, O₃, NO_x, and sulphur dioxide, SO₂) are reported in Table 2.2.

Table 2.2. Air pollutants and their health effects based on respiratory and cardiovascular diseases (source: EC, 2005; Hurley et al., 2005).

Group of health effects	Specific effect	Air pollutant			
		PM	O ₃	NO _x	SO ₂
Acute and chronic mortality	Reduction in life expectancy	X	X	X	X
Acute effects on morbidity	Asthma episodes		X	X	X
	Respiratory hospital admissions	X	X	X	X
	Cardiac hospital admissions	X		X	X
	Consultations with primary care physicians	X		X	X
	Use of respiratory medication	X	X	X	X
	Use of bronchodilator	X			
	Lower respiratory symptoms	X			
	Restricted activity days	X	X	X	X
Chronic effects on morbidity	Bronchitis	X			
	Cough in children and asthmatics	X			

In general, a reduction in average life expectancy due to short and long-term exposure to the reviewed air pollutants is expected. In order to quantify the magnitude of these effects, many epidemiological studies combining meta-analyses recorded during air pollution episodes have been conducted to provide statistical associations by relating unit changes in ambient concentrations and different types of health outcomes (i.e. specific effect of exposure to air pollutants) (Costa et al., 2014). These concentration-response functions (CRF) are based on relative risk (RR) models that are applied to translate concentration changes into health impacts, and take into account a greater health risk for certain vulnerable groups within a population (e.g. elderly people, children and those with underlying diseases) (Pervin et al., 2008; WHO, 2013b). As result, linear or non-linear CRF, which may or not contain threshold exposure values, have been designed. Nevertheless, the vast majority of the available methodologies assumes that the cause-effect relation is linear, in the form of a Poisson regression, which usually does not reflect the real situation, since there is a threshold exposure value below which the physical impact is no longer felt. Therefore, these approaches are considered more appropriate for situations in which the increase in pollutant levels is marginal and when the supposed linearity is not violated and, hence, the applicability domain (i.e. concentration and exposure range) of the model should

be clearly stated (Marques et al., 2013; Pizzol et al., 2010). On the other hand, due to unavailability/lack of epidemiological studies based on country data, CRF are often taken from international epidemiological studies that are regarded as reference studies by the scientific community. According to these studies, the cause-effect relationship is stronger for PM compared to other air pollutants (EHA, 2006; Pervin et al., 2008) and, thus, their effects are better documented and quantified (e.g. Mechler et al., 2002; R ckerl et al., 2011).

To assess the exposure, defined as the pollutant concentration existing in a person's breathing zone over a specified period of time, the following methods can be used (WHO, 2002):

- exposure monitoring, with the advantage of producing accurate exposure data on individuals in known and real life conditions. However, a personal exposure monitoring programme is normally more laborious and costly, and when selecting the individuals there is a tendency for behavioural changes, thus potentially modifying the exposure;
- exposure modelling has some advantages comparatively to personal monitoring, allowing exposure assessments for past and future periods; its use is recommended for estimating potential long-term effects and for densely populated areas.

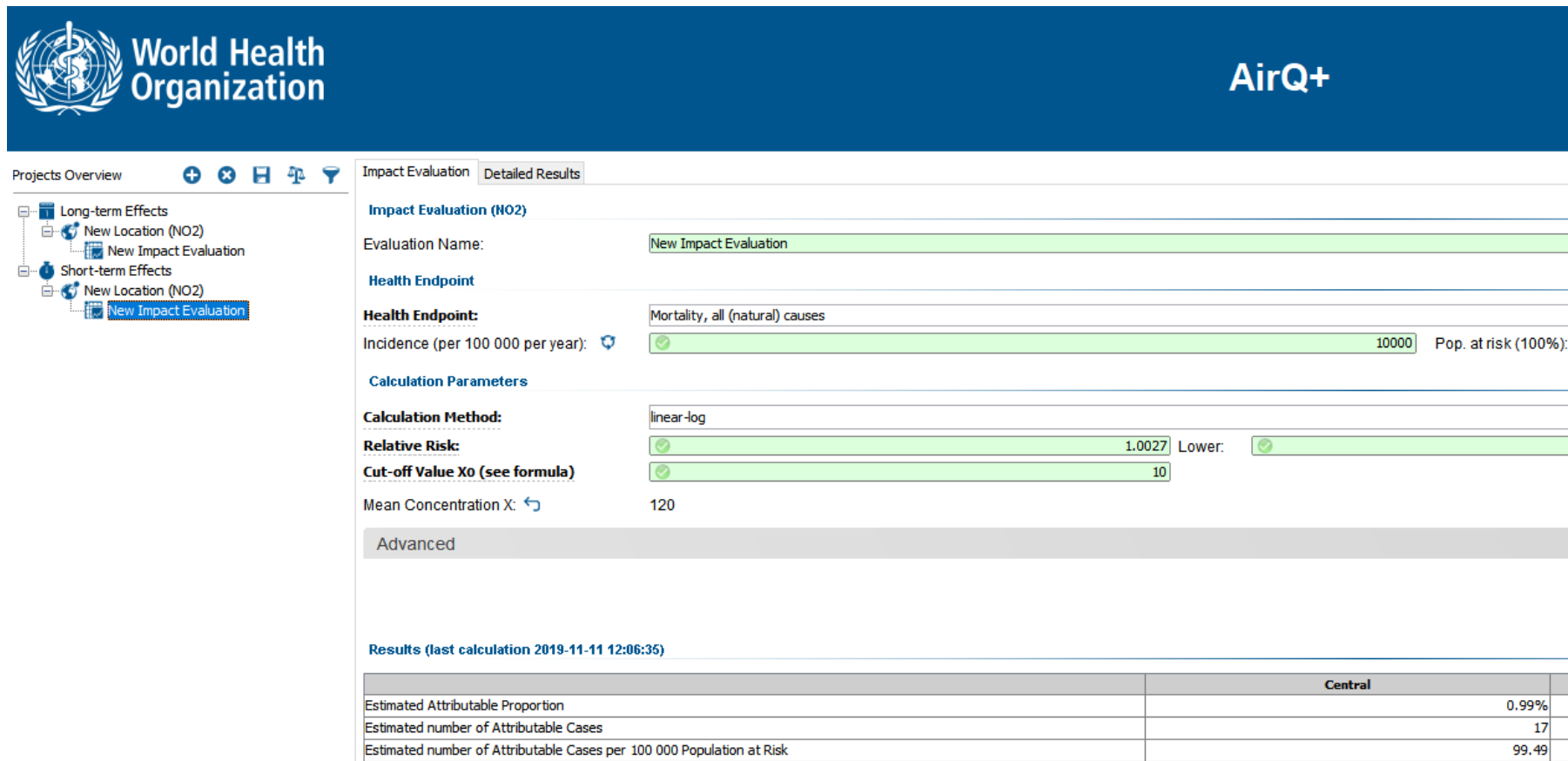
In epidemiological studies, exposure modelling techniques are often applied, since large cohorts and populations of entire cities over long periods of time are needed to design the overall effect of air pollution. However, to support these long-term exposure assessments, adverse health effects due to short-term exposure are usually accounted by the cumulative effect over time, which is expressed through mortality indicators (e.g. years of life lost) and incidence/prevalence of specific chronic diseases (Costa et al., 2014; Seethaler et al., 2003; WHO, 2013c). Short-term exposure studies, that represent only a part of the health problem, are usually focused on exploring the high variability of acute health effects using time-series of hourly and daily changes in pollutant concentration (R ckerl et al., 2011). In addition to the air pollution, seasonal factors, as the time of year and weather conditions, also produce important short-term effects that are more significant during the cold season, thus modifying the relationship between air quality and acute health outcomes (Ostro, 2004; WHO, 2002). In turn, long-term epidemiological evidences assess the increase in mortality risk (age-specific death rates) due to chronic exposure to outdoor air pollutants (H roux et al., 2015; R ckerl et al., 2011; WHO, 2013a).

2.2.2. Quantification of physical health impacts

Despite the widespread consensus that air pollution is a serious concern for the health and welfare of the society, the quantification of its impacts has often been overlooked in modelling studies aimed at assessing air quality improvement strategies (Miranda et al., 2015). This happens because the EU Ambient Air Quality Directive 2008/50/EC establishes ambient air quality standards oriented towards public health protection, but not identifying the need to estimate effects. Nevertheless, health impacts triggered from air pollution are increasingly being addressed and documented due to the joint collaboration of experts in different scientific areas, as air pollution, public health, sociology, economics, among others. Based on the shared knowledge and identification of key aspects aimed at integrating these thematic areas, a set of health impact assessment (HIA) tools have been developed. According to Brenk (2018), who assessed the suitability of these tools for European cities using criteria as their usefulness at city level, the possibility of calculating multiple health effects for different air pollutants as well as adjusting input parameters (e.g. RR, age structure, incidence rate) led to the adoption of two main HIA tools: AirQ+ and GGD. The latter is directed to the Dutch public health services, not being applicable to other European countries. Therefore, the AirQ+ tool, developed by the WHO, is the best option for a comprehensive assessment of health impacts derived from air pollution.

The latest AirQ+ version 1.3 was released in October 2018 and is freely available to download from the WHO website (URL1). The AirQ+ software is designed to calculate the magnitude of health impacts due to short and long-term exposures to outdoor air pollution from several pollutants (PM_{2.5}, PM₁₀, NO₂, O₃ and black carbon) using methodologies and CRF well established by epidemiological studies. Moreover, AirQ+ can also be used to estimate the effects of household air pollution related with solid fuel combustion (indoor air pollution). Notwithstanding its graphical interface (Figure 2.2) intended for any stakeholder who wants to carry out HIA, it is possible to highlight that:

- users have the possibility to use values for a pollutant not included in the AirQ+ database, if RR and other input data are available. In this case, it is highly recommended using results from a meta-analysis rather than from a single local study;
- for each air pollutant and health indicator a separate impact evaluation has to be carried out, implying intensive work to conduct a complete HIA with all the available pollutants and health indicators.



World Health Organization **AirQ+**

Projects Overview + × ⏪ ⏩ 🔍

- Long-term Effects
 - New Location (NO2)
 - New Impact Evaluation
- Short-term Effects
 - New Location (NO2)
 - New Impact Evaluation

Impact Evaluation Detailed Results

Impact Evaluation (NO2)

Evaluation Name:

Health Endpoint

Health Endpoint:

Incidence (per 100 000 per year): Pop. at risk (100%):

Calculation Parameters

Calculation Method:

Relative Risk: Lower:

Cut-off Value X₀ (see formula):

Mean Concentration X:

Advanced

Results (last calculation 2019-11-11 12:06:35)

	Central
Estimated Attributable Proportion	0.99%
Estimated number of Attributable Cases	17
Estimated number of Attributable Cases per 100 000 Population at Risk	99.49

Figure 2.2. Graphical interface of the AirQ+ software.

The impact evaluation can be done through two calculation methods: log-linear and linear-log, that only differ in the adjusted RR function for different air concentrations. The log-linear RR function assumes a linear relationship between concentration and risk (hereinafter referred as linear RR) (Eq. 2.1), whereas the linear-log method uses a RR function in which health risks decrease non-linearly with increasing concentrations (hereinafter referred as non-linear RR) (Eq. 2.2).

$$RR_{(p,i)} = \exp [\beta (X - X_0)] \quad (\text{Eq. 2.1})$$

$$RR_{(p,i)} = \exp [\beta (\ln (X + 1) - \ln (X_0 + 1))] \quad (\text{Eq. 2.2})$$

Where:

$RR_{(p,i)}$ correlates a pollutant p 's concentration variation ($X - X_0$) with the probability of experiencing or avoiding a specific health indicator i ;

β coefficient denotes the change in the RR for unit change in concentration X (expressed as the natural logarithm of RR);

X is the pollutant p 's concentration ($\mu\text{g}\cdot\text{m}^{-3}$): daily values to calculate the short-term exposure risk, or annual averages if long-term RR is required;

X_0 indicates the pollutant p 's cut-off or counterfactual concentration value ($\mu\text{g}\cdot\text{m}^{-3}$) above which health impacts are calculated.

AirQ+ provides default values of RR and X_0 , but they may be adjustable. RR values are often presented with a confidence interval of 95 %, and result from a systematic review done in the scope of the HRAPIE project (WHO, 2013a), which included published epidemiological studies and their meta-analyses. Given the nature and geographic framework of the majority of these studies, the use of these default RR values is essentially recommended for Western Europe and North America regions. Regarding the default counterfactual values, the WHO AQG are suggested since they provide global guidance on thresholds and limits for key air pollutants harmful for the human health.

In order to test the behaviour of these RR methods, the mortality risk (all natural causes) due to the short-term exposure to NO_2 was estimated for a hypothetical case, using the following data: default RR of 1.0027 per $10 \mu\text{g}\cdot\text{m}^{-3}$ change (recommended by WHO, 2013a); daily maximum 1-

hour mean (X) up to $120 \mu\text{g.m}^{-3}$; and the X_0 threshold is set at $10 \mu\text{g.m}^{-3}$ (default value used in URL1). Figure 2.3 shows the estimated RR based on the two methods.

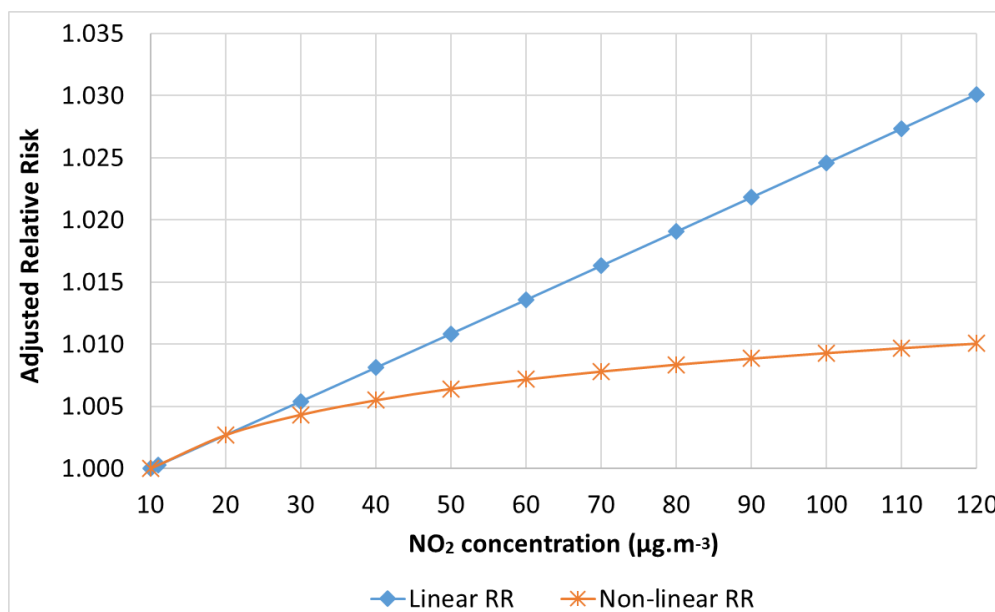


Figure 2.3. Estimated mortality risk due to the short-term NO₂ exposure using the two RR methods (linear RR and non-linear RR).

For lower concentrations (up to $25 \mu\text{g.m}^{-3}$), the trendline of the non-linear RR function shows a trend similar to the linear method. After this value, the logarithmic form considered in non-linear RR leads to a smaller increase of the adjusted RR (i.e. response) in association with NO₂ concentration (i.e. exposure) increases. The option for a non-linear risk model is based on the assumption that a simple linear extrapolation produces large overestimates of burden of disease, mainly when high air concentrations are observed (Burnett et al., 2018; Nasari et al., 2016).

Beyond the adjusted RR calculation, other input parameters, as population data and background incidence/prevalence rate for the chosen morbidity and mortality indicators, are required for impact evaluation using the AirQ+ tool. Thus, the general equation (Eq. 2.3) to estimate physical health impacts from air pollution is described as follows:

$$HI_{(p)} = \sum_{i=1}^n [(pop_{(p,i)} \times Inc_{(i)}) \times RR_{(p,i)}] \quad (\text{Eq. 2.3})$$

Where:

$HI_{(p)}$ represents the number of unfavourable implications (cases of disease, deaths) over all health indicators ($i = 1, \dots, n$) avoided, or not, due to pollutant p 's short and/or long-term exposure;

$pop_{(p,i)}$ is the population at risk (all ages or certain age group) associated to the RR meta-analysis;

$Inc_{(i)}$ corresponds to the baseline incidence/prevalence rate of a specific health indicator i (expressed as the number of new cases per 100000 individuals per year).

The Impact Pathway Approach (IPA), designed within the ExternE (External Costs of Energy) project (EC, 2005), is another health modelling tool that has often been used by the scientific community, at least until the development of the AirQ+ (end of 2016), in order to obtain damage estimates for different impact categories. For quantifying health impacts from air pollution, the IPA uses a similar methodology to the linear RR-based AirQ+ tool, but it does not include the counterfactual value; therefore, any air concentration changes result in health damage estimates.

In addition to the estimate of new cases of disease and deaths attributable to air pollution, other health metrics are also quantified in many HIA studies (e.g. APPRAISAL, 2013b; Costa et al., 2014; Hurley et al., 2005; Likhvar et al., 2015), such as:

- Years of life lost (YLL) in the target population due to changes in mortality risk. YLL can be calculated by multiplying the number of premature deaths with the remaining life expectancy at the age of death, reliably represented through life table methods. This health indicator is also implemented within the AirQ+ software, allowing the user to do life table calculations for assessing the decline in life expectancy, assuming that population and mortality risk rates are known.
- Years lost due to disability (YLD) reflecting the extent of the disability associated to a specific disease. YLD can be estimated by multiplying a disability weight factor, which varies between 0 (perfect health) and 1 (death), with the average duration of the disease.
- Disability-adjusted life years (DALY) provide a relevant measure of the overall disease burden, because it combines both mortality and morbidity. Thereby, DALY are the sum of the YLL with YLD, which account for the number of years lived in less than optimum health.

2.2.3. Economic evaluation

Economic evaluation studies on air pollution-related health impacts aim to raise awareness about the need of improving the air quality, especially in urban areas, providing an important support for the definition of strategic action plans (Silveira et al., 2016). For that purpose, several techniques to estimate the economic costs and benefits that result from air quality changes have been employed (DEFRA, 2019a; Holland et al., 2005). However, it is not a straightforward procedure, since many of the health effects have no market value and, consequently, the monetary valuation is often discarded in HIA studies (Belhaj and Fridell, 2008). These health damage costs arising from air pollution are known as negative externalities, also referred as external costs to repair a given reference situation or avoid welfare losses (van Essen et al., 2011), and are generally quantified through the cost-of-illness (COI) methodology (Eq. 2.4) (Pervin et al., 2008; WHO, 2008). According to this approach, total health costs per case (C_{health}) are determined by the sum of direct (C_{direct}), indirect ($C_{indirect}$) and intangible ($C_{intangible}$) costs.

$$C_{health} = C_{direct} + C_{indirect} + C_{intangible} \quad (\text{Eq. 2.4})$$

Direct costs include both health care and non-health care costs associated with treatment and caring. These costs are based on market values for e.g. medical staff, examinations, laboratory tests, medication, consumables and hospital facilities as well as for caregivers' time, and are estimated using bottom-up or top-down accounting methods (Pervin et al., 2008).

Indirect costs include costs associated with loss of productivity due to morbidity as well as loss of production due to morbidity or mortality. These costs are based on market values for e.g. wages, incomes and earnings, and are estimated using the human capital approach (HCA) or the friction cost approach (FCA) (Hanly et al., 2012; Pervin et al., 2008). The HCA approach assesses an individual's productivity and production losses from health deterioration, based on the time foregone from productive activities over the individual's lifetime and against the relevant wage rate (Tranmer et al., 2005). The FCA approach assesses a firm's productivity and production losses from health deterioration, based on the time needed to restore initial production levels (friction period) and assuming vacancies are filled by unemployed (low opportunity cost) employees (Koopmanschap and van Ineveld, 1992).

Finally, intangible costs include non-market costs associated with pain and suffering. These costs are based on non-market values for pain and suffering from morbidity and mortality, and are estimated using quality-adjusted-life-year (QALY) and willingness-to-pay (WTP) or willingness-to-accept (WTA) approaches (Hammitt, 2005). The QALY approach assesses the change in QALYs, and corresponding monetary values, due to an expected change in health. Estimates are invariably dependent on life expectancy, future health and latency, though rarely dependent on income or risk characteristics. The “willingness-to” approaches assess an individual’s willingness to spend money for an expected health improvement (WTP; compensating variation) or, alternatively, an individual’s willingness to receive money to resign an expected health improvement (WTA; equivalent variation). Estimated values may be a function of income, education and age as well as environmental quality (Hammitt, 2005; Seethaler et al., 2003).

For each health indicator, after identifying the different cost components related with the impacts and determining how to assess them in monetary terms, the overall health damage costs over a given region due to air pollutants exposure are estimated as follows (Eq. 2.5):

$$Costs_{(i,p)} = HI_{(i,p)} \times C_{health} \quad (\text{Eq. 2.5})$$

Where:

$Costs_{(i,p)}$ express the overall damage (€), occurred or avoided, on the health indicator i due to pollutant p ’s short and/or long-term population exposure over a given region;

$HI_{(i,p)}$ represents the number of unfavourable implications associated to the health indicator i , that could be avoided or not, due to pollutant p ’s short and/or long-term population exposure over a given region;

C_{health} is the monetary value (€) to repair a person’s initial health status or, at least, to remediate the damages of air pollution on the health indicator i .

Health impacts (HI) and overall damage costs (Costs) avoided reflect the expected benefit with the implementation of air quality improvement strategies. In this context, since a typical HIA is focused on individual air pollutants, it is necessary to add the impact/benefit from the related health indicators.

2.2.4. Overview of epidemiological and economic studies

This section gathers scientific/technical information on epidemiological evidences and economic evaluation of impacts linking the exposure to the most common air pollutants (PM_{2.5}, PM₁₀, O₃, NO₂ and SO₂) with different health indicators (respiratory and cardiovascular diseases). In each pollutant-effect pair, the following aspects are considered: affected age groups, exposure time, impact functions (as RR) and damage/external costs per unit (as C_{health}) (Table 2.3).

Table 2.3. Epidemiological data and economic evaluation of health effects related to the most common air pollutants (PM_{2.5}, PM₁₀, O₃, NO₂ and SO₂).

Health indicator (pollutant)	Age group	Study design	RR (95% CI) per 1 µg.m ⁻³	Damage cost (prices per unit)		Reference
				€ (base year)	Unit	
Cough (PM _{2.5})	Children		0.22			Hurley et al. (2005)
	Adults		0.28			Hurley et al. (2005)
	Children <16 yr		0.45	59 (2006)	Day	Brandt et al. (2013)
	Adults >15yr		0.28	59 (2006)	Day	Brandt et al. (2013)
Cough (PM ₁₀)	Children		0.13			Hurley et al. (2005)
	Adults		0.17			Hurley et al. (2005)
Cough (O ₃)	Children 5-14 yr		0.093	31 (2002)	Day	Maibach et al. (2008)
Cough	All ages			42 (2000)	Day	Belhaj and Fridell (2008)
Chronic cough (PM _{2.5})	Children	Long-term	3.46E-03			Hurley et al. (2005)
Chronic cough (PM ₁₀)	Children	Long-term	2.07E-03			Hurley et al. (2005)
Chronic cough	Children			240 (2000)	Case	Belhaj and Fridell (2008)
Asthma (PM ₁₀)	Children 5-19 yr	Short-term	0.1028 (0.1006-0.1051)			WHO (2013a)
	Children <15 yr		0.1044 (0.1027-0.1062)			Seethaler (1999)
	Adults ≥15 yr		0.1039 (0.1019-0.1059)			Seethaler (1999)
Asthma (O ₃)	All ages		4.29E-03			Hurley et al. (2005)
Asthma				31	Day	Seethaler et al. (2003)
				85 (2000)	Day	Belhaj and Fridell (2008)
Acute bronchitis (PM ₁₀)	Children	Short-term		131	Day	Seethaler et al. (2003)
Bronchitis (PM ₁₀)	Children <15 yr		0.1306 (0.1135-0.1502)			Seethaler (1999)
	Children 6-18 yr	Long-term	0.108 (0.098-0.119)			WHO (2013a)
Bronchitis (NO ₂)	Children 5-14 yr	Long-term	1.021 (0.99-1.06)			WHO (2013a)
Chronic bronchitis (PM _{2.5})	Adults	Long-term	3.90E-05			Hurley et al. (2005)
	Adults		8.20E-05	52962 (2006)	Case	Brandt et al. (2013)
	Adults		2.45E-05			Hurley et al. (2005)
Chronic bronchitis (PM ₁₀)	Adults >18 yr	Long-term	0.1117 (0.1040-0.1189)			WHO (2013a)
	Adults >25 yr		0.1098 (0.1009-0.1194)			Seethaler (1999)
	Adults >27 yr		2.65E-05	153000 (2002)	Case	Maibach et al. (2008)
Chronic bronchitis incidence				168840 (2000)	Case	Belhaj and Fridell (2008)
				209000	Case	Seethaler et al. (2003)
				190000	Case	Holland et al. (2005)
Congestive heart failure (PM _{2.5})	Over 65		3.09E-05			Hurley et al. (2005)
	Over 65		3.09E-05	16409 (2006)	Case	Brandt et al. (2013)
Congestive heart failure (PM ₁₀)	Over 65		1.85E-05			Hurley et al. (2005)
Congestive heart failure	Over 65			3360 (2000)	Case	Belhaj and Fridell (2008)

Table 2.3. Epidemiological data and economic evaluation of health effects related to the most common air pollutants (PM2.5, PM10, O₃, NO₂ and SO₂) (cont).

Health indicator (pollutant)	Age group	Study design	RR (95% CI) per 1 µg.m ⁻³	Damage cost (prices per unit)		Reference
				€ (base year)	Unit	
Respiratory HA (PM2.5)	All ages	Short-term	3.46E-06	7931 (2006)	Case	Hurley et al. (2005)
	All ages		0.1019 (0.0998-0.1040)			WHO (2013a)
Respiratory HA (PM10)	All ages	Short-term	3.46E-06	1900 (2002)	Case	Brandt et al. (2013)
	All ages		2.07E-06 7.03E-06			Hurley et al. (2005)
	All ages	0.1013 (0.1001-0.1025)	Maibach et al. (2008)			
	All ages	0.08	Seethaler (1999)			
Respiratory HA (O ₃)	Over 65	Short-term	1.25E-05	7931 (2006)	Case	DEFRA (2019b)
	All ages		3.54E-06 0.075 (0.030-0.120)			Maibach et al. (2008)
Respiratory HA (NO ₂)	All ages	Short-term (day mean)	0.1018 (0.1012-0.1024)	4400 (2000)	Case	WHO (2013a)
	All ages	Short-term (day max)	0.1002 (0.0999-0.1004)			WHO (2013a)
	All ages	Short-term	0.05			DEFRA (2019b)
Respiratory HA (SO ₂)	All ages	Short-term	2.04E-06	7931 (2006)	Case	Hurley et al. (2005)
	All ages		0.05			Brandt et al. (2013)
Respiratory HA	All ages			4400 (2000)	Case	DEFRA (2019b)
Cardiovascular HA (PM2.5)	All ages	Short-term	0.1009 (0.1002-0.1017)	1900 (2002)	Case	Belhaj and Fridell (2008)
	All ages		4.34E-06			WHO (2013a)
Cardiovascular HA (PM10)	All ages	Short-term	0.1013 (0.1007-0.1019)	1900 (2002)	Case	Maibach et al. (2008)
	All ages		0.08			Seethaler (1999)
	All ages	0.06 (0.03-0.09)	DEFRA (2019b)			
	All ages	0.09 (0.04-0.15)	Hurley et al. (2005)			
Cardiovascular HA (O ₃)		Short-term	0.011 (-0.006-0.027)			Ballester et al. (2006)
Lung cancer (PM2.5)		Short-term	0.113 (0.104-0.122)	21152 (2006)	YLL	Mechler et al. (2002)
			1.26E-05			Brandt et al. (2013)
Respiratory mortality (PM10)	All ages	Short-term	0.1013 (0.1005-0.1020)			WHO (2008)
Respiratory mortality (O ₃)	Adults >30 yr	Short-term	0.1014 (0.1005-0.1024)			WHO (2013a)
Cardiopulmonary mortality (PM2.5)	Adults >30 yr	Long-term	0.108 (0.102-0.114)			Mechler et al. (2002); WHO (2008)
Cardiovascular mortality (PM10)	All ages	Short-term	0.1009 (0.1005-0.1013)			WHO (2008)
Acute mortality (PM2.5)			0.068			Hurley et al. (2005)
Acute mortality (PM10)			0.040			Hurley et al. (2005)
Acute mortality (O ₃)	All ages		0.059 0.03	60500 (2002)	YLL	Hurley et al. (2005) Maibach et al. (2008)
Acute mortality (SO ₂)			0.072			Hurley et al. (2005)
Acute mortality				25800 (2017)	YLL	DEFRA (2019b)
Chronic mortality (PM2.5)	Adults >30 yr		1.138E-03 0.6 (0.4-0.8)	77199 (2006)	YLL	Brandt et al. (2013)
	All ages		4.00E-04	49900 (2017)	YLL	DEFRA (2019b)
				40300 (2002)	YLL	Maibach et al. (2008)

Table 2.3. Epidemiological data and economic evaluation of health effects related to the most common air pollutants (PM2.5, PM10, O₃, NO₂ and SO₂) (cont).

Health indicator (pollutant)	Age group	Study design	RR (95% CI) per 1 µg.m ⁻³	Damage cost (prices per unit)		Reference
				€ (base year)	Unit	
Total mortality - All causes (PM2.5)	Age >9 months		6.68E-06			Brandt et al. (2013)
	Adults >30 yr	Long-term	0.106 (0.102-0.110)	63447	YLL	Mechler et al. (2002); WHO (2008)
	Adults >30 yr	Long-term	0.1062 (0.1040-0.1083)			WHO (2013a)
Total mortality - All causes (PM10)	Age <1 yr	Long-term	0.104 (0.102-0.107)			WHO (2013a, 2008)
	Adults >30 yr		0.1043 (0.1026-0.1061)	63447	YLL	Seethaler (1999); WHO (2008)
	All ages	Short-term	0.1006 (0.1004-0.1008)	63447	YLL	WHO (2008)
	All ages	Short-term	0.1012 (0.1005-0.1020)			WHO (2013a)
Total mortality - All causes (O ₃)		Short-term	0.034 (0.012-0.056)			DEFRA (2019b)
Total mortality - All causes (NO ₂)	All ages	Short-term (day max)	0.1003 (0.1002-0.1004)			WHO (2013a)
	All ages	Long-term	0.1055 (0.1031-0.1080)			WHO (2013a)
		Long-term	0.09 (0.06-0.13)			DEFRA (2019b)
Total mortality - All causes (SO ₂)		Short-term	0.06			DEFRA (2019b)

Notes:

- RR is the relative risk per person and per 1 µg.m⁻³ change in pollutant concentration;
- Brandt et al. (2013), Hurley et al. (2005) and Maibach et al. (2008) used RR functions derived from the ExternE project (baseline annual rate included in RR);
- For long-term studies annual mean concentrations are used, whereas short-term pollutant exposure is designed from daily average or maximum values;
- HA - Hospital admissions; YLL - Years of life lost.

As shown in Table 2.3 and mentioned in Section 2.2.1, statistical associations between PM concentrations and health effects have been most extensively investigated.

For certain health indicators the pollutant effect on a given age group reveals considerable variation in terms of CRF (i.e. relative risk) and damage costs, which can be explained by the differing methodologies, the geographical coverage and socio-economic conditions across studies. The research studies reported in Table 2.3 are designed for Europe as a whole (e.g. Brandt et al., 2013; WHO, 2013a), while some studies are country specific (e.g. DEFRA, 2019b; Seethaler, 1999).

The variability in CRF may be associated with several factors, namely the population structure (density, affected age groups and their distribution), source of data gathering, and unavailability or improper format of routinely gathered health indicator data for use in economic evaluations. In addition, the inclusion/exclusion of threshold exposure values as well as cumulative effects over time have contributed to the variation in derived risk functions (Hurley et al., 2005).

The variability in external cost estimates is particularly large when these build on WTP studies. WTP studies are based on interviews in which personal interpretation of the questions as well as strategic behaviour by respondents can lead to biased outcomes (Pervin et al., 2008). Furthermore, these values might also depend on additional variables, such as income and age and, probably, differ between health effects. The WTP approach has the advantage of acquiring the full range of personal costs associated with the disease (Pervin et al., 2008), thereby noting that many of those costs have no market value (Belhaj and Fridell, 2008). As a consequence, several health effects due to air pollution are often neglected and, hence, results are probably an underestimation of the total health costs (WHO, 2008).

2.2.5. Uncertainties in health impact assessment

In HIA, the uncertainty analysis should be performed in all stages, from air pollution exposure assessment to quantification of physical health impacts and corresponding external costs. Uncertainties are often based on 95% confidence intervals (CI) around the mean to provide an estimate of the precision of the HIA outcomes, and result from a simplification or shortcomings of the methodologies used and assumptions for obtaining the input data.

Regarding the exposure assessment, the major uncertainty sources are related with the choice of the air pollutants, their measured and/or modelled concentrations over a given region, and estimated number of people exposed. Usually only a few pollutants are considered in HIA instead of the entire mixture of air pollutants, and it is very likely that this approach does not reflect the real exposure and subsequent health impacts, but it is currently the most acceptable, since the importance of any individual pollutant for the overall mixture is unclear (DEFRA, 2019b; Ostro, 2004). Furthermore, the extent of the effects of some pollutants or any combination of different pollutants on human health is not always known, mainly due to the lack of epidemiological evidences (i.e. CRF). Even when there is a reasonable association between a specific type of exposure and a health effect, some doubts about the causality and impact of time lags might still exist (WHO, 2008). From the point of view of the concentration-exposure relationship, large uncertainties are associated to the modelling, representativeness of measurements and assumptions to link them. Thus, when using air quality modelling results to derive exposure, it is not certain that the estimated exposure coincides with the observed ambient concentrations in a given location (DEFRA, 2019b). In terms of spatial representativeness, HIA assumes that either individual exposure measurements or population-weighted average exposure estimates are

representative of the population exposed over a particular area. Even if the population exposure is well estimated, individual exposures can vary substantially, as a result of spatial differences in air concentrations, and due to the individuals' activity patterns (WHO, 2016b). As a consequence, an alleged low correlation between personal exposure and ambient concentration contributes to weakening the power of epidemiological studies to detect effects.

Moving from exposure to the quantification of potential health impacts, uncertainties about the number of deaths or cases of disease may be found for a variety of reasons:

- the use of different methodologies to calculate the value of health impacts could result in very significant variations, even if the equations are based on the same input data sets (e.g. AirQ+ methods);
- possible double counting of health effects from several air pollutants, since one health outcome may be captured from different pollutants, or the same effect may be added from two health indicators (e.g. mortality due to a specific cause is a part of all-cause mortality) (Héroux et al., 2015; WHO, 2016b);
- the choice of CRF derived from epidemiological studies inevitably introduces some uncertainty into the results, given the random effects and high variability in the CRF estimates. Moreover, epidemiological experiments on air pollution are often designed using an exposure threshold, and are scarce or absent in many regions around the world, limiting their reliability and applicability to these exposure ranges and countries where cohort studies were undertaken. It should be noted that most epidemiological studies have been conducted in developed countries, and the range of studied exposures does not necessarily represent what is observed worldwide (Héroux et al., 2015; Ostro, 2004; WHO, 2016b);
- baseline incidence and prevalence rates for health indicators of interest may also be highly uncertain with regard to the impact of ambient air pollution. These baseline rates are usually expressed as national statistics, available for most countries through the following online platforms: Global Health Observatory data repository (URL2) and European Health for All database (URL3). In the case of mortality rate, the number of premature deaths per a specific cause (e.g. ischaemic heart disease) is estimated from the joint effect of ambient and household air pollution. However, for calculating health impacts, this air pollution-related mortality rate should not be combined with CRF linking mortality to all natural causes, unless other environmental risk factors (e.g. climate change, contaminated water, waste disposal) are added to the mortality rate. In turn, largest uncertainties are associated to morbidity indicators, because the national health

outcomes may come from certain risk factors, not specifying the contribution from the air pollution;

- the introduction of a counterfactual level of air pollution, assuming no health impacts below that reference exposure value, raises some doubts about the theoretical minimum concentration that results in minimum population risk. This uncertainty degree becomes more noticeable when different air pollution management policies are tested in order to quantify air quality and health benefits (WHO, 2016a).

As a last step for analysing uncertainties in HIA, comes the economic evaluation of health impacts, which represents the overall estimate of effects, aggregated and converted to monetary values based on the pollutant-health outcome pairs (Héroux et al., 2015; Holland et al., 2005). In most economic studies (as mentioned in the previous section), the total health costs were probably underestimated for two main reasons:

- several known health effects related with a specific pollutant are often neglected, due to the lack of epidemiological evidences (i.e. CRF);
- certain damage costs, namely intangible costs, have not been quantified, or their evaluation is clearly biased. Within this cost component, the QALY and WTP values vary greatly and are sensitive to how the studies are conducted, usually through personal interviews reporting the individual's willingness to spend money aiming an expected health improvement, or to avoid a particular health risk. Moreover, these values might depend on additional variables, as income and age, and probably differ between health effects (WHO, 2008).

2.3. Summary

The review and analysis of multiscale air quality and health modelling state-of-the-art allowed to evaluate the current scientific developments, to identify the strengths and weaknesses in these research areas, and to define a set of guidelines with practices to overcome some existing methodological limitations. Moreover, this literature review and the guidelines were determinant to give response to the research question 1, aimed to select the most appropriate methodologies and modelling tools to be used in designing the multiscale modelling system, and to better understand how to integrate them into a single system. Thus, for the development of the integrated multiscale modelling system, the following aspects were taken into account:

- *Air quality modelling*
 - (i) to carefully couple different types of air quality models to cover multiple spatial scales and resolutions. Background and boundary meteorological and chemical conditions extracted from an urban scale simulation should be properly assimilated by the local scale model;
 - (ii) to model regional and urban air quality, the option for an online mesoscale model is recommended, because it has the advantage of integrating meteorology-chemistry feedbacks, allowing a better characterization of the time-resolved atmospheric processes and dispersion of air pollutants within the atmospheric boundary layer;
 - (iii) the link to the local scale should be done with a CFD model, in order to accurately reproduce the spatial variability and pollutant dispersion around the urban structure (e.g. buildings);
 - (iv) to apply the modelling system, starting with the mesoscale model in two-way nesting (3-5 ratio) and increasing resolutions (up to 1 km² or less), in order to provide high-resolution outputs to be used by the local scale model;

- *Health impacts modelling*
 - (v) to assess the human exposure to air pollutants at urban scales or in densely populated areas, it is recommended the use of modelling techniques for estimating potential short and long-term effects;
 - (vi) to quantify the resulting physical health impacts (number of cases or YLL), the linear and non-linear RR methodologies integrating the AirQ+ tool developed by the WHO, are the most suitable at the city level, and might be applicable to a wide range of environmental conditions;
 - (vii) finally, to evaluate the health damage costs, national statistics or comprehensive economic evaluation studies including WTP should be preferentially used.

Chapter 3

Development of an integrated multiscale modelling system

3.1. Architecture of the modair4health system

3.2. Air quality modelling

3.2.1. WRF-Chem description and input data processing

3.2.2. VADIS description and input data processing

3.3. Health impacts modelling

3.4. Operationalizing the modair4health system

3.5. Summary

3. DEVELOPMENT OF AN INTEGRATED MULTISCALE MODELLING SYSTEM

According to the objectives of the thesis, the design of a multiscale modelling system that combines both components, air quality and health, is undoubtedly the biggest proposed challenge.

The conceptual framework of the developed system, called modair4health - multiscale air quality and health risk modelling, is described as follows. Section 3.1 presents the general structure of the modair4health system, in relation to the used air quality and health models and links among them, and to the required input data and key simulation outputs, which are also used to feed the chain of models. A detailed description about these models and input data processing is provided in Sections 3.2 and 3.3, for air quality and health impacts, respectively. After the methodological consolidation and definition of the information flow, the modair4health system was linked and operationalized for research and end-user purposes (Section 3.4).

3.1. Architecture of the modair4health system

The core of the multiscale modelling system is composed by two air quality models able to simulate atmospheric concentrations from regional/urban scales (WRF-Chem) to the local scale (VADIS), and a health module for estimating health impacts and damage costs caused by short and long-term human exposure to air pollutants (Figure 3.1).

For air quality modelling from regional to urban scales, the Weather Research and Forecasting model with Chemistry (WRF-Chem) was chosen, because it is an online model that takes into account meteorology-chemistry feedbacks, but also due its performance, since it employs appropriate parametrizations for simulating air quality and meteorological fields at urban scale. As main inputs to run the WRF-Chem, static data characterizing the surface (e.g. land cover, topography), reanalysis data of weather observations, chemical boundary conditions from global CTM and atmospheric emissions, are needed.

The link with the local scale air quality modelling was carried out through the CFD model VADIS (pollutant DISpersion in the atmosphere under VAriable wind conditions), taking advantage of its numerical prediction capabilities and using much higher spatial resolutions to capture the large heterogeneity near the surface, with respect to the dispersion of turbulent flows and air concentrations in small simulation domains (building scale). To that end, initial meteorological conditions extracted from the higher resolution WRF-Chem results are used as input to the CFD model, namely air temperature and winds fields

(direction and wind speed) at a reference height. Besides this information source, elements describing the urban structure (buildings volumetry and streets configuration) and local emissions (point and/or line sources) are also required. As a last step of the multiscale air quality modelling, WRF-Chem urban background concentrations are added to the VADIS air quality estimates to account for the pollutant fraction that is not generated within the local simulation domain. Both air quality models are configured to produce hourly resolution outputs.

Finally, the resulting air quality assessment is then integrated in a health module, based on the AirQ+ methodologies, in order to estimate long and/or short-term health impacts and underlying damage costs associated to each pollutant-health outcome pair. In addition to the estimated ambient air concentrations and reference exposure value (i.e. counterfactual concentration level), other variables for quantifying physical health impacts and corresponding costs are needed:

- population size and its distribution by age groups (provided from country's population census);
- baseline mortality and disease incidence rates (usually derived from country statistics);
- impact functions expressed as RR for experiencing or avoiding a specific health indicator (derived from epidemiological studies);
- and monetary valuation of the health impacts, individually translated in damage costs per case/day over a health indicator (preferentially, should include all cost components: direct, indirect and intangible costs).

More details about the adopted models, recommended configurations, input data processing, and linking as a whole are presented in the following sections.

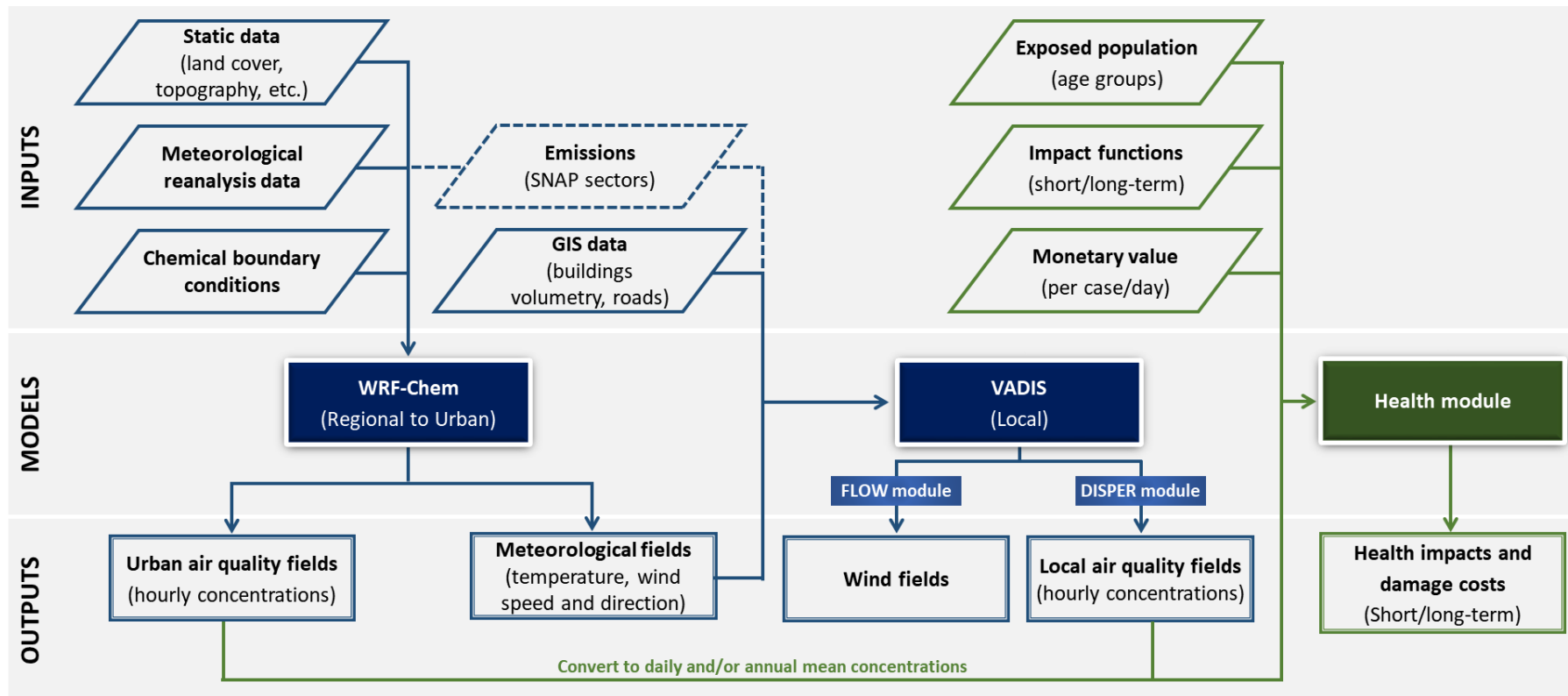


Figure 3.1. Flowchart of the modair4health system.

3.2. Air quality modelling

From the point of view of the multiscale air quality modelling, the selection and setup of the models to be integrated into the system was duly weighted, either through the critical analysis of the state-of-the-art, as well as through the performance evaluation of modelling tests aimed at finding the best parametrizations and input datasets.

In Sections 3.2.1 and 3.2.2, a description of the selected models, WRF-Chem and VADIS respectively, main inputs required and methods and modelling tools used for processing data, is provided.

3.2.1. WRF-Chem description and input data processing

WRF-Chem is an online model, developed and periodically updated by the NOAA's Earth System Research Laboratory (NOAA/ESRL) in collaboration with other research groups, with a chemistry module completely embedded within the Weather Research and Forecasting (WRF) model. This online coupling allows the simultaneous calculation and consequent feedback between meteorological and chemical variables, sharing the same simulation grids (i.e. horizontal and vertical levels), physical parametrizations, transport schemes and vertical mixing (Fast et al., 2006; Grell et al., 2005).

The WRF-Chem enables a variety of chemical and physical-dynamical parameterizations. Physical options include, for example, different schemes of microphysics, radiation, cumulus, and land surface and planetary boundary-layer representations. With regard to chemical options, the model allows several configurations for integrating anthropogenic and biogenic emissions, and includes a set of gas-phase chemical mechanisms (e.g. RADM2, RACM, CBM-Z) and aerosol schemes (e.g. MADE/SORGAM, MOSAIC, GOCART), which can be combined using different photolysis options. The aerosol interaction with the atmospheric radiation, photolysis and microphysics routines can be tested through aerosol direct or indirect effects. In terms of application scale, the model is suitable for simulations from mesoscale to urban environment.

Structurally, the WRF-Chem software consists of two major components: WRF Preprocessing System (WPS) and WRF solver including chemistry (WRF). The WPS aims to prepare some inputs (static and meteorological reanalysis data) for initializing the WRF, and is composed by three executable programs: geogrid, ungrib and metgrid. Geogrid defines the projection, geographic location and dimension of the simulation domains and, horizontally interpolates static terrestrial data. Ungrib uses meteorological fields (i.e. surface and pressure levels in GRIB file format) extracted from global atmospheric reanalyses. To complete the WPS, metgrid gathers the outputs from the previous programs and

horizontally interpolates the meteorological fields for the simulation grids. Data required for these programs (inputs and parametrizations) should be previously edited in the “namelist.wps” file and, after that, the programs could be run following the order above. The resulting metgrid files and vegetation data used for online calculation of biogenic emissions are then integrated as an input for the real program inside the WRF component, that along with chemical boundary conditions provide initialization fields for running the WRF-Chem (i.e. wrf program). In addition to these initialization data, anthropogenic emissions disaggregated in space and time are also used and, as main results of the model, meteorological and chemical fields are generated (Figure 3.2).

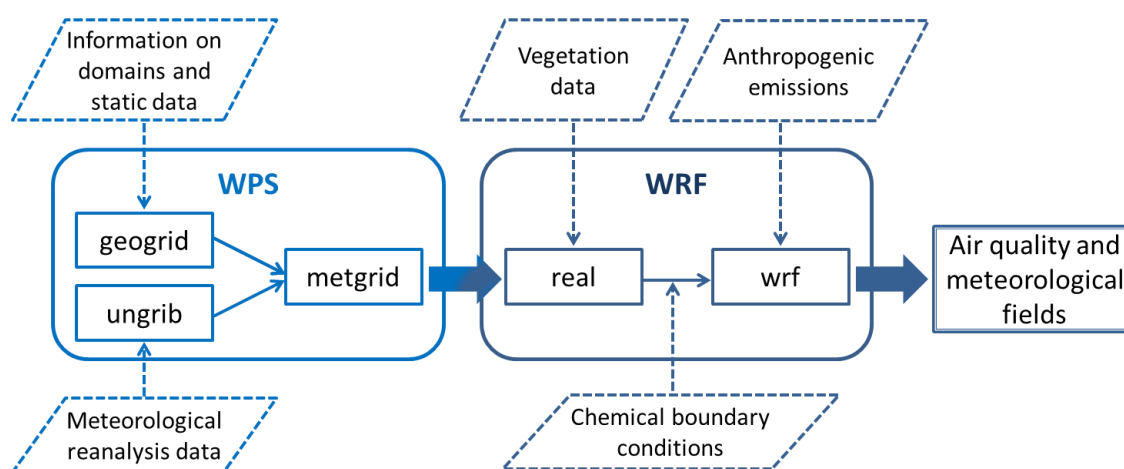


Figure 3.2. General structure of the WRF-Chem model.

A more detailed description of the WRF-Chem model can be found in Grell et al. (2005), and its application can be guided through tutorial exercises available online.

For processing the main input data in the format required by the WRF-Chem, the following methodologies and tools were used:

- **Static data**

Within this category, a set of physical and vegetation parameters that characterize the Earth’s surface dynamics are included, as topography, land cover, soil type and erodibility, vegetation fraction, albedo, etc. These static fields can be downloaded from the DTCenter website (URL4), and they are ready to be used into the geogrid program. Nevertheless, if more detailed and recent information is available, efforts to prepare these data to the geogrid binary format are recommended. In that sense, after a preliminary analysis of the role, magnitude and spatial distribution of available parameters ready for the geogrid and

their comparison to existing databases, it was decided to improve the land cover (LC) classification to be inputted to the WRF-Chem model.

LC is as a prevailing driver of important interactions (i.e physical and chemical processes) within the atmospheric boundary layer, directly influencing the Earth's energy budget, and emission and deposition rates of air pollutants (Jiménez-Esteve et al., 2018; Wu et al., 2012; Xu et al., 2016).

The analysis of the 24-classes of the United States Geological Survey (USGS) database provided with the WRF-Chem package against high accuracy and validated LC maps, based on the Corine land Cover (CLC) dataset for Europe, which contains 44 classes created from visual interpretation of 2012 satellite images with a 100 m positional accuracy, and more detailed and specific LC data for Portugal (hereinafter referred as COS2010) (DGT, 2017), indicated that the USGS LC does not reproduce with enough detail needed LC information (Figure 3.3a). Therefore, a new LC classification combining CLC and COS2010 data was developed, allowing to get a better representation of reality (Figure 3.3b). In a first step, these LC databases were integrated in Geographic Information Systems (GIS), using the ArcGIS software, and reclassified according to the new 33-classes USGS nomenclature following the Pineda et al (2004) suggestions (Appendix A). In this LC reclassification process, the inclusion of three different urban classes should be highlighted: low-intensity residential (class 31), high-intensity residential (class 32) and industrial or commercial (class 33). Then, the resulting LC was processed with COS2010-based 100 m² resolution for Portugal and CLC-based 5 km² resolution over Europe in order to be assimilated by the WPS geogrid program. However, it should be noted that the spatial interpolation from very fine resolution data to coarse grid cells leads to considerable losses of detail, not taking the best advantage of the relevance of these inputs. Ideally, the LC database and the simulation grid spacing should have the same resolution. This advice is particularly useful for studies over urban areas, where adjusted urban parametrizations and higher input and output resolutions are essential to improve the modelling performance.

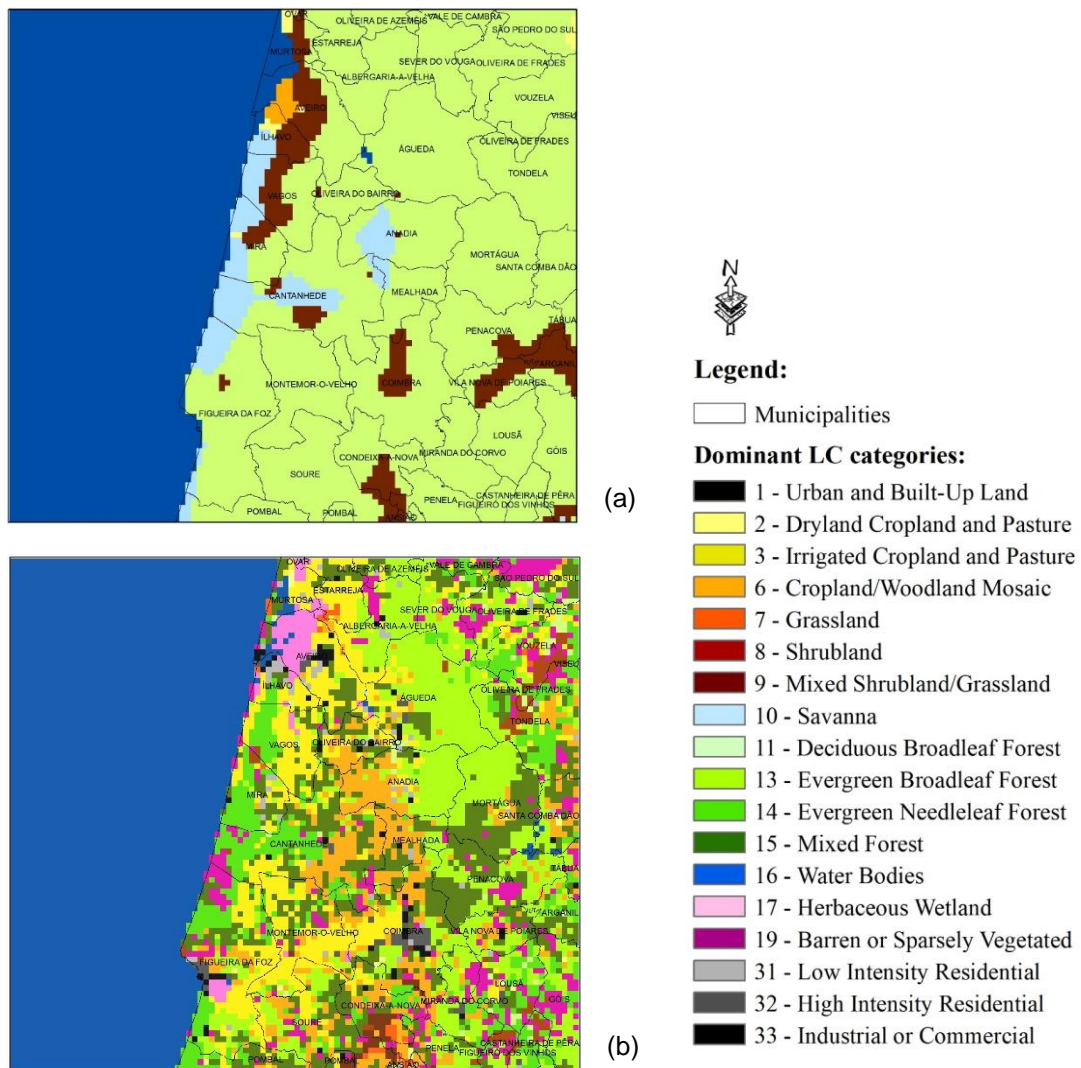


Figure 3.3. Dominant LC categories mapped for a regional domain coverage over central Portugal, resulting from interpolation onto a 1 km² resolution grid based on: (a) default USGS LC; and (b) new LC classification.

- Meteorological reanalysis data

Meteorological reanalyses are conducted from data assimilation systems, using observations for model initialization and to recreate the lateral boundary conditions. To run the WRF-Chem, ERA-Interim’s global reanalysis data, provided by the European Centre for Medium-Range Weather Forecasts (ECMWF) at 6-hour intervals for surface and pressure levels, were used. These datasets can be collected from the ECMWF website (URL5) and are available from 1979 until nowadays, with a spatial resolution of approximately 80 km² and 60 vertical levels from the surface up to 0.1 hPa. For each

simulation domain, the required fields are regridded and prepared as meteorological variables applying the WPS ungrib program.

- **Chemical boundary conditions**

Chemical lateral boundary conditions are needed to account for the influence of the transboundary transport of air pollutants, and are particularly relevant for predicting longer-lived species, as O₃ and carbon monoxide (Pendlebury et al., 2018; Tang et al., 2007). These time-variant chemical conditions were extracted from the global Model for OZone And Related chemical Tracers (MOZART-4/GEOS-5) considering updated data every 6 hours with 1.9° x 2.5° horizontal resolution and 56 vertical levels. The integration of these boundaries into the coarser WRF-Chem domain is performed after running the real program, using the preprocessing tool mozbc (URL6) to design these chemical variables over the resulting real outputs.

- **Emission data from anthropogenic and natural sources**

Anthropogenic emissions from the European Monitoring and Evaluation Programme (EMEP) database with a 0.1° x 0.1° horizontal resolution were used (URL7). This annual emission inventory (EI) is available by Gridding Nomenclature For Reporting (GNFR) including estimated emissions of classic air pollutants (e.g. PM₁₀, NO_x, NMVOC), heavy metals and persistent organic pollutants for key activity sectors (e.g. road transport, industry). The spatial allocation for the simulation grids based on the LC, vertical distribution and application of default time profiles by activity sector considering the seasonality, day of week and daily cycle, as well as speciation and aggregation of emissions into WRF-Chem species, are performed using the emissions interface (called EMIWRF) built by Tuccella et al. (2012).

In turn, biogenic, sea-salt and dust emissions are calculated online by activating WRF-Chem-coupled specific modules and preprocessing tools that create initialization fields. For computing biogenic emissions, the Model of Gases and Aerosols from Nature (MEGAN – version 2.04) is initialized with monthly leaf area index data, fraction by plant functional type and emission factors previously prepared from the bio_emiss utility (URL6). Further information about this MEGAN model version is provided by Guenther et al. (2006).

3.2.2. VADIS description and input data processing

VADIS is a CFD model developed in 1998 at the Department of Environment and Planning of the University of Aveiro, which has been updated and, recently, copyrighted and registered as a trademark under the class 9 of the Nice classification, including instruments for research purposes, technologic and audiovisual equipment, among other goods/services. The latest model version is designed for 3D microscale numerical simulations of flow and dispersion of urban air pollution due to point and line (road traffic) emission sources in urban built-up areas. Its capacity to support multiple obstacles, and flow fields and traffic emissions that vary in time, allows to more realistically evaluate the maximum short-term local concentrations over complex urban geometries, especially with low wind speed conditions (Borrego et al., 2003).

The model is structured in two main programs: the FLOW, which is based on an Eulerian approximation for solving the Navier-Stokes equations at the atmospheric boundary layer (i.e. urban canopy) and; the DISPER, which is based on the lagrangian calculation of the trajectory of particles. FLOW is a Reynolds Averaged Navier-Stokes (RANS) prognostic model with a standard $k-\epsilon$ turbulence closure that calculates wind components, turbulent viscosity, pressure, turbulence kinetic energy and temperature, taking into account a set of obstacles located over a 3D Cartesian grid. The DISPER module uses the 3D atmospheric flow estimated by FLOW to calculate 3D concentrations of inert pollutants following a typical lagrangian approach. This methodology assumes that the pollutant spatial and temporal dispersion is conveniently represented by the trajectory of a large number of particles randomly released in the flow. The numerical separation between flow estimates and pollutant dispersion modelling can be seen as a major advantage compared to other CFD models (e.g. ANSYS Fluent), which solve the advection-diffusion equation coupled with the Navier-Stokes equations (Vardoulakis et al., 2003). Thus, it is possible to obtain a flows database for a particular urban area, which will be available, at any time, for estimating the pollutants dispersion with a lower processing time. The numerical principles of the VADIS CFD model are described by Borrego et al. (2003). Figure 3.4 shows how these programs are related, and what input data are needed for running the VADIS modelling system.

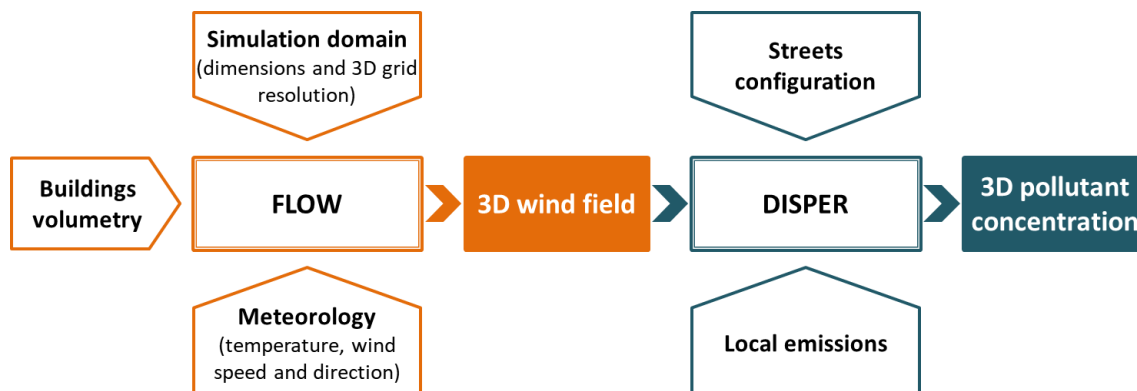


Figure 3.4. General structure of the VADIS model.

The main input data could be grouped into three types: (i) geographic features that portray the urban area of interest, starting by defining the simulation domain and, thereafter, the buildings volumetry and streets configuration with known emission rates; (ii) meteorological conditions, including air temperature and wind speed and direction at a specific reference height, used for initializing the FLOW module; and (iii) local emissions from point and/or line sources required to run the DISPER module. For processing this information according to the VADIS requirements, the following methodologies and tools were used:

- **Geographic features**

The preparation of the geographic data, from its spatial representation to the format required for the VADIS simulations, is performed in two steps. Firstly, once defined the simulation domain (i.e. case study), the buildings and streets inside that area should be drawn in parallelepiped sections using a GIS software. For the buildings, average heights also need to be provided. After this stage, the resulting geographic information, namely the coordinates of the vertices of each polygon and buildings height, are introduced into a VADIS preprocessing tool, which designs these data, aligned or in angle, under a structured mesh.

- **Meteorological conditions**

Meteorological variables to feed the FLOW can be obtained from measurements or using modelled data. In the scope of the modair4health system, it was decided to use meteorological fields extracted from the WRF-Chem simulations, considering modelled results over the inner domain.

- **Local emissions**

For quantifying the pollutants dispersion over the simulation domain, local road traffic emissions estimated by the TRansport Emission Model for line sources (TREM) are used. TREM was also developed at the Department of Environment and Planning of the University of Aveiro, with the main objective of obtaining high spatial-temporal resolution traffic emission estimates based on available traffic counts and fleet composition statistical data, in order to be used in air quality modelling. Thereby, streets are considered as line sources and traffic emissions are calculated for each road segment taking into account detailed traffic counts and vehicle fleet data. Basically, the total emission of the pollutant p (E_p) for each road segment is estimated as follows (Borrego et al., 2003):

$$E_p = \sum i [e_{pi}(v) \times N_i] \times L \quad (\text{Eq. 3.1})$$

Where:

$e_{pi}(v)$ is the emission factor for the pollutant p and vehicle category i as a function of the average speed, engine capacity, vehicle mass and emission reduction technology (v);

N_i is the number of vehicles of the category i ;

L is the road segment length.

Fleet composition data and emission factors are extracted from the COPERT 2014 database for Portugal (URL8). Among these data, the distribution of the number of vehicles by category is treated in smaller territorial units. This information is available for each district on the *Associação Automóvel de Portugal* website (URL9), and it is disaggregated to the municipality level using the municipality-district ratio in terms of number of inhabitants (URL10). Regarding the traffic counts, Open Transport Map data (URL11) based on traffic volume estimates in national highways are used and interpolated to other main roads.

3.3. Health impacts modelling

Incorporating health impact modelling tools into the system is useful for assessing physical and economic health damages due to air quality changes, but also provides an important support to stakeholders and decision-makers when defining air pollution control policies at different scales. To quantify the extent of these health impacts over a particular urban area, pollutant-health outcome pairs are evaluated. Figure 3.5 shows the different steps involving

a classic HIA scheme, as well as the methodologies adopted and input data required to run the health module.

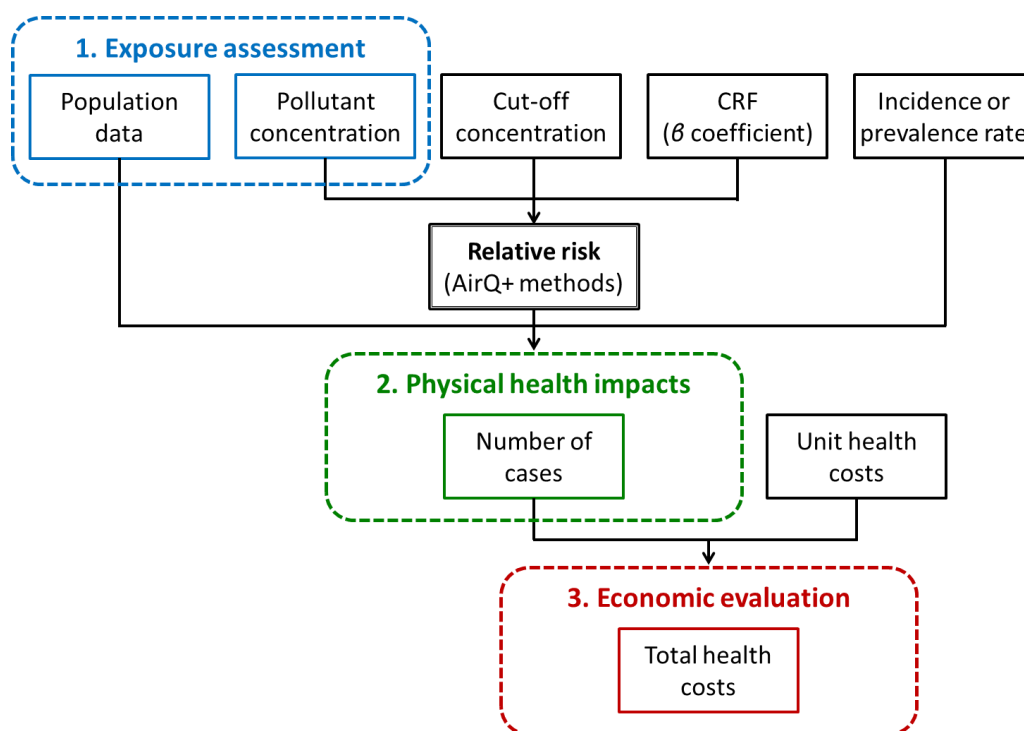


Figure 3.5. General structure of the health module.

The dissemination of HIA results is often based on short and/or long-term exposures for a given pollutant. Therefore, the effect on health indicators related with the exposure to a single pollutant should be added.

- **Exposure assessment**

In the first step, exposure assessment is described as a function of the estimated pollutant concentration and its spatio-temporal variability, to which citizens are or may be exposed. Thus, for each grid cell of a simulation domain, the population exposure is calculated through the resulting concentrations and the number of inhabitants per age groups that could be affected. Concentrations are usually presented as daily average or daily maxima values for designing short-term exposures, whereas annual average concentrations are used for long-term exposure modelling. The examined age groups are based on epidemiological evidences (i.e. CRF) relating the pollutant, exposure time and health indicator. This exposure modelling approach has been widely used to study large geographic regions (e.g. city scale) or densely populated areas (APPRAISAL, 2013b;

Brenk, 2018), where is unfeasible the elaboration of individual exposure monitoring programmes focused on time-activity patterns, and even if population samples are selected, that sampling might not be representative of the case study. For the same reasons, epidemiological models continue to use ambient concentrations rather than exposure measurements.

- **Quantifying physical health impacts**

When moving from exposure assessment to physical health impacts quantification, the linear and non-linear AirQ+ methodologies, described in Section 2.2.2, are implemented into the health module. Both methodologies use the same general equation (Eq. 2.3), differing only in the RR calculation. For a specific health indicator, the RR of the human exposure to an air pollutant is derived from CRF, estimated concentration in each grid cell, and cut-off concentration value above which health impacts are quantified. Concerning the CRF and cut-off values, in the absence of consolidated air quality and epidemiological studies over the target geographic region, reference values reported from the WHO are recommended. Besides the RR, other inputs to quantify the number of cases of disease or premature deaths are required, namely, population data organized by age groups and baseline incidence or prevalence rates associated to each pollutant-health outcome pair. Demographic data are provided from country's population census, whereas baseline rates related to certain health indicators are usually derived from national statistics, or if not available, using scientific references designed for regions with similar environmental conditions.

- **Economic evaluation of health impacts**

Economic evaluation of the quantified physical health impacts, at least from the perspective of governing bodies, is seen as one of the most important milestones of a comprehensive HIA, since it reflects the societal costs associated to these health damages. This costs component is incorporated into the health module, considering economic cost figures, as health costs per case or cost by YLL. Such monetary valuation for the different health indicators related to the most common air pollutants is based on economic studies (Section 2.2.4), and results from the sum of direct, indirect and intangible costs (Section 2.2.3). Focusing the HIA on a given pollutant-health indicator relationship, the product between these unit health costs and the number of cases due to short or long-term human exposure represents the total health cost to repair/remediate the initial health status of the affected

people. Lastly, taking as a basis the target pollutant and exposure time, the total health costs estimated for the associated health indicators are added.

3.4. Operationalizing the modair4health system

After defining the methodological principles, focused on the use of the chosen air quality and health models and the preparation of input data, the models and input-output matrices were operationalized and linked as a whole, resulting in the modair4health system.

The operational chain of the modelling system, in terms of automating processes, was thought for research and end-user purposes, using python and bash shell script's programming tools for its design. In general outlines, the coupling between models and specific input data processing tools, as well as the information flow management, represent the main innovations of the developed modelling system. The user is guided from different system options (Appendix B, e.g. target pollutant, required simulation period, include or not integrated analysis, data postprocessing) and can easily adapt the baseline configurations (e.g. domains, parametrizations and input data) according to a specific case study and research objectives.

The modair4health system is organized in modules, which are used for input data processing, and in executable programs oriented towards multiscale air quality and health modelling. Additionally, a postprocessing module to handle the air quality outputs is also incorporated (Figure 3.6).

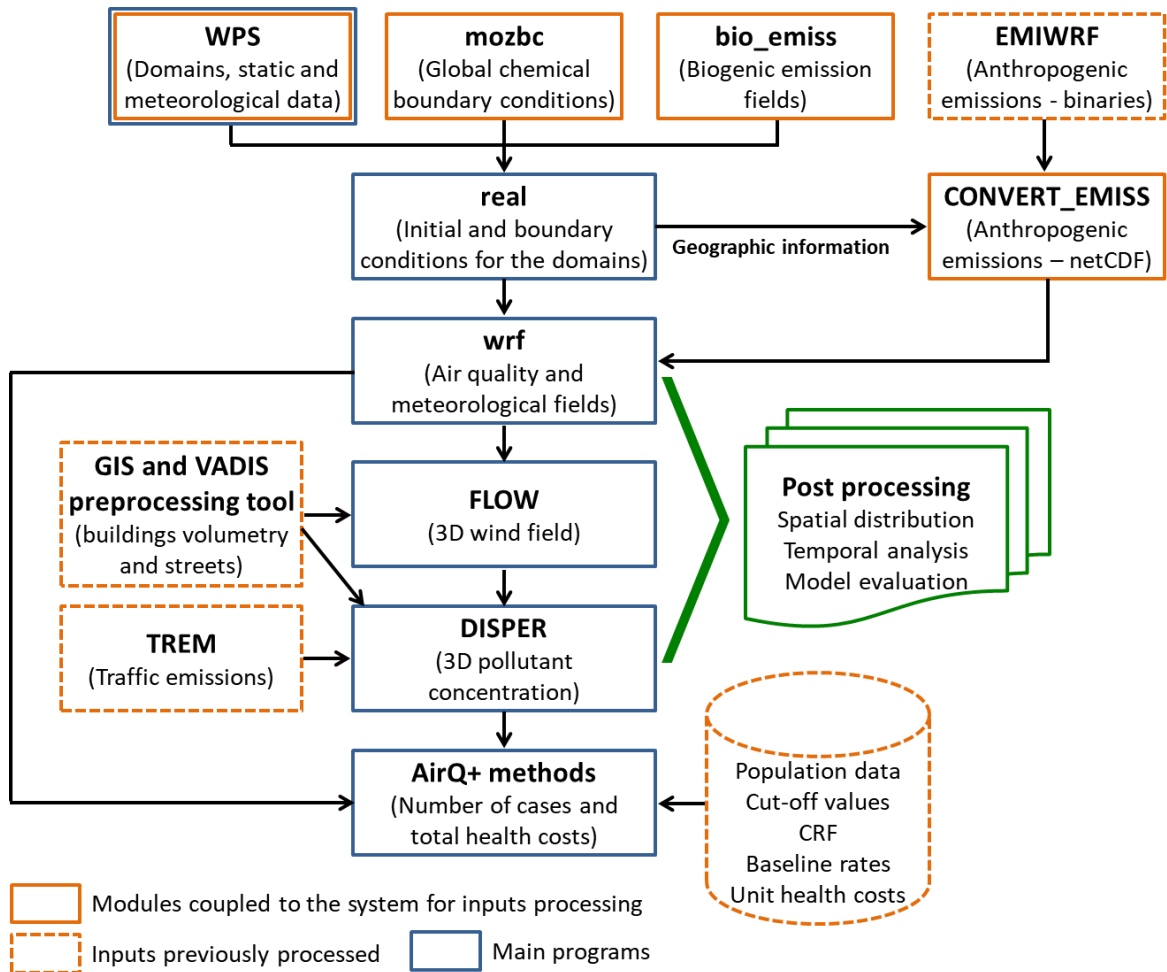


Figure 3.6. Schematic representation of the operational chain of the modair4health system.

Structurally, the operationalization of the system is done at the level of the air quality models and health and postprocessing modules, focusing on key determinants used for their connection.

- WRF-Chem

For air quality modelling from regional to urban scales, the WRF-Chem model script, composed by the WPS and main real and wrf programs, was prepared to simultaneously run multiple domains, because the source code of the CONVERT_EMISS module (available within the chemistry component), used to convert binary anthropogenic emission files into the required netCDF format, is only able to run each domain separately. To that end, anthropogenic emissions for the simulation grids should be previously processed using the EMIWRF utility to generate binary files with time and space varying emissions and, then, the script-embedded CONVERT_EMISS routine is applied to each domain. The spatial

allocation of emissions is performed through geographic information extracted from the model initialization files. Once the anthropogenic emissions processing is completed, these are called every hour when running the wrf program. To provide initial and boundary conditions for the domains, the WPS, mozbc and bio_emiss modules, available for the WRF-Chem community, were coupled to the model script. WPS is used to process information about the domains and static and meteorological reanalysis data; mozbc defines MOZART chemical boundaries; and bio_emiss creates initialization fields for online processing of biogenic emissions. After processing these input data, the wrf program is executed, producing 3D air quality and meteorological fields with hourly resolution for the nested simulation domains.

- **VADIS**

The downscaling for the local scale air quality modelling is done through the VADIS model, which accurately reproduces turbulent flows (FLOW) and pollutant dispersion (DISPER) within the urban structure. With this purpose, hourly meteorological fields (air temperature and wind speed and direction), extracted from the WRF-Chem's inner domain grid cells that intersect the local domain, are used as an input for the VADIS simulations, promoting thus the link between models (i.e. offline coupling). Besides the meteorology, to automate the VADIS model script, other inputs for the local case study are required, namely geographic features (buildings volumetry and streets configuration) and streets-allocated traffic emissions. These inputs should be previously processed following the methodologies described in Section 3.2.2, which briefly identify the use of a GIS software and VADIS preprocessing tool to treat the geographic elements, and the TREM model to estimate traffic emissions for each road segment. In operational terms, some adaptations and improvements in the VADIS functioning scheme were implemented:

- i. to automatically change the namelist that gathers the required input data to run the model. This condition is applicable, for example, when hourly resolution simulations for a large time period are needed, which implies changing the date, meteorology and emissions every hour. When using the model outside the script, these data will have to be changed manually;
- ii. to build traffic emission profiles with hourly temporal disaggregation. These profiles are calculated based on air quality measurements from a station located within or near the domain (preferably under traffic influence), and background concentration values estimated from the WRF-Chem. In alternative, default or user-defined emission profiles could be used;

- iii. to represent the VADIS outputs in GIS, assigning the same system projection that was used in editing the geographic features. The current model version represents the X and Y coordinates according to the Cartesian grid spacing;
- iv. to account for the pollutant fraction that is not emitted within the simulated local case study, higher resolution WRF-Chem concentrations for the grid cells that intersect the domain are added to the VADIS results as background values.

- **Health module**

For quantifying physical health impacts resulting from the multiscale air quality modelling, translated in number of unfavourable cases, the two AirQ+ methodologies (linear and non-linear) were coupled to the system. Thus, when running the health module using one of these approaches, the individual and the overall effect of a single pollutant on health indicators are estimated, contrary to the AirQ+ software, which only allows distinct impact evaluations by pollutant-health outcome pair. For a particular health indicator, both AirQ+ approaches use the same input dataset (pollutant concentration, cut-off value, exposed population, CRF and baseline rates) and the impacts calculation only differs in the RR formulation. As the selection of the input data is dependent on several factors, such as target pollutant, associated health indicators, exposed age groups and exposure time, the script of the health module (i.e. inputs for the AirQ+ equations) have to be adapted according to the specificities of each study. Nevertheless, when choosing impact evaluations due to short or/and long-term exposures, hourly modelled concentrations will be automatically processed in the required format: daily averages/maxima for short-term, and annual averages for long-term exposure. Regarding the economic evaluation, in which the physical health impacts are converted in monetary losses, the estimation is made for each health indicator, considering total health costs per case or YLL obtained from economic studies. These damage costs are included into the health module, in order to first quantify total health costs per health indicator (number of cases x costs per case), and then compute the HIA per pollutant (sum of the cost of all indicators).

Following this structure, a set of instructions for computing potential health benefits derived from air pollution management strategies (i.e. differences between scenarios) is also included into the module.

- **Postprocessing module**

The creation of a postprocessing module oriented to the multiscale air quality assessment is very useful for quickly analysing the performance of the models using different parametrizations and input data. The module is divided in two main parts: spatial analysis and model evaluation, where the user only needs to define the simulation domain, time period and plots (e.g. maps, time series) of interest. All available options are documented in Appendix B.

3.5. Summary

The conception and operationalization of the modair4health system, following the functioning schemes of the models and described methodologies, were the most challenging achievement of the thesis. As key aspects of this developed system, it is possible to highlight the link among models and scales, the integration of a health module to assess short and long-term air pollution exposure effects, and the automated data pre- and postprocessing capabilities. Thus, when applying the modair4health system to cover multiple scales and resolutions, it is possible to more quickly and comprehensively assess the ambient pollution levels and their potential impacts on human health.

Chapter 4

Modair4health system application and assessment

4.1. Case study characterization

4.2. Air quality modelling from regional to urban scales

4.2.1. WRF-Chem setup

4.2.2. Model evaluation

4.3. Air quality modelling at local scale

4.3.1. VADIS setup and input data

4.3.2. Model evaluation

4.4. Quantification of health impacts

4.4.1. Selected health input metrics

4.4.2. Comparative analysis of the health impact methodologies

4.5. Summary

4. MODAIR4HEALTH SYSTEM APPLICATION AND ASSESSMENT

The application and assessment of the modair4health system allowed to identify the most appropriate parametrizations and input datasets for the simulation domains, focusing particularly on the smallest domain (case study).

Structurally, this chapter is organized as follows. Section 4.1 presents the selected case study and the reasons for its selection, as well as the description of the most relevant characteristics. The base air quality modelling setup, tests performed with different configurations and inputs, and models evaluation from regional/urban (WRF-Chem) to local (VADIS) scales are presented in Sections 4.2 and 4.3, respectively. The WRF-Chem tests resulted in the following publications:

Test 1 - Investigating feedbacks of online meteorology-chemistry coupling

Silveira C., Martins A., Gouveia S., Scotto M., Miranda A.I., Gama C., Monteiro A. “The role of the atmospheric aerosol in weather forecasts: investigating the direct effects using WRF-Chem model”. Submitted to *Atmospheric Research Journal* (under review).

Test 2 - Influence of a high-resolution land cover classification

Silveira C., Ascenso A., Ferreira J., Miranda A. I., Tuccella P., Curci G., 2018. Influence of a High-Resolution Land Cover Classification on Air Quality Modelling. *International Journal of Environmental and Ecological Engineering*, 12(9), 563-571.

Section 4.4 addresses the link between air quality and health impact estimates that is carried out for the case study considering short-term human exposure, and the comparison of health results using the two AirQ+ methodologies.

4.1. Case study characterization

The selected case study is located within the city of Coimbra, the largest city of the Centre Region (Figure 4.1) and the fourth largest urban centre of Portugal, with 105842 inhabitants in its urban perimeter (2011 census) and a municipality area of 319.4 km² (URL10). The largest urbanized areas are mainly concentrated along the Mondego river valley and in the historical zone, in contrast with other areas of the city, which present a high degree of urban dispersion.

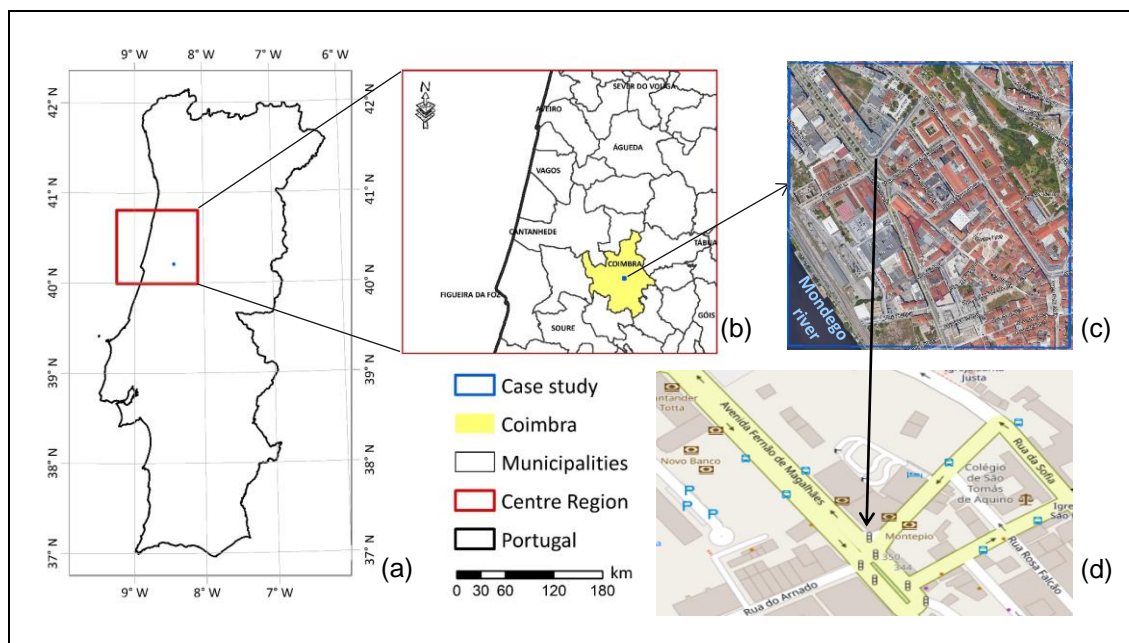


Figure 4.1. Geographic location of the case study area: a) framework, b) part of the Centre Region, c) case study, and d) part of the Fernão de Magalhães Avenue.

Coimbra plays a strategic role in connecting the north to the south, and the coast to the inland of Portugal. At north, the landscape is characteristically more fragmented and complex, whereas towards the south, down the Tejo river, large homogeneous territorial units predominate. Regarding the coast-inland link, the city is located 50 km away the Atlantic Ocean (Figueira da Foz), and at 40 km distance there is the mountain “Serra da Lousã” (1205 m) (Figure 4.2). The proximity to both the sea and the mountains is a determinant factor for intensifying urban/local atmospheric dynamics. These geographical nuances greatly contribute to the region’s climate, which is affected by Atlantic and Mediterranean influences. Based on the 30-year average climatological normal (1971-2000) obtained from the Coimbra meteorological station, it can be concluded that the summer is typically warm and dry, with average minimum and maximum temperatures of 15 °C and 28.5 °C, respectively, reaching 40 °C or more in certain days. In winter, these values decrease to 4.6 °C and 14.6 °C, and high rainfall is recorded: total average and daily maximum precipitation for January reached 112.2 mm and 47.6 mm, respectively (URL12).

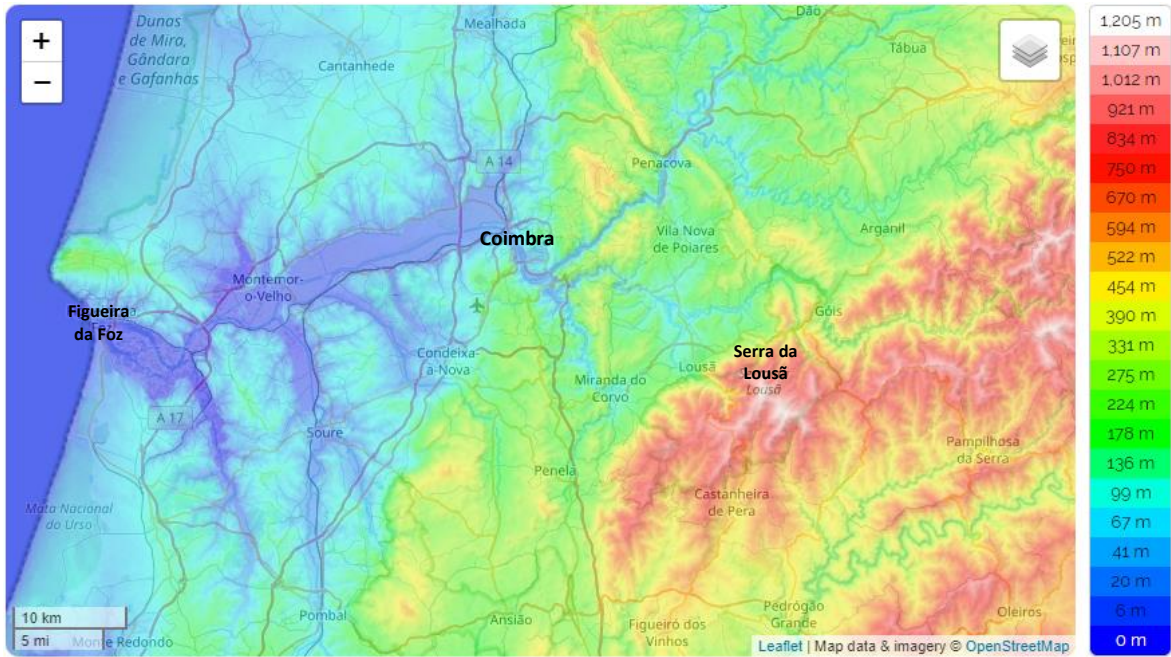


Figure 4.2. Altimetry (m) of the Coimbra region (source: OpenStreetMap - URL13).

Regarding accessibility, currently, the city of Coimbra is the major input-output pole of the region. However, the public road transport services serving the city have to be improved due to the long travel time and lack of articulation with the internal services (CIM-RC, 2018). These are some reasons that discourage the use of public transports from/to Coimbra and, as a consequence, high road traffic volume due to the increased use of private vehicles has been observed in the main arteries of the city and in certain day periods with traffic congestion.

From the point of view of urban air quality, high air pollution levels are also associated to streets with intense road traffic activity. Thereby, in the current context of the city of Coimbra, and in many other urban areas, the road traffic is seen as one of the major environmental concerns, being the atmospheric pollution identified as a potential cause of many diseases and premature deaths. However, for the Coimbra urban area in general, and for the characterization of local effects under complex geometries in particular, few studies addressing the emissions, transport and dispersion of air pollutants in urban environment (e.g. Dias et al., 2019, 2016) and subsequent health implications have been performed. Nevertheless, in a broader geographic context and according to the EU Ambient Air Quality Directive 2008/50/EC, transposed into national law through the Decree-Law no. 408/2010, the elaboration of an air quality improvement plan for the Centre Region was mandatory (Regulation no. 408/2014) (CCDRC, 2010). This plan covered the Coimbra, Aveiro/Ílhavo and Litoral Noroeste do Baixo Vouga zones, where exceedances to the PM10

LV were recorded in the years 2003-2009. The set of proposed measures for reducing the PM₁₀ levels was focused on traffic management and control strategies, industrial regulations and on small combustion sources (residential and commercial). Among the traffic-related harmful air pollutants, beyond PM₁₀, NO₂ is also considered a problematic contaminant for both health and environment, which is largely emitted from the road traffic activity. It contributes significantly to the ground level O₃ formation, primarily during heatwave episodes. Moreover, air quality studies based on NO₂ have rarely been explored for the urban Coimbra area.

For the aforementioned reasons, in particular the intense traffic in some areas, the chosen case study is one of the busiest road traffic areas of the city of Coimbra (Fernão de Magalhães Avenue) and NO₂ was considered the target pollutant. This case study is integrated in a densely build-up and populated zone, where important municipal services are located, and a strong commercial activity is known.

4.2. Air quality modelling from regional to urban scales

This section focuses on nesting applications using WRF-Chem version 3.6.1, which were performed from regional to urban scales, with different configurations and input data to be tested and evaluated. The year 2015 was selected, because it was the most recent year with the required input data available: emissions, meteorology and boundary conditions (described in Section 3.2.1). Furthermore, the option for this year was supported on information reported by the EEA and the World Meteorological Organization (EEA, 2017; WMO, 2016), which indicate 2015 as the hottest and driest year in Europe since there are records, with a series of heatwaves that affected Europe from May to September. The evaluation of the model performance was based on air quality observations recorded by the Portuguese monitoring network QualAr (URL14) (Figure 4.3), considering stations with more than 75% of data availability. A characterization of the QualAr network by geographic location of the stations, typology, measured pollutants and start of activity is presented in Appendix C.

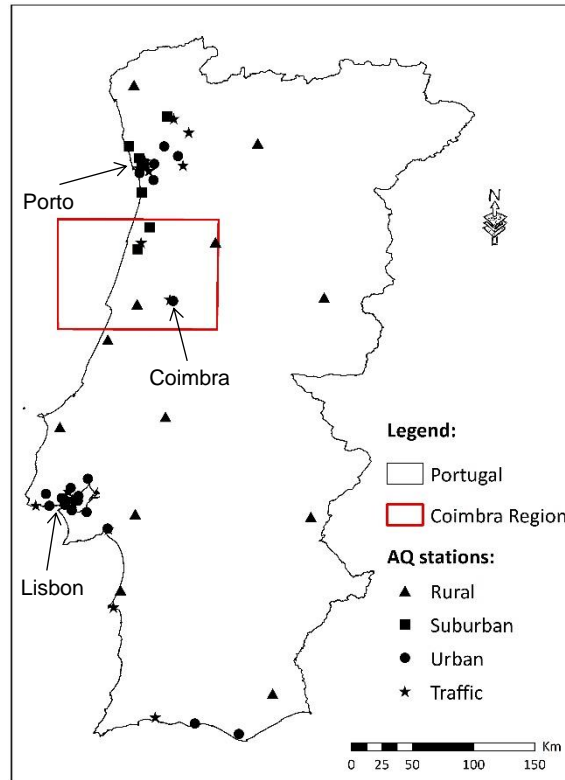


Figure 4.3. Portuguese air quality monitoring network characterized by station typology: rural, suburban, urban and traffic.

In total, 40 background influence stations are available in Mainland Portugal: 12 rural in inland regions, 8 suburban around the Greater Porto, and 20 urban sites that are mostly located in the Lisbon region. Within the urban areas, 14 traffic influence stations are also monitoring air pollutant concentrations. In the Coimbra region, 7 air quality stations are installed: 2 rural, 2 suburban, 1 urban and 2 traffic.

4.2.1. WRF-Chem setup

The WRF-Chem setup includes three nested domains covering from a large part of Europe and North Africa (D1), through a regional domain centred over Portugal (D2) to a Portuguese region (D3) (Figure 4.4). The main configurations used for the geographic projection of these domains, having as reference the central point (38.716° , -9.084°) of the parent domain (D1), are presented in Table 4.1. The vertical structure of the atmosphere was resolved with 29 vertical levels extending up to 50 hPa, being the lowest level at approximately 28 m above the surface.

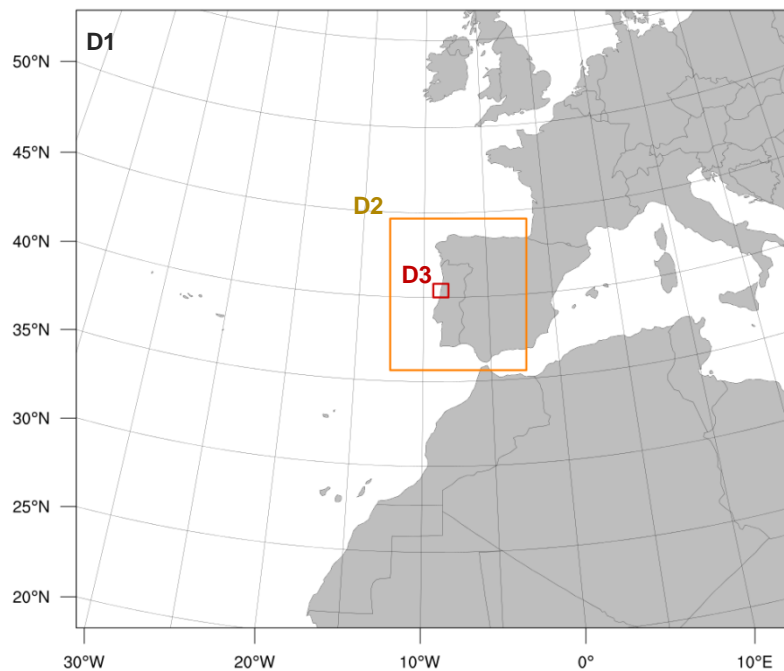


Figure 4.4. Spatial representation of the nested WRF-Chem simulation domains.

Table 4.1. Configurations used for designing the nested WRF-Chem simulation domains.

Domain	Description	Size (km ²)	Resolution (km ²)	Grid cells
D1	Background domain	4750 x 4075	25 x 25	190 x 163
D2	Regional domain	900 x 1000	5 x 5	180 x 200
D3	Coimbra region (Urban target domain)	100 x 90	1 x 1	100 x 90

The model was applied in two-way nesting mode from 24th December 2014 to 31st December 2015 on a daily basis and with hourly resolution, discarding the days of December 2014 as model spin up.

Table 4.2 shows the main physical and chemical parametrizations adopted for the base WRF-Chem simulations. These options were chosen taking into consideration the model performance in other applications under different simulation domains but with similar environmental conditions (e.g. Kong et al., 2015; Kuik et al., 2016; Palacios-Peña et al., 2017).

Table 4.2. Main physical and chemical parametrizations used in the numerical WRF-Chem simulations.

Processes	Options ¹	Remarks
Microphysics	Morrison double-moment	
Short-wave radiation	RRTMG	Called every 25 min
Long-wave radiation	RRTMG	Called every 25 min
Surface layer	Monin-Obukhov Similarity	
Land-surface model	NCEP Noah LSM	LC classification (to be tested)
Boundary-layer scheme	MYNN 2.5 level TKE	
Cumulus	Grell 3D	Only for D1 and D2
Photolysis	Fast-J	
Gas-phase mechanism	RADM2	Fixed version (chem_opt=2)
Aerosol module	MADE/SORGAM	
Aerosol-radiation feedback	Turned on/off	Direct and semi-direct effects (to be tested)
Aerosol optical properties	Volume approximation	

¹ The methodological assumptions of these options are described in the WRF and WRF-Chem user's guides.

Acronyms: LSM - Land Surface Model; MADE/SORGAM - Modal Aerosol Dynamics Model for Europe / Secondary Organic Aerosol Model; MYNN - Mellor-Yamada-Nakanishi-Niino; NCEP Noah - National Center for Environmental Prediction; RADM2 - Regional Acid Deposition Model, 2nd generation; RRTMG - Rapid Radiative Transfer Model for General Circulation Models; TKE - Turbulent Kinetic Energy.

Aiming to better understand the impact of different configurations and input data, some WRF-Chem modelling tests were performed. Table 4.3 summarizes these tests, identifying the target options that were compared.

Table 4.3. WRF-Chem tests to different configurations and input data.

Test	Option 1	Option 2
Test 1 - Investigating feedbacks of online meteorology-chemistry coupling	Include direct and semi-direct aerosol effects	Not include direct and semi-direct aerosol effects
Test 2 - Influence of a high-resolution land cover classification	New LC (33 classes)	USGS LC (24 classes)
Test 3 - Impact of grid spacing and its relationship with the land cover	1 km ² grid spacing	5 km ² grid spacing

In the first two tests, the aspects referenced in the option 1 were adopted for the base simulations, whereas the test 3 was oriented towards the evaluation of the impact of grid spacing, focusing on the D2 (5 km²) and D3 (1 km²) nested domains (Figure 4.4) and its relationship with the new LC classification (33 classes).

4.2.1.1. Test 1 - Investigating feedbacks of online meteorology-chemistry coupling

This first test aimed to evaluate the impact of considering, or not, direct and semi-direct aerosol effects on meteorological results, based on the application of the WRF-Chem model along 2015. To that end, besides the base simulation with direct and semi-direct effects, another WRF-Chem simulation for the same time period and input data was performed, disabling the options aerosol-radiation feedback and aerosol optical properties (i.e. without aerosol feedback). By definition, direct effects involve the scattering of solar radiation and subsequent reduction of shortwave solar radiation, whereas the semi-direct effects are associated to the absorption of solar radiation by black carbon and other absorbing aerosol compounds, producing a change in the ground surface temperature, relative humidity and atmospheric stability impacting the clouds formation (Chapman et al., 2009; Forkel et al., 2012; Liu et al., 2016; Palacios-Peña et al., 2017; San José et al., 2015; Zhang, 2008). For both simulations, D2 results (5 km² resolution) were explored based on agreement statistical methods and on spatial variability analyses in order to assess the importance of including the online-coupled aerosol radiative effect on the potentially more affected meteorological variables: shortwave solar radiation, air temperature and precipitation. The agreement between simulations (with and without aerosol feedback) was evaluated for each meteorological time series and defined in terms of the magnitude-squared coherence function, $C_{xy}(f)$, as:

$$C_{xy}(f) = \frac{|G_{xy}(f)|^2}{G_{xx}(f) G_{yy}(f)} \quad (\text{Eq. 4.1})$$

Where:

x and y are the (zero-mean) time series of the WRF-Chem outputs without and with aerosol feedback, respectively;

$C_{xy}(f)$ varies between 0 and 1, where 0 indicates no relationship between x and y at frequency f , and 1 corresponds to a perfect linear relationship between x and y at frequency f ;

$G_{xy}(f)$ is the cross-spectral density between x and y ;

$G_{xx}(f)$ and $G_{yy}(f)$ represent the spectral density of x and y , respectively.

More details about these agreement statistical methods can be found in Kay (1988).

Figure 4.5 shows the spatial distribution of agreement for the set of meteorological variables.

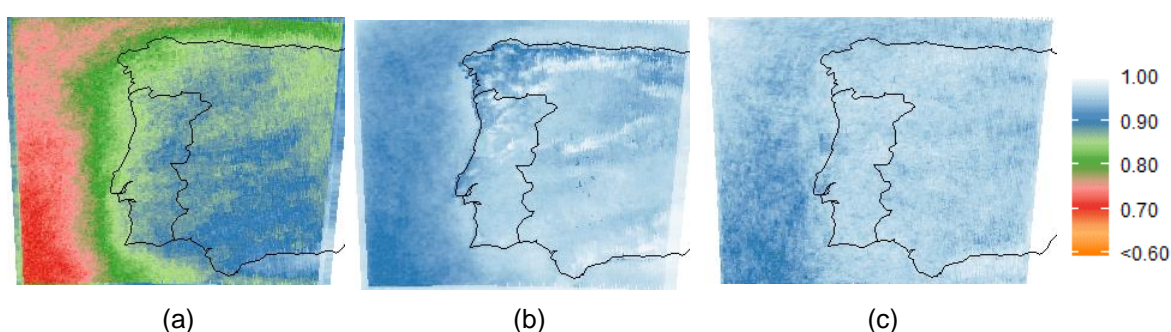


Figure 4.5. Agreement between the WRF-Chem simulations, with and without aerosol feedback, for the analysed meteorological variables: (a) solar radiation; (b) air temperature; and (c) precipitation.

Air temperature and precipitation have agreement values ranging from 0.87 up to 1.00, while solar radiation presents a lower agreement, varying between 0.68 and 0.98. Solar radiation agreement is lower over the ocean (0.68-0.75) comparatively to land regions (0.75-0.98), probably due to ocean-land differences based on the extent, height and type of clouds and their interaction with the atmospheric aerosol. The higher variability over the ocean comparing both simulations is largely associated to the approach used for quantifying semi-direct aerosol effects, since their influence on the radiative forcing induces changes in other meteorological variables (surface temperature, relative humidity, wind speed) impacting the cloud cover (Archer-Nicholls et al., 2016; Briant et al., 2017; Chapman et al., 2009; Forkel et al., 2015; Thomas et al., 2015).

By analysing the monthly variation of agreement values, it is possible to observe that once again solar radiation exhibits larger variability than temperature and precipitation (Figure 4.6).

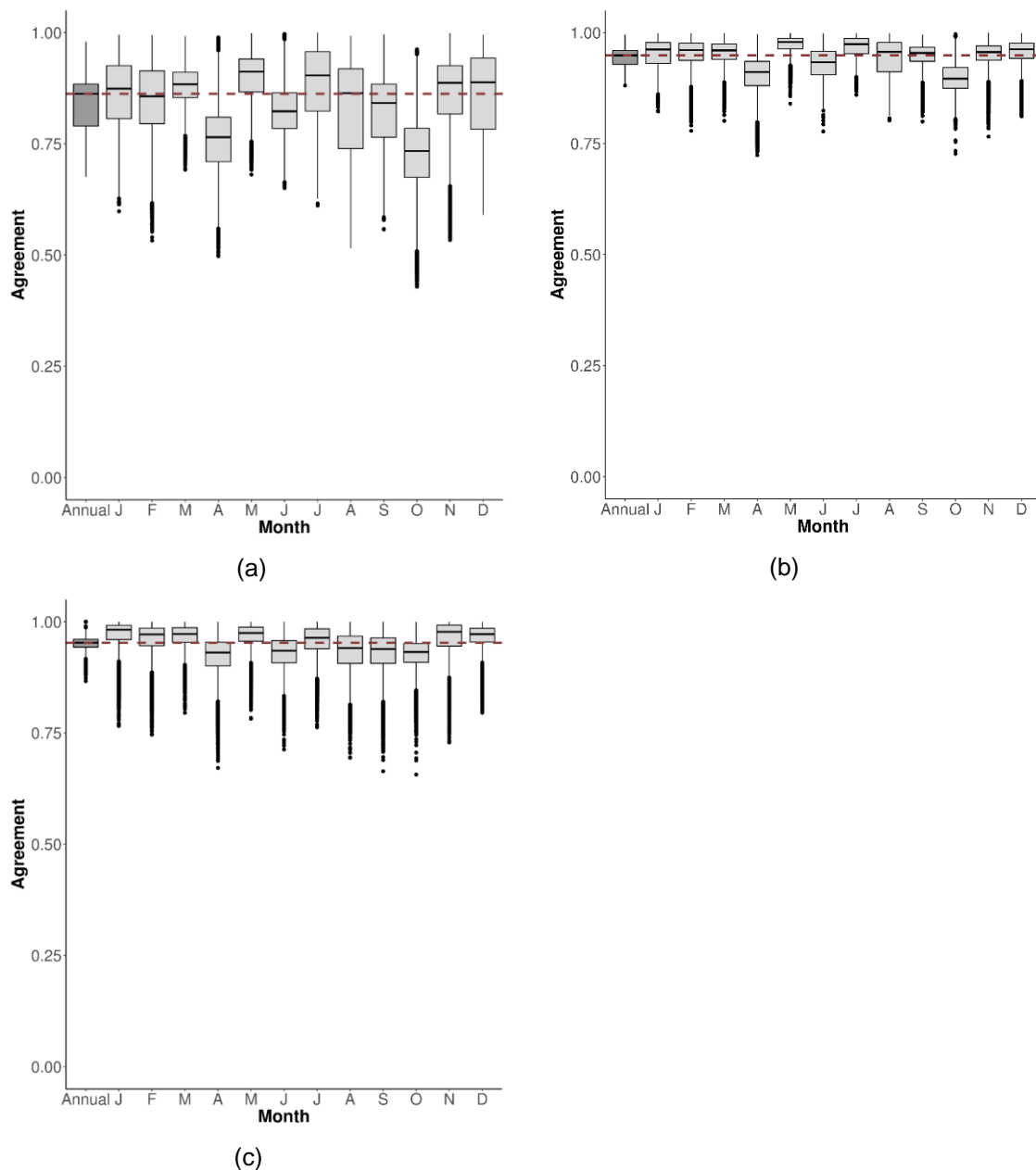


Figure 4.6. Monthly agreement between the WRF-Chem simulations, with and without aerosol feedback, for the analysed meteorological variables: (a) solar radiation; (b) air temperature; and (c) precipitation. Dark grey box represents the annual average distribution of agreement for the domain grid cells, while light grey boxes indicate the monthly distribution of agreement for the domain grid cells. Red dashed line shows the median of the annual agreement.

For all meteorological variables, agreement values in April, June and October are lower compared to the annual average agreement. One-way analysis of variance (ANOVA) for these months showed statistically significant differences from the annual mean ($p < 0.05$). Several reasons might justify the larger variability during these months: higher shortwave

solar radiation, increased biogenic emissions leading to the formation of secondary organic aerosol, more dynamic atmospheric boundary layer, or even predominance of particles due to Saharan dust episodes and agricultural activities (EEA, 2017; Sporre et al., 2019; Werner et al., 2017).

Besides the statistical analysis, annual mean and maximum spatial differences between simulations (with feedback – without feedback) for the solar radiation (Figure 4.7) and air temperature (Figure 4.8) are also presented.

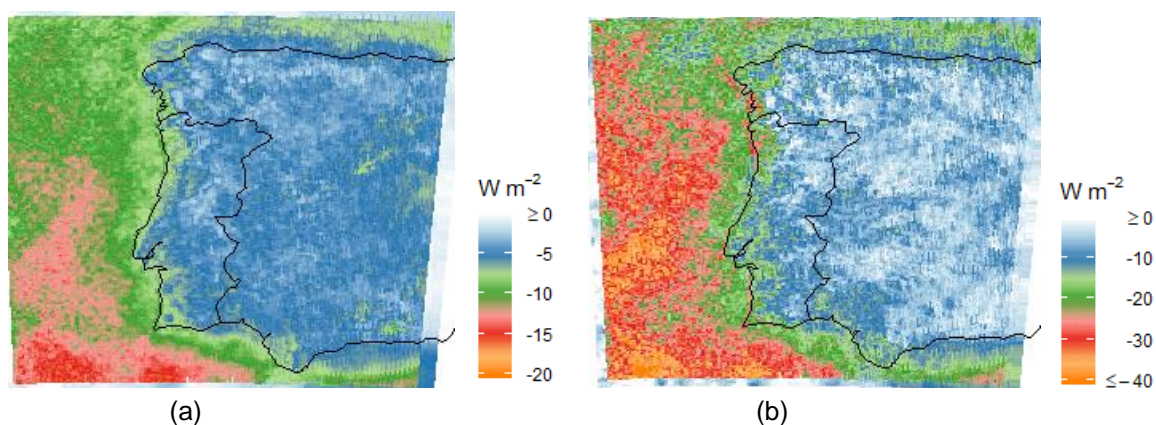


Figure 4.7. Spatial differences of solar radiation comparing both simulations (with feedback – without feedback): (a) annual average including all hourly values; and (b) annual average of daily maximum values.

Looking at the maps of solar radiation differences, the higher mean values were estimated when the aerosol feedback was neglected, mainly over ocean regions (negative differences in Figure 4.7a). This radiation variability (up to $20 W m^{-2}$) is associated to the methodological assumptions used for estimating aerosol effects (direct and semi-direct) and their relationship with the aerosol optical properties, as well as to spatial and vertical distribution of both aerosol and cloud layers. Therefore, overall, the aerosol feedback favoured the scattering and absorption of the shortwave and longwave solar radiation into the atmosphere (direct effect), leading to its warming and subsequent decrease of the amount of solar energy that reaches the ground surface. On the other hand, the higher differences over the ocean, which resulted in a lower agreement (Figure 4.5a), could be related with the aerosol-cloud dynamics (semi-direct effect), since the cloud physical characteristics (e.g. geometry, water content, particles size) significantly differ between land and sea, influencing the Earth-atmosphere radiative energy budget (Chen et al., 2017; Forkel et al., 2012; San José et al., 2015; Thomas et al., 2015; Zhang et al., 2012). Similar spatial pattern and the same sign of the mean radiation was found when mapping the maximum solar radiation differences (up to $40 W m^{-2}$) (Figure 4.7b).

Regarding the impact on the air temperature near the surface, very small differences were estimated (up to 0.5 °C) (Figure 4.8).

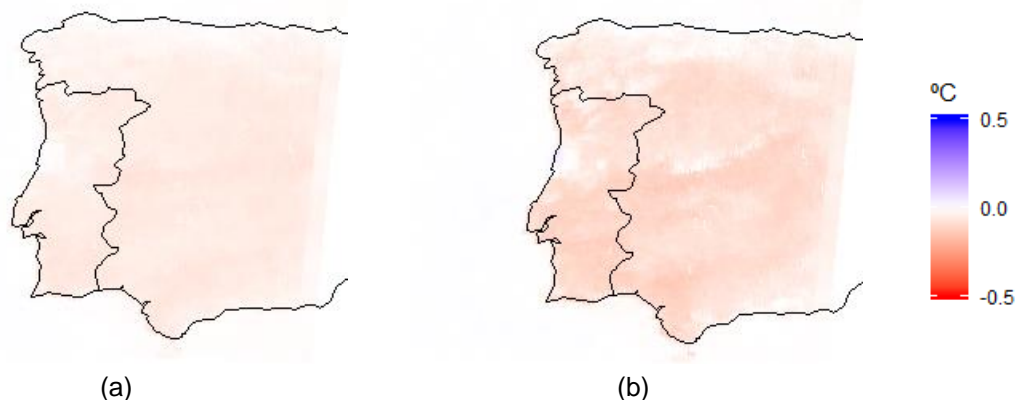


Figure 4.8. Spatial differences of air temperature comparing both simulations (with feedback – without feedback): (a) annual average including all hourly values; and (b) annual average of daily maximum values.

On land, as expected, the used aerosol schemes contributed for a slight decreasing of both solar radiation and temperature, whereas on the ocean the aerosol had the opposite effect on the meteorological variables, that is, the largest radiation reduction led to a very small increase of the surface temperature. These solar radiation and air temperature variations, related with the direct aerosol effect, especially those estimated on land surfaces, are in the range of other studies using WRF-Chem over Europe (Forkel et al., 2015, 2012; Palacios-Peña et al., 2017; Werner et al., 2017).

In summary, these results confirm that the aerosol particles have a key role in the atmosphere dynamics, influencing the net radiation budget and underlying meteorological conditions. Therefore, the accounting for the aerosol effect, only possible through the use of online atmospheric models, is recommended, either to improve the weather predictions, but also to obtain more accurate air quality estimates, since the potential meteorology-chemistry feedbacks favour the numerical resolution, in very small time steps, of the physical and chemical processes occurring within the atmospheric boundary layer.

4.2.1.2. Test 2 - Influence of a high-resolution land cover classification

The objective of this test was to evaluate the influence on the air quality of the two LC databases described in Section 3.2.1: 24-classes USGS (provided with the model package) and 33-classes USGS (new LC classification). For this purpose, besides the base simulation using the model setup with the aerosol effect turned on (Table 4.2), another

WRF-Chem simulation for the same time period (year 2015), replacing the new LC classification by the default 24-classes USGS LC, was performed. To assess the impact of the LC changes on air quality, Portugal and O₃ as target pollutant were chosen for this test due to the following reasons:

- the spatial differences comparing both LC databases (Figure 3.3) show a greater discretization of the new LC classification, with several vegetation categories that significantly influence the emission of O₃ precursors (mainly NMVOC). Thereby, the option for the O₃ will allow to better evidence the impact of these LC changes;
- to assess the resulting O₃ changes, Portugal was selected as study domain because, in particular during the spring/summer, O₃ pollution episodes are often recorded, leading, sometimes, to non-compliance of the existing air quality standards;
- another important aspect is related with the detail and higher LC spatial resolution for Portugal (100 m²) than the reclassified CLC data over Europe (5 km²).

The assessment of the modelled O₃ concentrations in Portugal using different LC classifications was based on D2 outputs (5 km² resolution), considering the spatial variability for the seasons with higher O₃ levels: spring (Apr – Jun) and summer (Jul – Sep). As support, Leaf Area Index (LAI) and air temperature data, responsible for boosting NMVOC emissions and favouring the O₃ production, were also examined. These interactions between the Earth's surface characteristics and the planetary boundary layer height are closely related with the Noah LSM scheme used in both simulations (Table 4.2), since it assumes a prominent role in connection with the LC, incorporating vegetation parameters for each LC category that correspond to annual minimum/maximum values. LAI and emissivity vary in proportion to vegetation fraction, whereas the albedo varies conversely with it.

Figure 4.9 maps the Portuguese LC obtained for the D2 based on the two LC classifications, which were spatially aggregated to the 5 km² grids resolution by dominant category. Relevant differences are visible when comparing both LC spatial distributions, but the new LC seems to be closer to reality (Figure 4.9b), because it is possible to observe the complex landscape fragmentation characterizing the Portuguese territory, as well as to clearly distinguish some categories of interest (e.g. 31, 32 and 33 as urban areas).

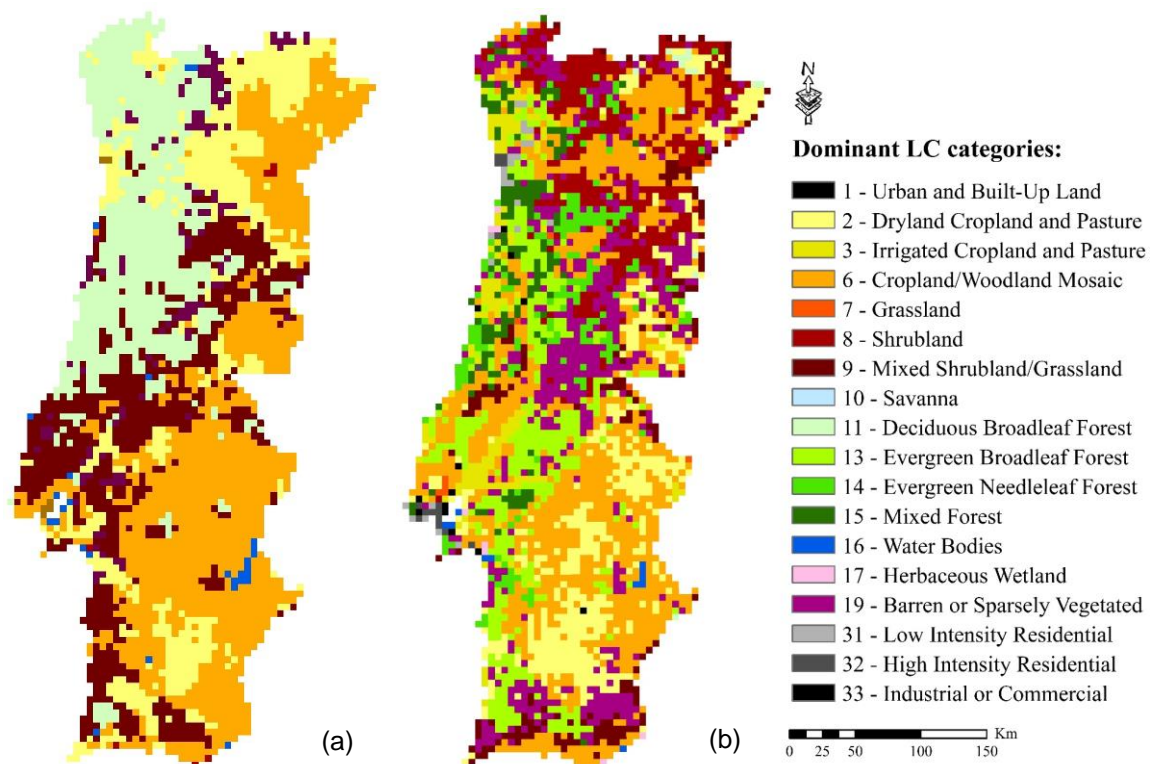
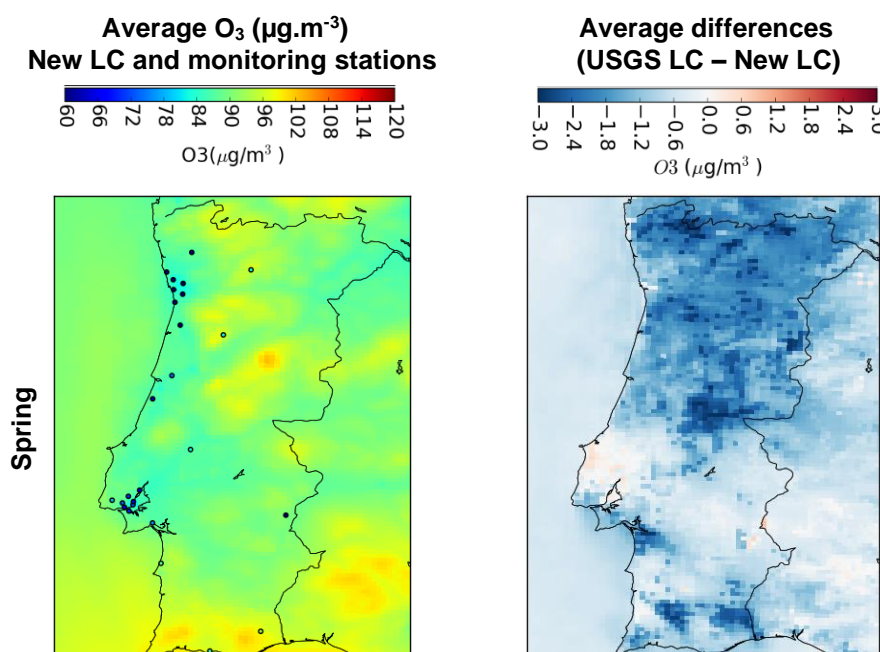


Figure 4.9. LC databases for the domain 2, over Portugal: (a) USGS LC; and (b) new LC.

In order to capture the impact of LC changes and vegetation dynamics, spatial variations in modelled O_3 concentrations by season (spring and summer), were analysed (Figure 4.10).



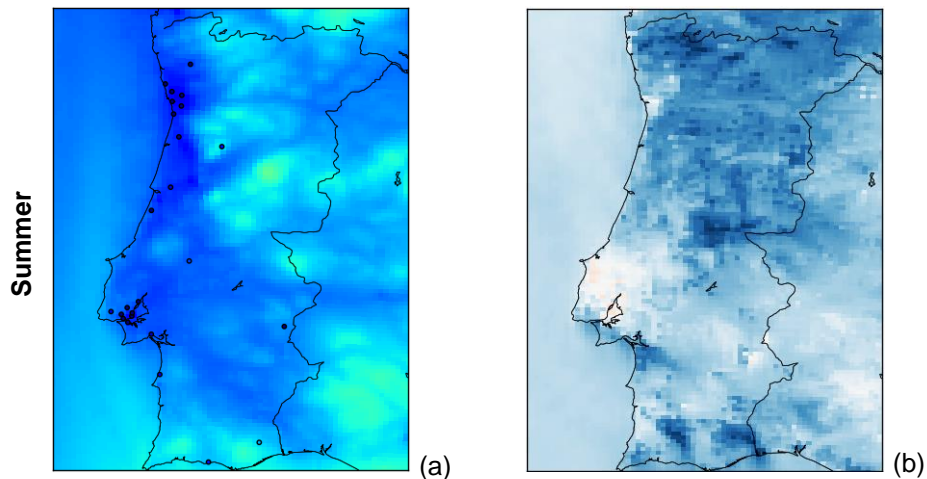


Figure 4.10. Spatial distribution of the modelled O₃ concentrations ($\mu\text{g}\cdot\text{m}^{-3}$) by season: (a) new LC-based average O₃ concentration (dots represent O₃ averages from background monitoring stations); and (b) average differences between USGS LC and the new LC.

In Figure 4.10a, average O₃ concentrations based on the new LC classification are presented, serving as a reference for quantifying the average differences in relation to the USGS LC. Overall, averaged O₃ levels are higher in spring, indicating the most favourable environmental conditions for the formation of this secondary pollutant during this period. Regarding the spatial differences comparing O₃ results from both LC approaches (Figure 4.10b), higher average values for the spring and summer using the new LC database as an input (up to $3 \mu\text{g}\cdot\text{m}^{-3}$) were estimated (Figure 4.10b). Moreover, the higher differences in both seasons are verified in the regions where bigger differences between the LC databases are observed (half north of the territory and specific areas in the south). Therefore, these differences could be explained by the joint influence of the identified LC classes, associated vegetation parameters and their relationship with the meteorology. To complement this analysis and better understand the O₃ spatial variability, LAI and air temperature spatial variations are also analysed (Figure 4.11). The latter is only mapped for the new LC, because no relevant temperature differences were found in comparison with results from the USGS LC approach.

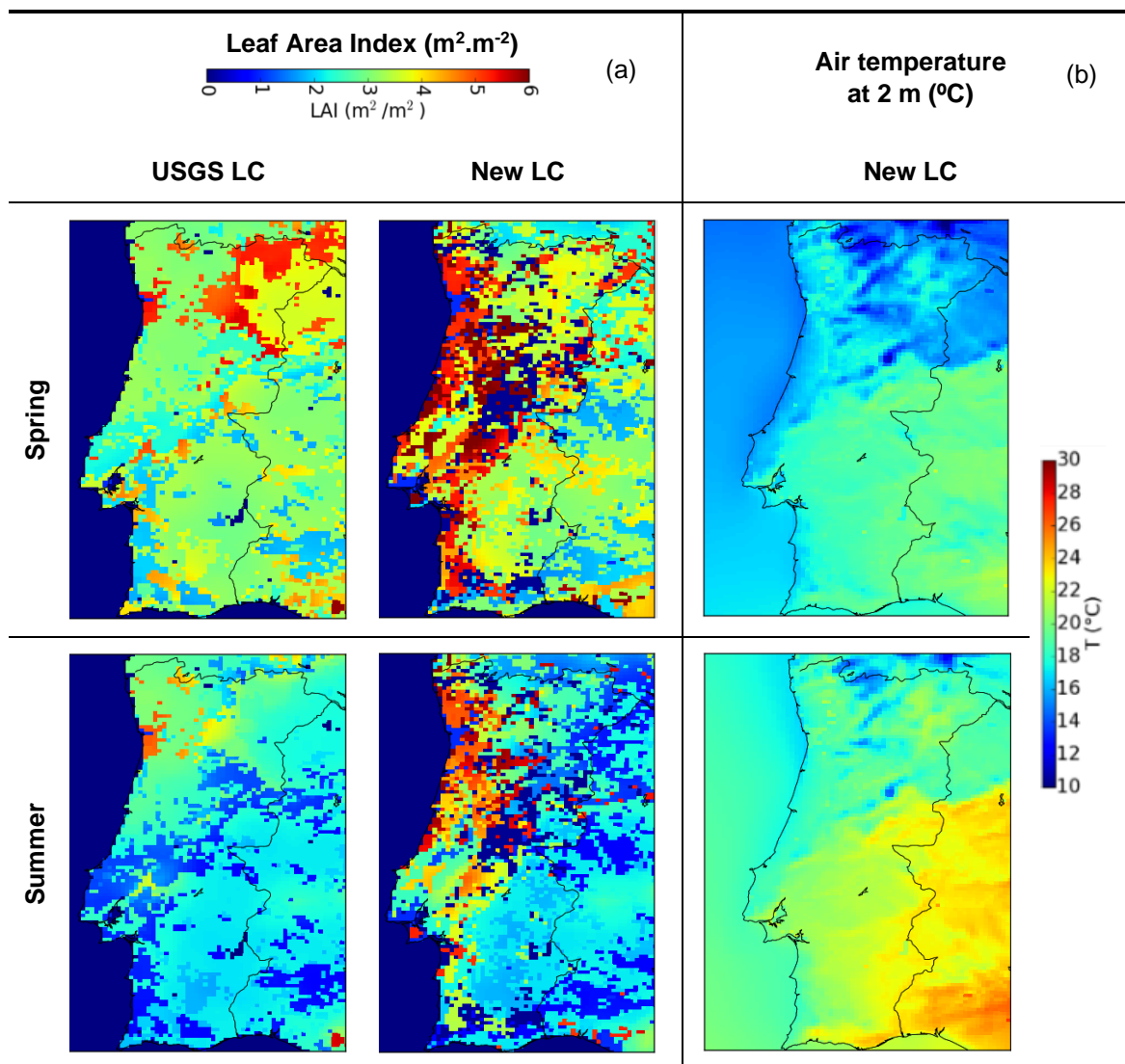


Figure 4.11. (a) Average Leaf Area Index ($m^2 \cdot m^{-2}$) for the spring and summer seasons using both LC approaches; and (b) 2 m average air temperature ($^{\circ}C$) for the spring and summer using the new LC approach.

As regards the LAI, calculated as a function of the LC classes, higher values were recorded in spring, in full vegetation growth (i.e. maturity stage), favouring the emission of biogenic NMVOC. Relating the LAI spatial information with the average air temperature, it is notorious a direct proportionality to the average O_3 concentrations (Figure 4.10a), although other factors must also be considered in the O_3 photochemistry, as availability of other precursors (mainly NO_x), orography and atmospheric synoptic transport. In summer, the highest average air temperatures do not linearly correspond to increased O_3 production, because during this season there is a decrease of the vegetation fraction, which leads to lower LAI values, and consequently, decreases the emission of biogenic NMVOC.

To evaluate the model performance on an hourly basis using both LC approaches, the following statistical metrics were calculated by season and background station typology (rural, suburban and urban): Pearson’s correlation coefficient, BIAS and Root Mean Square Error (RMSE) (Figure 4.12).

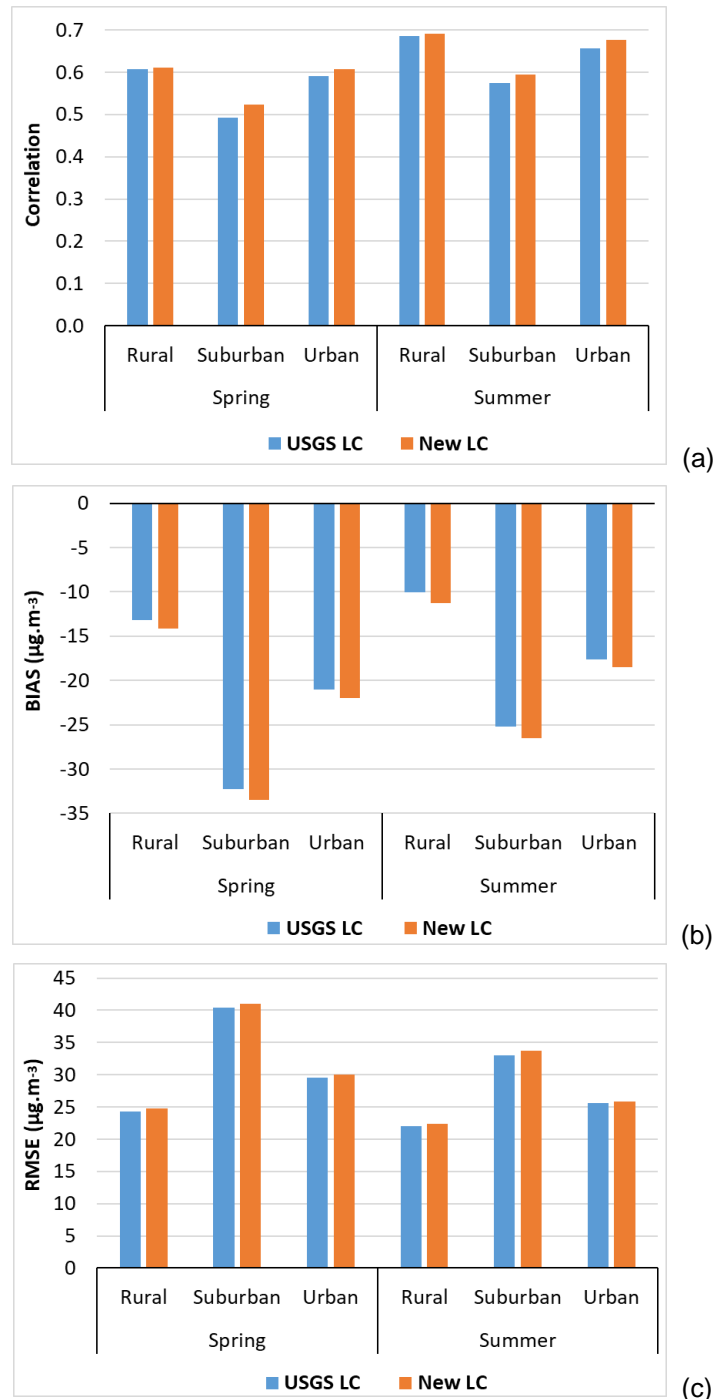


Figure 4.12. (a) Correlation, (b) BIAS, and (c) RMSE between observations from background air quality stations and hourly modelled O_3 concentrations ($\mu\text{g}\cdot\text{m}^{-3}$) by season and station typology using both approaches USGS and new LC for Portugal.

As expected, the best seasonal performance was achieved in rural influence stations: moderate correlation (0.6 – 0.7), and lower BIAS (10 – 14 $\mu\text{g}\cdot\text{m}^{-3}$) and RMSE (22 – 25 $\mu\text{g}\cdot\text{m}^{-3}$). Moreover, in these rural sites, higher O_3 concentrations are often observed. In turn, the validation for suburban stations had the worst performance, mainly for BIAS and RMSE. The location of these stations around the Greater Porto (Figure 4.3), associated to high emission rates of O_3 precursors and to favourable environmental conditions for the local photochemical production of O_3 , were determinant factors for high deviations between observed and modelled O_3 concentrations. For urban stations, mostly located in Lisbon region (Figure 4.3), the reasons are similar to those indicated for suburban stations.

Concerning the LC effect, this statistical analysis based on average values from grouping air quality stations by typology was not very conclusive, although a slightly greater correlation was obtained with the new LC (Figure 4.12a). Negative BIAS in both LC approaches and for all seasons and background stations, indicate an overestimation of the modelled O_3 concentrations (Figure 4.12b), which is in line with the dispersion measure between the observations and modelled data (i.e. RMSE, Figure 4.12c). When crossing the average O_3 concentrations obtained using the new LC approach with the dots representing observation values from background monitoring stations (Figure 4.10a), it can be concluded that the modelled seasonal averages have an acceptable agreement with the observations, mainly in summer.

Based on the performed spatial and statistical analyses to evaluate the influence of the LC on O_3 concentrations, it is demonstrated that the new LC classification represents an added value in atmospheric modelling and, therefore, its use is recommended.

4.2.1.3. Test 3 - Impact of grid spacing and its relationship with the land cover

This last test focuses on the model setup adopted for the base simulation, which includes the aerosol effect and the new LC database, and on the target pollutant for the local case study, in order to assess the background chemical conditions that will be passed to the local scale air quality modelling. Therefore, the variability of NO_2 concentrations estimated in the two smaller domains, D2 and D3, having 5 and 1 km^2 horizontal grid resolutions, respectively, was investigated. Spatial variability was examined based on the new LC classification specifically processed for both domains, giving particular emphasis to urban areas, where the major anthropogenic pollution sources are located, and to NO_2 concentrations, for which the road traffic is a main contributor. Figure 4.13 shows the LC mapped for the D3 area that resulted from its aggregation for 1 and 5 km^2 grid spacing.

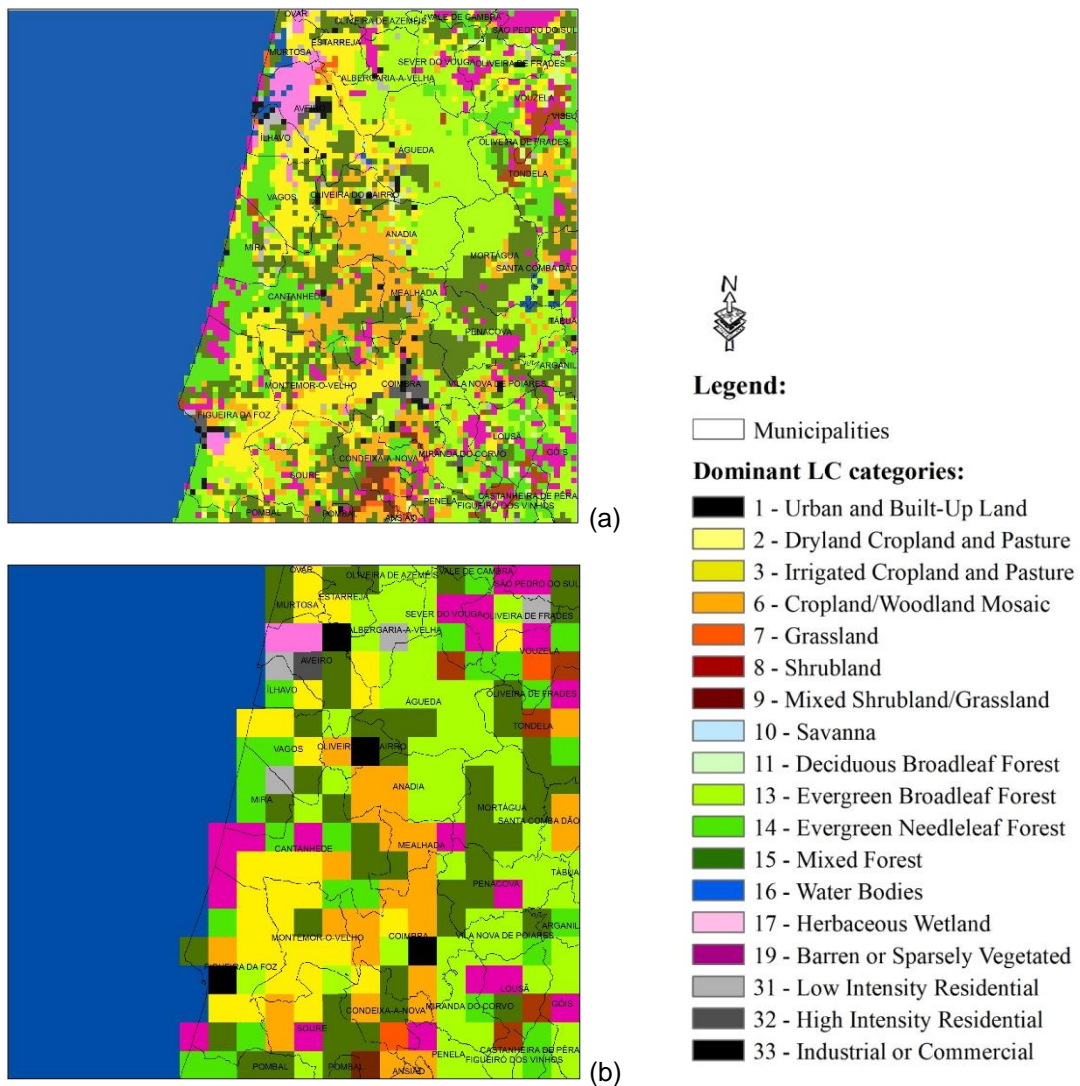


Figure 4.13. Dominant LC categories mapped for the domain 3 coverage resulting from interpolation of the new LC: (a) 1 km² grid spacing; and (b) 5 km² grid spacing (D2 cut on D3 area).

As a starting point to analyse the influence of the horizontal grid resolution on NO₂ concentrations, annual mean spatial differences between D3 and the part of D2 that overlaps D3 (D3 – D2 for each grid cell of D3) were quantified (Figure 4.14).

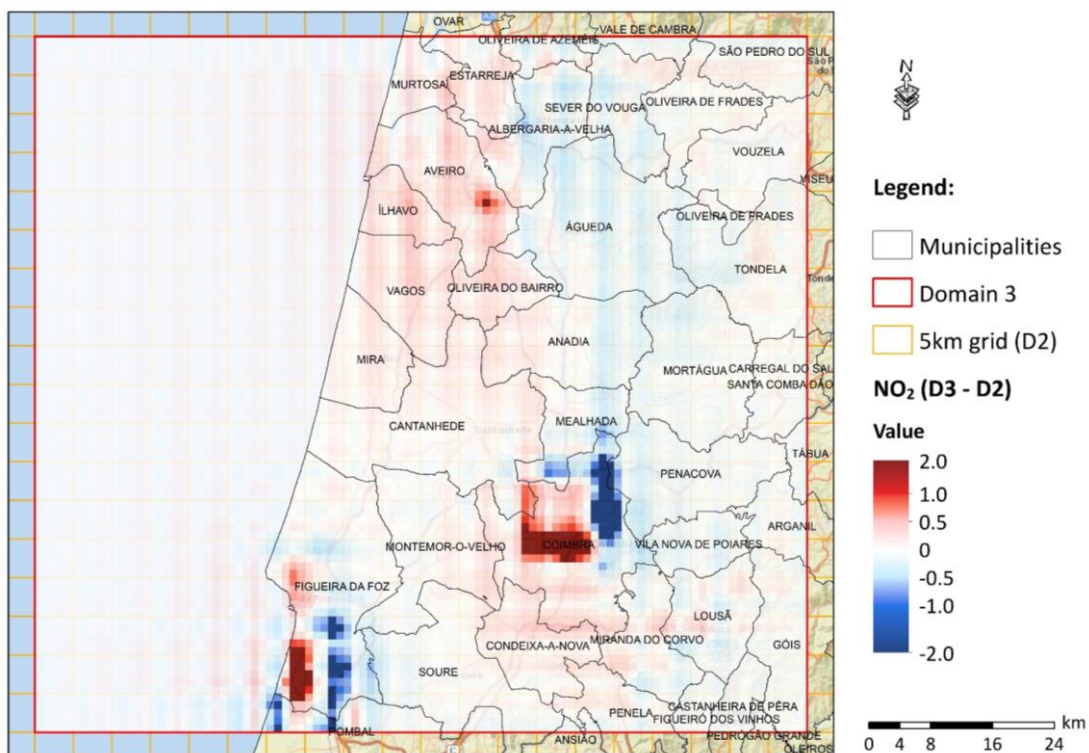


Figure 4.14. Map of the annual mean NO₂ differences (µg.m⁻³) between D3 and D2 results.

Looking at the spatial distribution of the annual mean NO₂ differences, it is notorious the influence of the LC interpolation process on the simulation grids. The highest resolution from the domain 3 better resolves the geographic location of the LC categories and, consequently, an improved representation of the main emission sources and amount of emitted pollutant is expected. Hence, higher positive differences of NO₂ concentrations (up to 2 µg.m⁻³) in pollution hotspots were found, which, to a certain extent of the domain 2 results, are not properly captured, or even not identified. For the Aveiro and Figueira da Foz municipalities more pronounced positive differences occur near the large industrial point sources, whereas for Coimbra, the resulting LC characterization and associated road traffic activity were determinant for raising the NO₂ concentrations over the domain 3. In contrast, for the surrounding area of these hotspots, higher concentrations were estimated for the domain 2 (negative differences up to 2 µg.m⁻³), probably due to the way the emissions were spatially distributed by the simulation grids, attributing a more uniform pattern to domain 2. As a support to this information, Figure 4.15 presents the annual mean NO₂ differences between D3 and D2 for each dominant LC category.

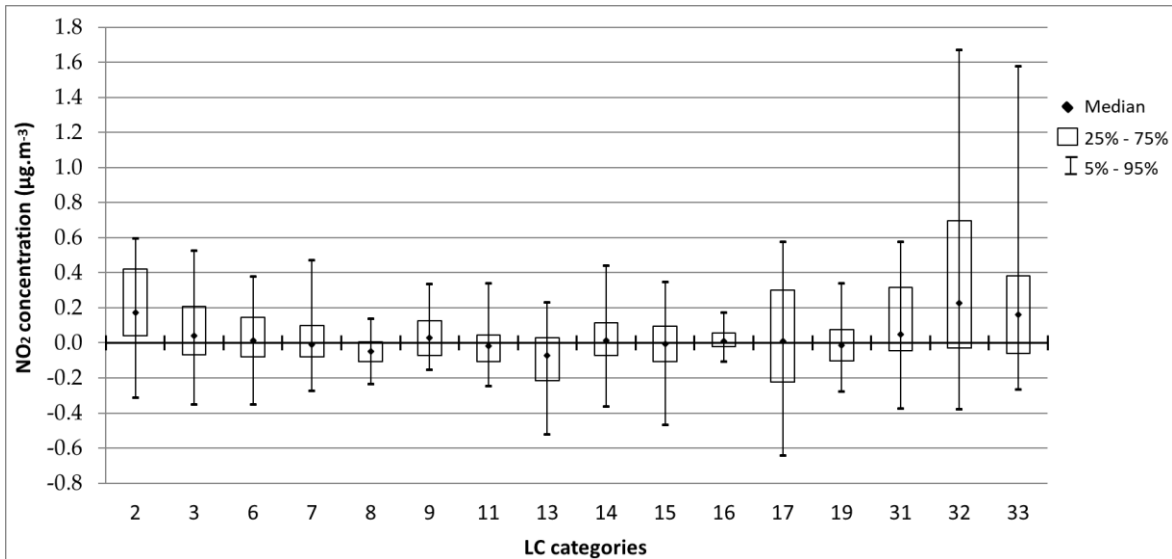


Figure 4.15. Annual mean NO₂ differences (µg.m⁻³) between D3 and D2 grouped by dominant LC category. For the legend of LC categories, see Figure 4.13.

The dominant LC categories for the D3 cells, mainly the classes 32 and 33 (high-intensity residential and industrial or commercial, respectively), contributed to higher NO₂ values in relation to the D2 estimates (positive differences).

As mentioned before, this test represents the base model setup that was applied for producing NO₂ results to be used as background conditions for the air quality modelling at local scale. In the next section, it is presented the model evaluation for the D2 and D3 domains, in order to select the domain that will provide outputs to the local air quality modelling.

4.2.2. Model evaluation

The hourly predicted NO₂ levels for D2 and D3 were compared with observations from air quality stations common to both simulation domains, taking into account the station type. In total, results for seven locations representing air quality stations (inside the Coimbra region - Figure 4.3) are presented: 2 rural (FRN, MOV), 2 suburban (ILH, TEI), 1 urban (IGE) and 2 traffic (AVE, COI). Figure 4.16 shows the variability of the hourly observed and modelled NO₂ concentrations on these sites.

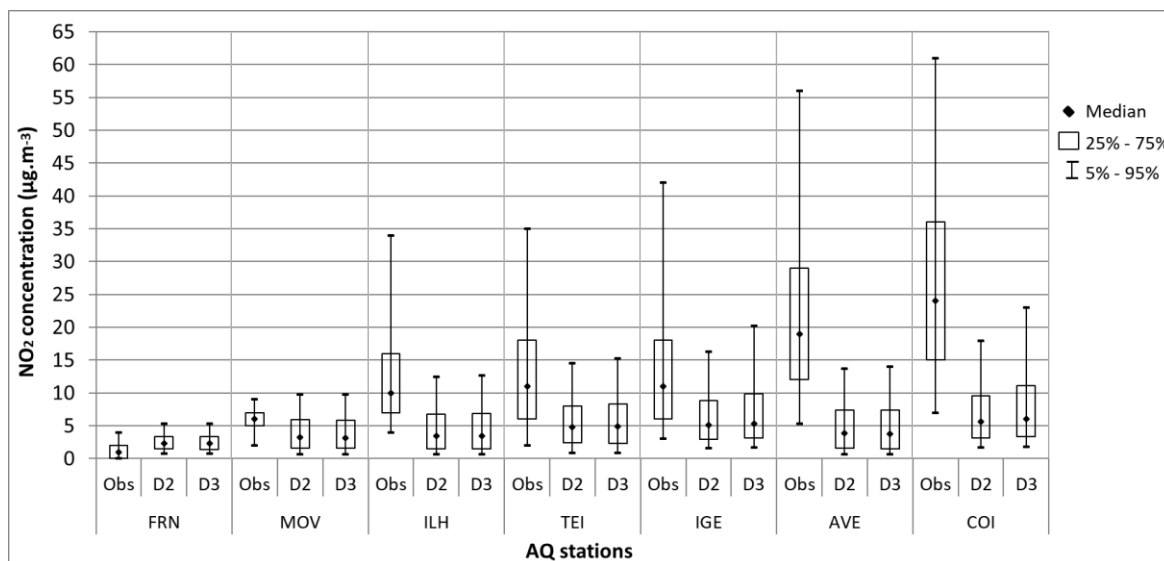
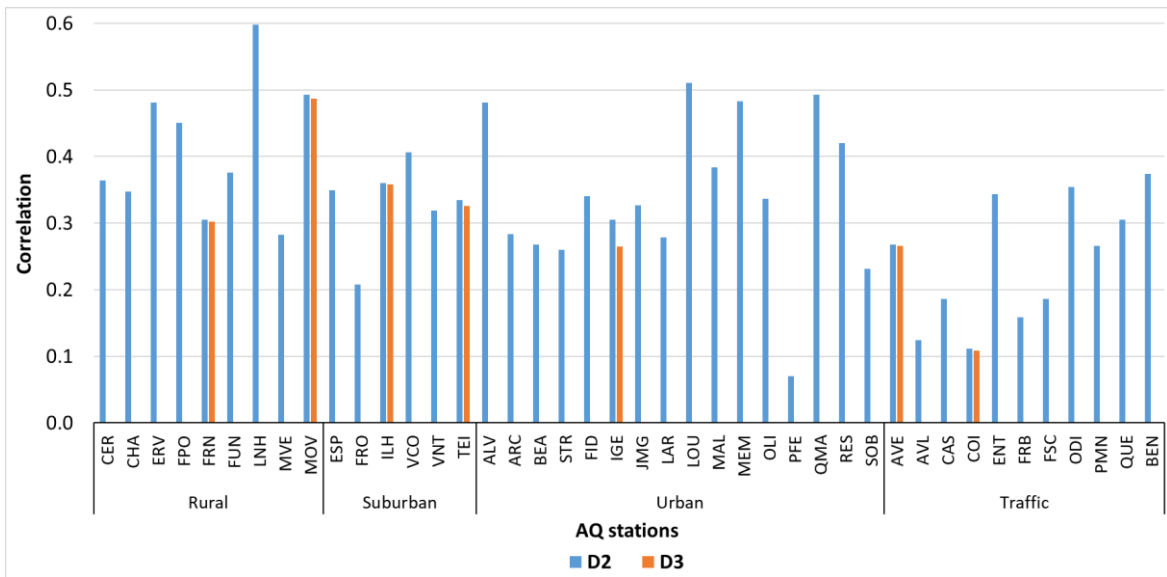


Figure 4.16. Boxplot of the hourly NO₂ concentrations (µg.m⁻³) observed (Obs) and modelled in the D2 and D3 domains.

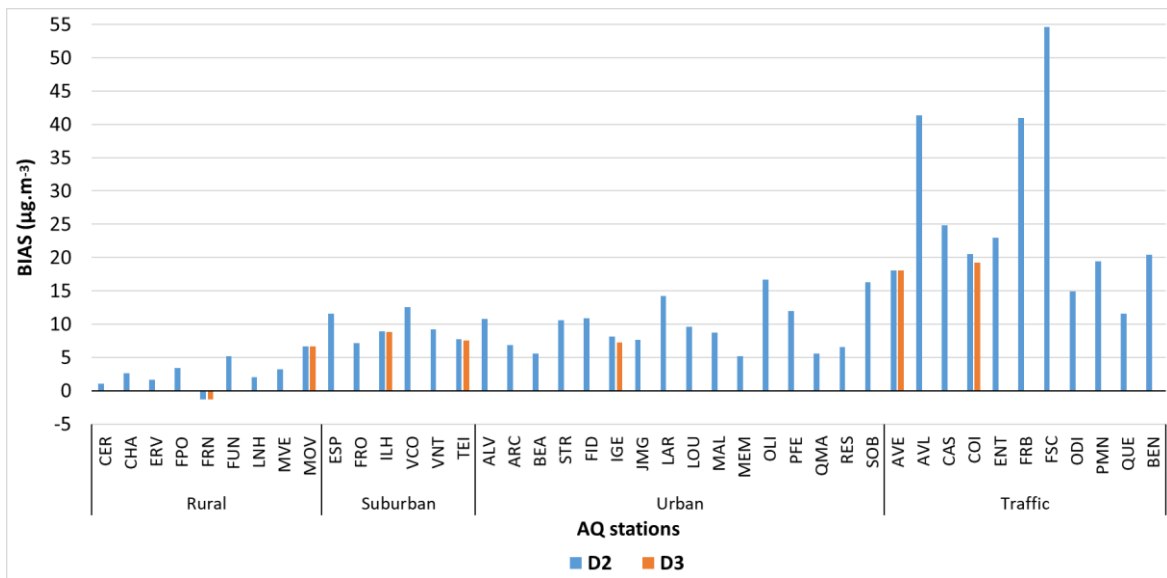
A good agreement between observations and estimates was obtained for background rural locations (FRN, MOV), where the numerical resolution of the processes within the atmospheric boundary layer is easier. In turn, as expected, highest measured values were recorded in traffic stations (AVE, COI), due to the intense road activity and its major contribution to the urban NO₂ pollution. The model was not able to reproduce the magnitude of these values because, despite the reasonable grids resolution to portray urban areas, in particular of the domain 3 (1 km²), the used EI has a resolution (approximately 10 km²) which does not allow to solve urban-scale air pollution patterns. The low resolution of the EI and its use in all simulation domains contributed to the relatively small differences between D2 and D3. Nevertheless, there are other factors that could explain the variability of the modelled data and their underestimation, as the smoothing of areas with complex terrain, omission of emission sources or deficit emission rate, and poorly reproduced meteorological processes. When comparing the traffic stations results with the other typologies, differences between measured and modelled data tend to decrease, demonstrating that the traffic-related NO₂ emissions used for simulating air quality over urban areas with high traffic activity are clearly underestimated. At this scale, specific modelling tools and a detailed characterization of the local emission sources and urban geometry are required.

For a more comprehensive analysis of the agreement between base simulation results and observations, the model performance over the D2 and D3 domains using the entire Portuguese air quality monitoring network (Figure 4.3) was evaluated, considering annual

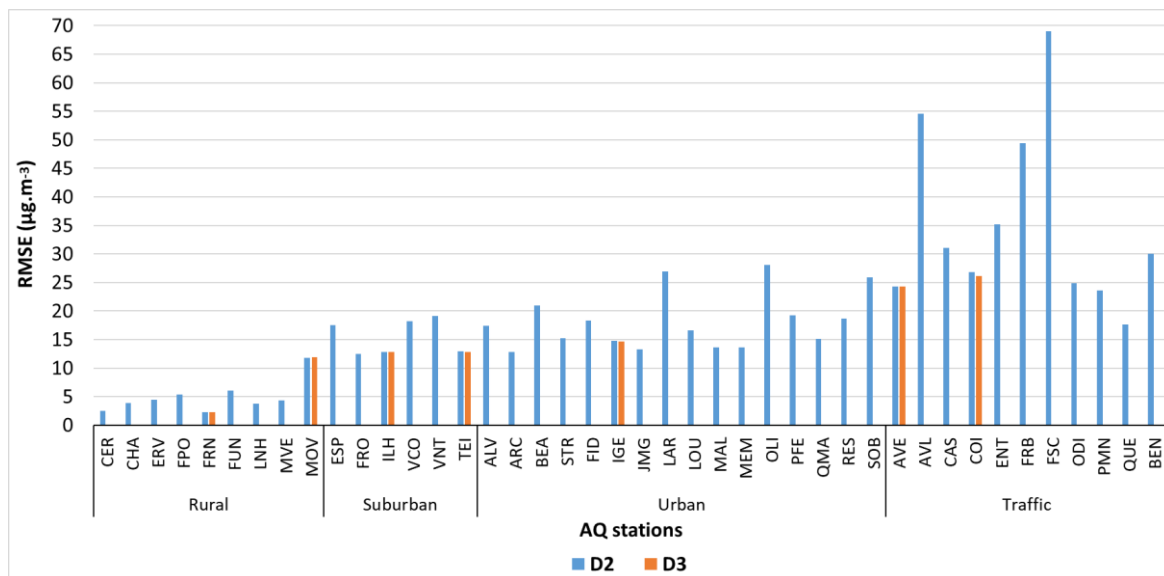
mean NO₂ results for each station, identified by typology, and the following statistical metrics: Pearson’s correlation coefficient, BIAS and RMSE (Figure 4.17).



(a)



(b)



(c)

Figure 4.17. (a) Correlation, (b) BIAS and (c) RMSE between NO₂ observations from the Portuguese air quality monitoring network and the modelled concentrations (µg.m⁻³) for the D2 and D3 domains.

These statistics, in a way, translate the hourly NO₂ results presented in Figure 4.16. Worst performance was found in traffic stations, with lower correlations and higher biases and RMSE. For the reasons previously mentioned, this model behaviour can be largely explained by the geographic location of these stations, since they are strategically positioned over urban street canyons with high traffic activity, and due to the low resolution of the used EI in all simulation domains, which contributed to a poor characterization of the emission sources, mainly for urban/local-scale modelling purposes. In turn, this limited representativeness of the EI, associated to emissions evenly distributed in space and more simplified terrain features were determinant for the best estimates on rural areas, leading to the highest correlations and lowest biases and RMSE. Comparing the modelled results for the sites common to both domains, the increase in the horizontal grid resolution from 5 km² (D2) to 1 km² (D3) did not greatly impact the model performance. However, the bias and the RMSE tend to decrease with the increasing resolution, while a slightly higher correlation was obtained for the lower resolution.

Although there is no clear evidence that shows what is the best model setup/resolution for the analysed simulation domains, the use of D3 outputs to provide background meteorological and chemical conditions for the local scale air quality modelling was adopted, because in the relationship with the LC, dominant urban categories aggregated for higher resolution cells and potential air pollution hotspots are better represented.

4.3. Air quality modelling at local scale

Local scale air quality modelling assumed a prominent role in the modair4health system development, because the local domain is the focus of this multiscale system. Thus, in this section, the VADIS model setup and used input data that characterize the local case study's urban structure are described. The response of the VADIS CFD model to certain traffic emission profiles was also evaluated, crossing modelled NO_2 concentrations with observations from a traffic influence monitoring station.

4.3.1. VADIS setup and input data

The local case study, as mentioned in Section 4.1, is located in one of the busiest road traffic areas of the city of Coimbra (Fernão de Magalhães Avenue), covering an area of 600 m x 600 m, where air pollution hotspots, in particular NO_2 , are expected to occur. The urban structure that influences the flow and dispersion of air pollutants in this geographic area was designed using a GIS software. In total, 125 buildings and 34 road segments were drawn in parallelepiped sections, considering also the average building heights (Figure 4.18).



Figure 4.18. Spatial representation of the local case study's urban structure (buildings volumetry and streets configuration) considered for the VADIS simulations. The traffic influence monitoring station used to evaluate the model performance is also identified.

The tallest building, with 49 m, served as a reference for defining the urban canopy, where atmospheric processes are solved by the CFD model. Thereafter, these geographic features, represented by their vertices and buildings height, were introduced into the VADIS preprocessing tool, which prepares these data as an input for the VADIS simulations.

The model was applied over the case study domain using a 3-D uniform grid resolution of 4 m and hourly resolution to produce NO₂ estimates for two simulation periods:

- winter (26th January to 1st February 2015);
- summer (15th to 21st June 2015).

It should be noted that the definition of the domain dimensions, grid resolutions and geometrical characteristics of the buildings and road segments including their orientation, were based on the COST 732 guidelines for CFD simulation of flows in urban environment (Franke et al., 2011).

The simulation periods were selected taking into account the seasonality, very connected to the local weather conditions and to daily activity patterns, and the highest NO₂ concentrations measured in the traffic station located in the Fernão de Magalhães Avenue (marked in Figure 4.18) for the year 2015. This traffic station, hereinafter referred as COI station, is in operation since 2008, and measures, in continuum, PM10, NO, NO₂, NO_x and carbon monoxide concentrations. Figure 4.19 shows the prevailing wind regimes that were simulated by the WRF-Chem model for the geographic location of the local case study and simulation periods.

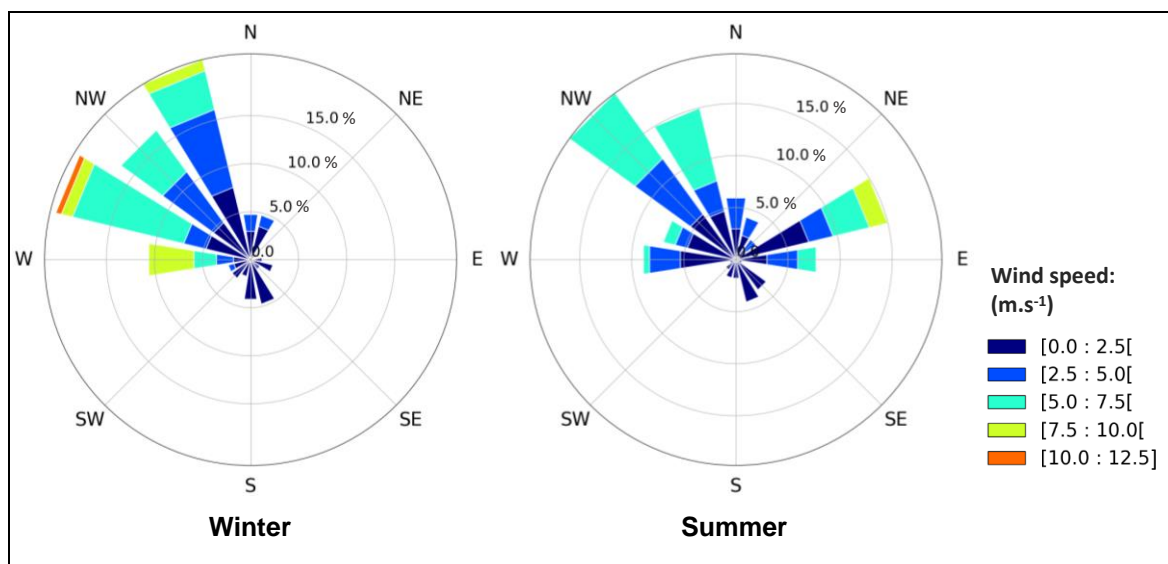


Figure 4.19. Wind roses that characterize the direction and speed wind simulated by WRF-Chem for the geographic location of the local case study and winter and summer simulation periods.

In winter, the wind mainly blew from the northwest sector, with wind speed values that achieved 10.9 m.s^{-1} (31st January at 12 p.m.), and an average of 3.5 m.s^{-1} . For the summer period, winds were predominantly from northwest and northeast, with an average wind speed of 3 m.s^{-1} , reaching a maximum value of 8.5 m.s^{-1} (18th June at 6 a.m.).

High resolution WRF-Chem meteorological results (D3), namely 2 m air temperature and 10 m wind fields (direction and wind speed), were used for VADIS initialization. For quantifying the impact of the road traffic activity on local NO_2 concentrations, traffic-induced NO_2 emissions estimated by the TREM model and then allocated to each road segment (REF information in Appendix D), were also included in the model setup. In order to account for the pollutant fraction that is not emitted within the case study, the WRF-Chem urban background NO_2 concentrations (1 km^2 resolution) extracted from grid cells that intersect the local domain were added to the VADIS NO_2 results.

Regarding the local traffic emissions, since their temporal evolution is very relevant, two methodologies were tested aiming to better represent their behaviour:

- **REF_def:** seasonal traffic profiles based on observed NO concentrations in the COI station during a 10-year period (2008-2017). The use of the NO levels as a traffic tracer can be explained by its suitability to portray the traffic-related air pollution around the COI station, since it is mainly directly emitted from traffic sources, while NO_2 is essentially a product of NO oxidation. For the area of interest, these profiles were constructed by season, considering hourly averaged concentrations for each season during the analysed 10-year period. Figure 4.20 shows the seasonal traffic emission profiles for the VADIS simulation periods: winter (Dec – Feb) and summer (Jun – Aug).

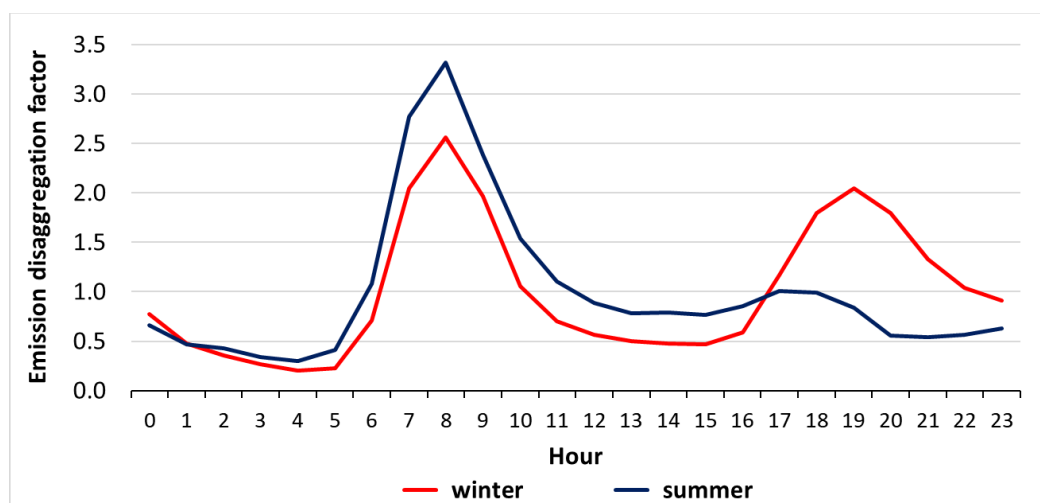


Figure 4.20. Seasonal traffic emission profiles (winter and summer) designed for the influence area of the COI station.

In winter a bimodal distribution is well visible, with two road traffic activity peaks, in the early morning and late afternoon, with people going and returning from their activities. At night, there might also be some influence from local domestic heating. During summer, the traffic volume is distributed in the afternoon, because it is a holiday period and activity patterns are different, with people going to the coastal areas in the morning.

- **REF_adj**: adjusted traffic profiles based on observed and modelled NO₂ concentrations. Emission disaggregation factors are automatically processed every hour when running the VADIS model, by applying the following equation:

$$Factor(h) = \frac{(OBS_h - MOD_h)}{\sum_h^N (OBS_h - MOD_h) / N} \leftrightarrow$$
$$If MOD_h > OBS_h \leftrightarrow Factor(h) = 0 \quad (Eq. 4.2)$$

Where:

Factor (h) is the emission disaggregation factor for each road segment and hour of the day (h = 0, ..., N = 23);

OBS_h corresponds to the observed NO₂ concentration (µg.m⁻³) in the COI station at each hour h;

MOD_h represents the WRF-Chem NO₂ concentration (µg.m⁻³) for each hour h at the location of the COI station.

The REF_adj approach is only applicable if observed and modelled background data for the local domain are available. Moreover, when the background is higher than the observations, a zero factor is assumed; therefore, no emission for these hours is considered and, consequently, the modelled NO₂ concentrations will only reflect the WRF-Chem background values.

4.3.2. Model evaluation

In this section, the modelled NO₂ concentrations for both simulation periods using the two emission temporal disaggregation approaches were evaluated based on COI station measurements. Looking at the time series (Figure 4.21), a better agreement between observations and modelled concentrations was reached with the REF_adj approach, slightly improving in the winter period.

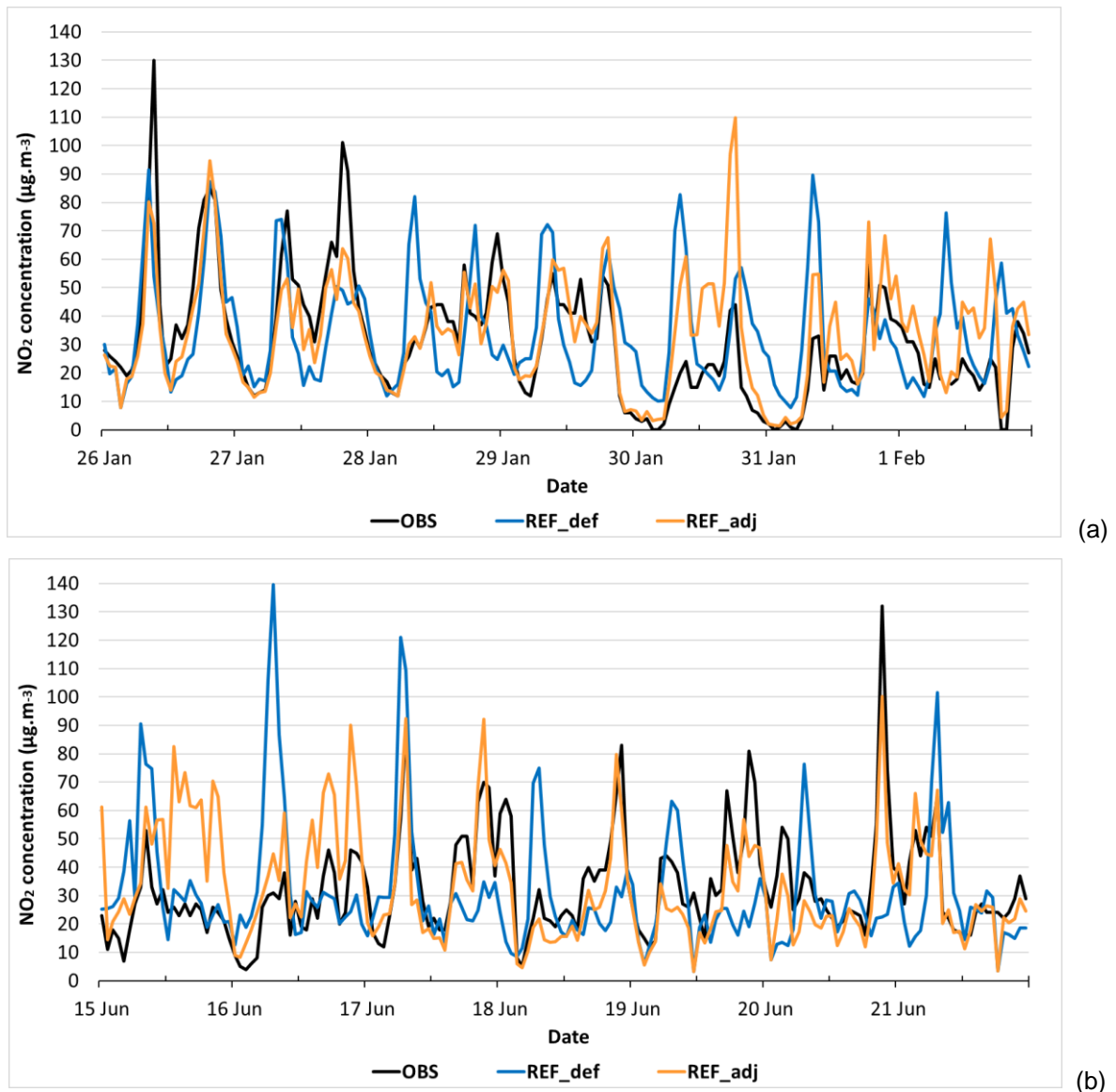


Figure 4.21. Time series of hourly observed and modelled NO_2 concentrations ($\mu\text{g.m}^{-3}$) in (a) winter and (b) summer periods considering the two approaches used for temporal disaggregation of traffic emissions: REF_def and REF_adj.

The overestimation of the REF_adj-based NO_2 concentrations in certain time periods (e.g. 30th January) occurred due to the higher background values (MOD_h) than NO_2 concentrations recorded at the COI station (OBS_h). In these cases, only WRF-Chem NO_2 estimates were considered.

In terms of daily profiles of NO_2 concentrations (Figure 4.22), based on hourly averages for each simulation period, as expected, when crossing this information with the contents of Figure 4.20, a similar curve for both periods using the REF_def approach was obtained, since chemistry is not considered (no chemical reactions) in the VADIS CFD model.

Relating the observed and modelled NO₂ concentrations, it is evident the remarkable role attributed to the REF_adj approach, which presents a very strong agreement with the observations. Using seasonal traffic-based profiles (REF_def), a clear overestimation of local NO₂ concentrations is observed in the early morning, because higher emissions (i.e. highest factors in Figure 4.20) were allocated to that time of the day.

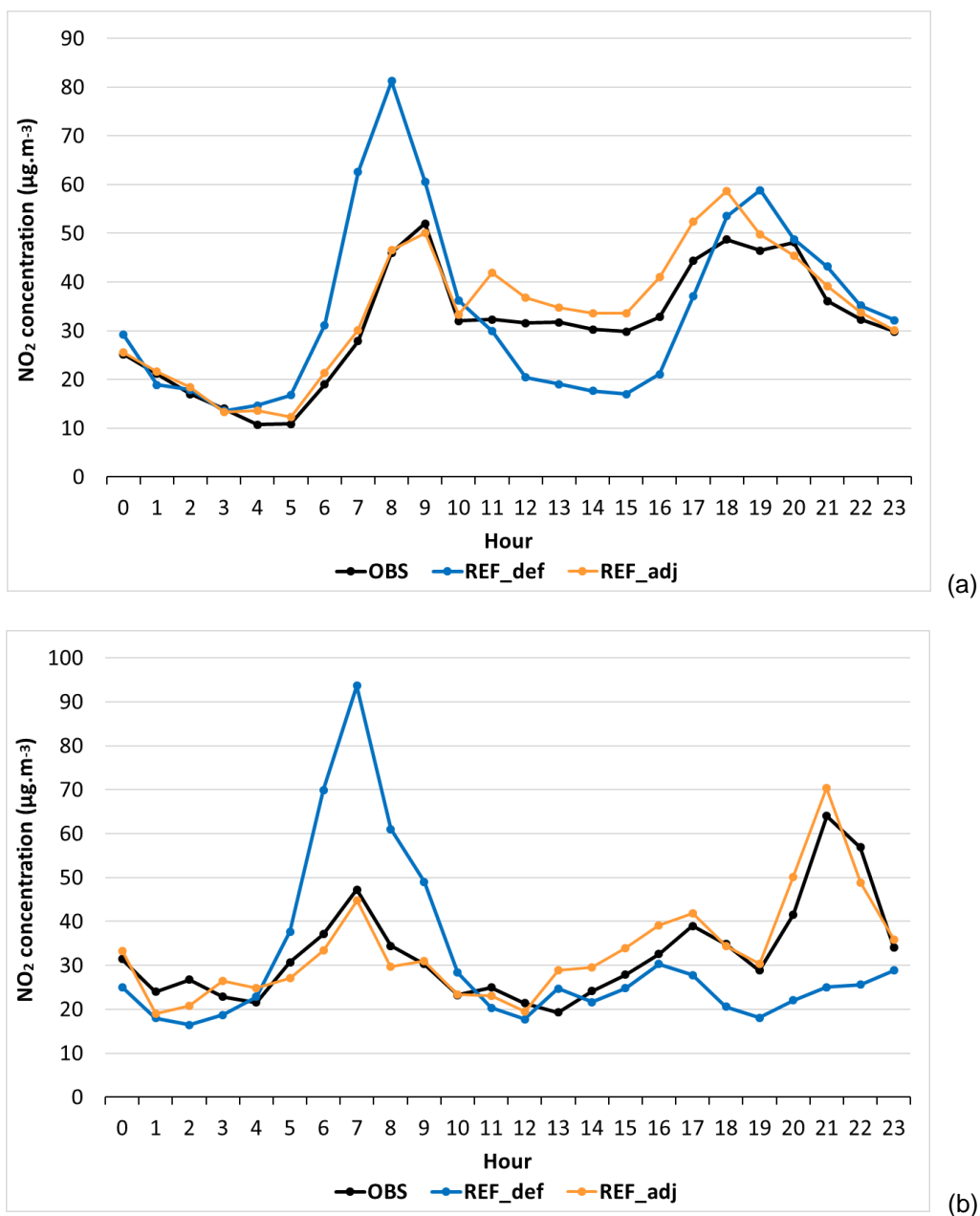


Figure 4.22. Daily NO₂ profiles including observations and modelled NO₂ concentrations (µg.m⁻³) in (a) winter and (b) summer periods, considering the two approaches used for temporal disaggregation of traffic emissions: REF_def and REF_adj.

To complement the previous analysis, the statistical performance of the model results was evaluated through the coefficient of determination (R^2) (Figure 4.23).

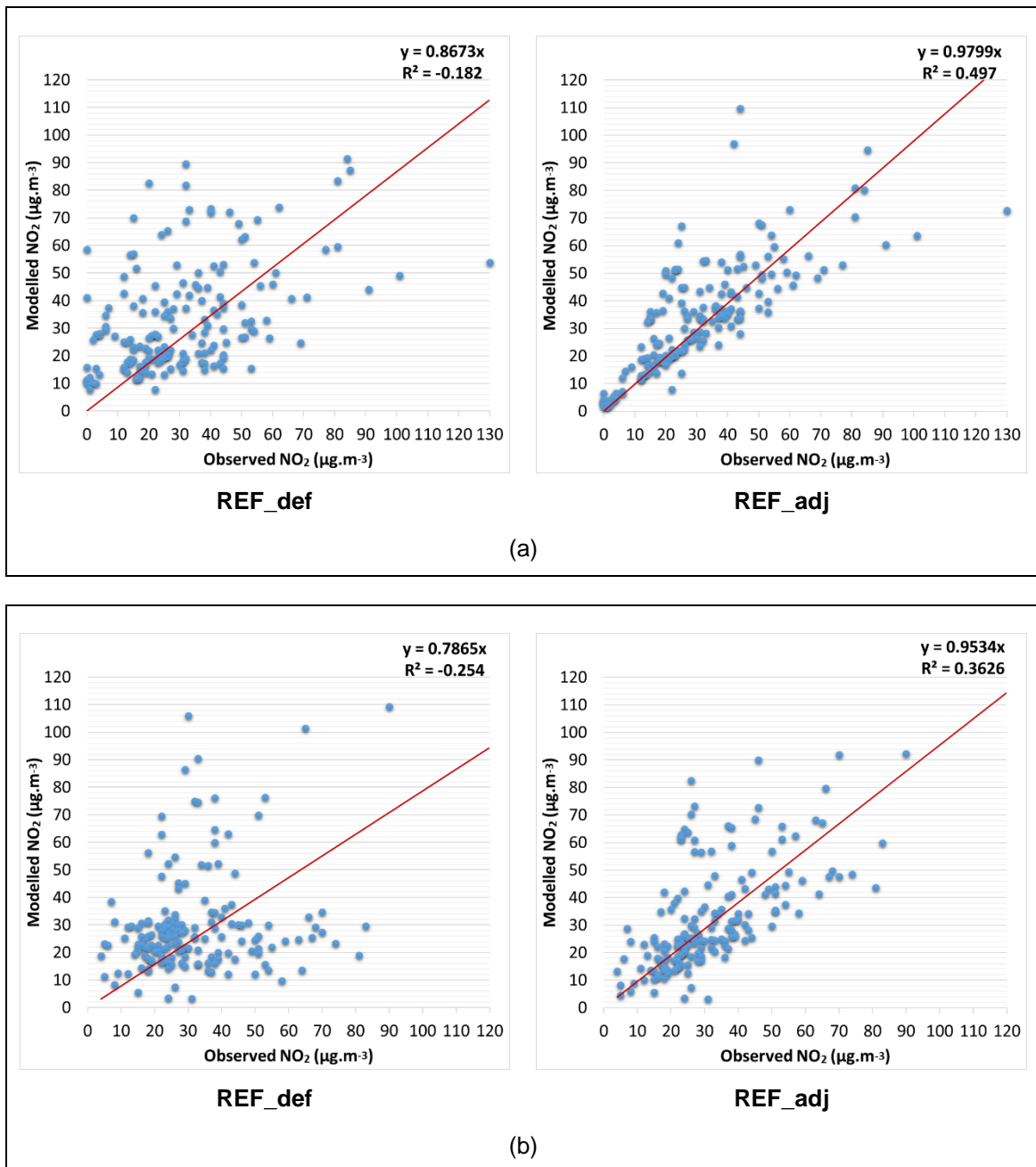


Figure 4.23. Correlation between observations and hourly modelled NO₂ concentrations (μg.m⁻³) in (a) winter and (b) summer periods, considering the two approaches used for temporal disaggregation of traffic emissions: REF_def and REF_adj.

Overall, the best performance to reproduce local NO₂ concentrations was achieved with the REF_adj approach, in particular for lower values, slightly worsening in the summer period,

probably due to the transport of polluted air from other regions, added to the CFD model outputs as WRF-Chem background concentrations. Negative R^2 associated to the REF_def approach indicates that modelled NO_2 concentrations do not follow the trend of the observations. It means, therefore, that the use of seasonal traffic profiles poorly fits resulting NO_2 estimates to local reality.

In summary, the modelled NO_2 results using the REF_adj approach showed a better agreement with the measurements, demonstrating their suitability to be used as an input for quantification of health impacts. Therefore, the option for this automated approach is recommended as long as the observations for the case study and modelled background values are available for the simulation periods.

4.4. Quantification of health impacts

Health impacts of ambient NO_2 pollution are expected to be greatest in urban areas, characterized by high NO_2 concentrations and population density. When the objective is to evaluate effects associated to frequent and high NO_2 pollution events, short-term human exposure studies may be more important than the variability of NO_2 concentrations over time (i.e. long-term mean exposure). For these reasons, health impacts derived from NO_2 pollution were quantified for the case study and simulation periods, considering health indicators that relate this pollutant with short-term human exposure. Therefore, in this section, the selected health input metrics based on these indicators are described, and then, they are used as inputs for application of the linear and non-linear AirQ+ methodologies and subsequent estimation of damage costs. A comparative analysis of the main results is presented.

4.4.1. Selected health input metrics

According to the survey of epidemiological and economic studies (Table 2.3), the following health input metrics associated to short-term NO_2 exposure were included in the HIA performed over the case study: health indicator, affected age group, reference period for NO_2 concentration, CRF (as RR), baseline rate and damage cost (Table 4.4).

Table 4.4. Health input metrics used to assess health impacts from short-term human exposure to ambient NO₂ concentrations.

Health indicator	Age group	Reference period	RR (95%) per 1 ug.m ⁻³	Baseline rate (%)	Damage cost Price (€)	Unit
Respiratory hospital admissions	All ages	Daily maximum	0.1002 (0.0999 - 0.1004)	0.05	8960	Case (8-days average duration)
Mortality (all natural causes)	All ages	Daily maximum	0.1003 (0.1002 -0.1004)	0.977	1844	YLL

Among these metrics, for each health indicator, the chosen RR function determines which potentially affected age group and reference period for NO₂ concentrations should be analysed. Regarding the RR functions, due to the lack of epidemiological evidences over the target geographic region, those recommended by the WHO (central value) were used (WHO, 2013a), whereas the baseline mortality and disease incidence rates were obtained from country statistics (URL2, URL3). In terms of affected age groups, total resident population data at the subsection level, extracted from the Portuguese National Statistics Institute (INE) (URL10), were used and disaggregated to the local case study's grid horizontal resolution (4 m²) (Figure 4.24).



Figure 4.24. Spatial distribution of the total resident population per grid cell (4 m² horizontal resolution) for the local case study.

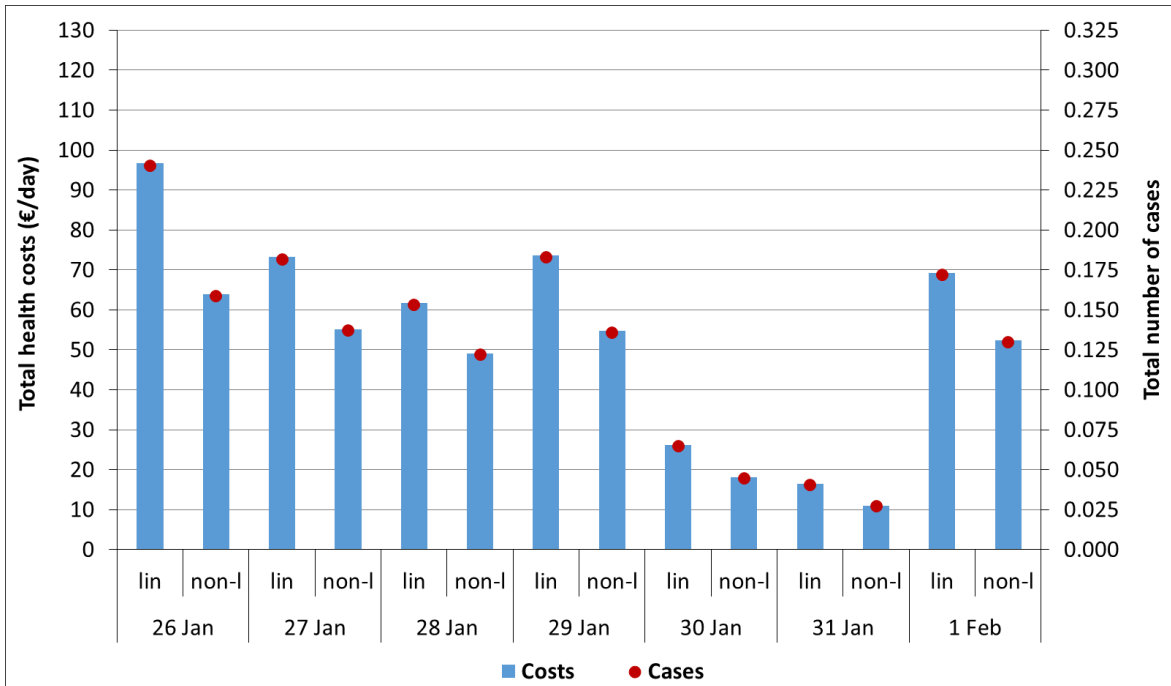
In total, 2005 residents were identified. To estimate the short-term human exposure, daily maximum NO₂ concentrations for the simulation periods and an exposure threshold (i.e. counterfactual concentration value) of 10 µg.m⁻³, were considered. The use of this threshold, above which physical health impacts are calculated, is suggested by the WHO (URL1).

Finally, to quantify the overall health damage costs resulting from the number of cases of disease or premature deaths that were estimated, cost figures (per case and YLL) based on Pervin et al. (2008), and updated for the reference year (2015) were considered. Nevertheless, since short-term health impacts are quantified on a daily basis, these costs were converted to the same time scale.

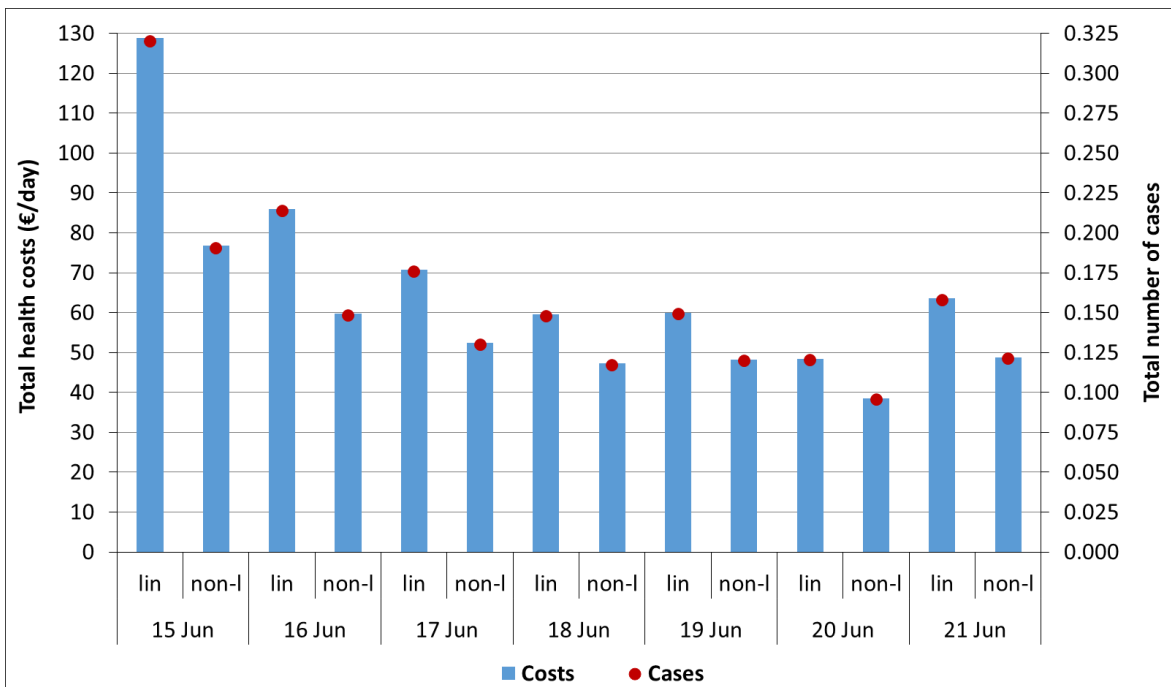
4.4.2. Comparative analysis of the health impact methodologies

Given the inherent uncertainty and high variability embedded in HIA studies, the results using different assumptions and methodologies need to be evaluated and communicated. Thus, based on the selected health input metrics, the linear and non-linear AirQ+ methodologies were applied to the local case study for the winter and summer periods, with the purpose of evaluating the number of unfavourable cases and health costs attributed to the short-term (daily) human exposure to ambient NO₂ concentrations. However, for each health indicator, due to the small dimensions and very fine resolutions of the case study, the health results hereinafter presented were quantified assuming that 1 % of the exposed population is vulnerable to both analysed health indicators (i.e. baseline rate equal to 1 %). For such a small area, this approach is reasonable to get a good screening of potential health impacts.

Figure 4.25 shows the daily total health impacts for the whole simulation domain including the sum of the two health indicators.



(a)



(b)

Figure 4.25. Daily total health impacts, translated in number of cases and damage costs due to short-term NO₂ exposure, for the (a) winter and (b) summer periods using the linear (lin) and non-linear (non-l) AirQ+ methodologies.

In general, estimated health impacts are higher using the linear approach, and the daily variability is directly related with the spatial distribution of the daily maximum NO₂

concentrations. Therefore, on the day-to-day analysis, the highest total number of cases and associated costs resulted from the combination of higher values of gridded population data (Figure 4.24) with daily maximum NO₂ concentrations. In contrast, the lowest values on 30th and 31st January 2015 occurred because a large part of the simulation domain presented daily maximum NO₂ levels below 10 µg.m⁻³ (i.e. exposure threshold), so no health impacts were calculated for these grid cells. Summing up the health impacts for each simulation period, in winter 415 € total health damage costs (1.04 cases) were estimated using the linear approach, whereas more moderate damages were obtained applying the non-linear method (305 € health costs and 0.76 cases). In the summer period, the total health results were slightly higher: 515 € and 370 € health damages (1.28 and 0.92 cases), using the linear and non-linear approaches, respectively. In average, each attributable case has a daily cost of 400 €.

As a support to the information provided in Figure 4.25, the Figure 4.26 gathers daily health outputs for the two simulation periods, with regard to the total number of estimated cases comparing the two AirQ+ methodologies. Of the exposed vulnerable population (1% of the residents), the range of daily attributable cases varies between 0.03 using the non-linear method on 31st January, and 0.32 applying the linear method on 15th June. Another aspect to note is the point where the line slope changes (0.16, 0.12), from which larger differences in number of cases tend to increase, leading to linear method-based values often overestimated with increasing NO₂ concentrations.

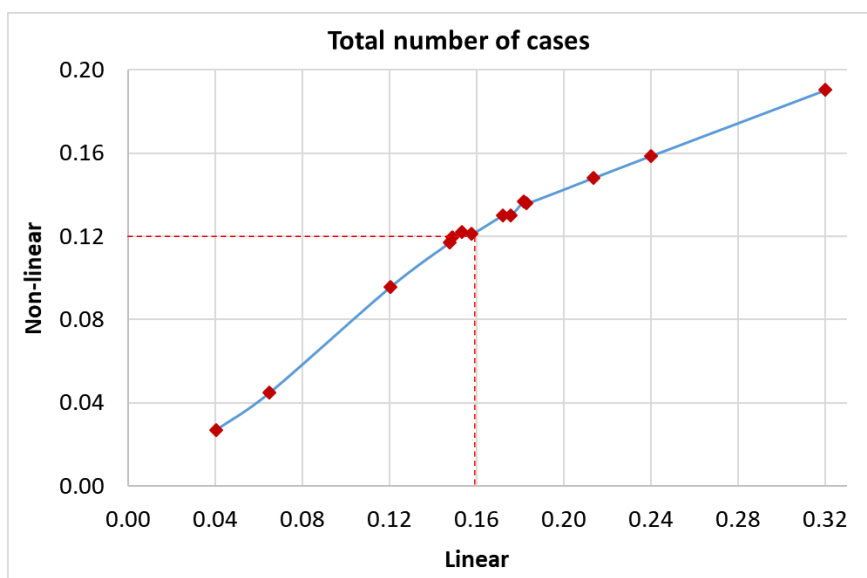


Figure 4.26. Total number of cases estimated for the winter and summer periods comparing the linear and non-linear AirQ+ methodologies.

Focusing on the health estimates for the days of each period with higher total differences comparing both approaches, 26th January and 15th June, there is a clear spatial relationship between the ambient NO₂ concentration (when combined with population data) and the health cost differences (linear – non-linear) (Figure 4.27). Thus, making this link, the linear AirQ+ methodology presents larger health costs for grid cells with higher population and daily maximum NO₂ concentration records. In turn, the more spatially pronounced cost differences on 15th June reflect the highest total difference among health approaches that was estimated over the simulation domain (Figure 4.25).

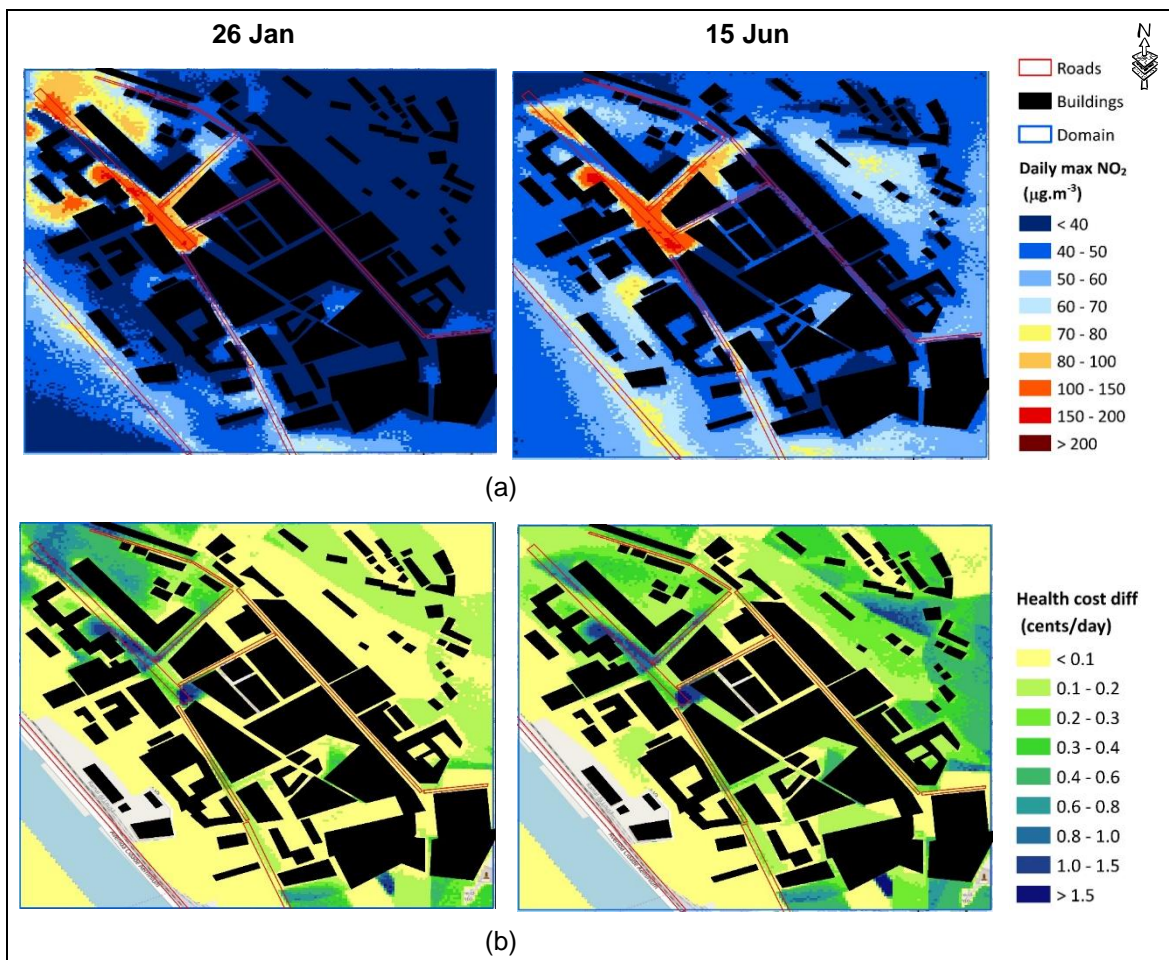


Figure 4.27. Spatial representation of the (a) daily maximum NO₂ concentrations (μg.m⁻³); and (b) short-term health cost differences (cents/day) between AirQ+ methodologies (linear – non-linear) for the local case study of 26th January (on the left) and 15th June (on the right).

The lowest health results using the non-linear AirQ+ methodology seem to be better adjusted to the local reality, mainly for higher NO₂ concentrations, where the linear model is associated to large overestimates of health impacts. In view of these conclusions, the

option for the non-linear methodology is recommended, especially when high ambient air pollution concentrations are recorded.

4.5. Summary

The application and assessment of the modair4health system contributed to identify some more appropriate configurations and input data for the multiscale simulations. In terms of base modelling setup, the WRF-Chem online model was applied over three nested domains (25, 5 and 1 km² resolutions) for the year 2015, and the inclusion of a new LC database and the aerosol effect represent the recommended options. The air quality and meteorological fields resulting from the inner domain were used as input to calculate flows and dispersion of air pollutants in the urban structure, considering a smallest domain with much finer resolution (local case study with 4 m grid spacing). For this purpose, the VADIS CFD model was applied for two simulation periods: one week in winter and another one in summer. To reproduce the behaviour of traffic emissions, an automated approach was considered the best option for local scale air quality modelling. The link with the health was tested for the case study using the two AirQ+ methodologies to quantify short-term human exposure effects. Lower health outcomes using the non-linear approach seem to be better adjusted to the local reality, and its use is recommended, mainly for high pollutant concentrations.

Chapter 5

Air quality and health management

5.1. Selected air pollution management strategies

5.2. Evaluation of the chain of impacts

5.2.1. Atmospheric emissions

5.2.2. Air quality

5.2.3. Human health

5.3. Summary

5. AIR QUALITY AND HEALTH MANAGEMENT

The conception of this chapter was meant towards the assessment of the modair4health system capabilities and its operability to support decision-makers and stakeholders in selecting the best strategies for urban air quality and health management. To that end, two traffic management scenarios were selected and tested over the local case study for the two simulation periods previously identified, in order to evaluate the entire chain of impacts: atmospheric emissions, air quality and human health. As a result, potential benefits with the implementation of these scenarios are expected regarding local pollution control and health improvement of the exposed population.

5.1. Selected air pollution management strategies

The definition of air pollution management strategies to be tested over the local case study was based on:

- the road traffic sector is the major air pollution source and the main contributor for high NO₂ levels;
- the existence of sustainable urban mobility plans for the Coimbra region, which include traffic management and control measures, incentives to electric mobility, promotion of smooth modes, among other mobility proposals (CIM-RC, 2018, 2016);
- air quality improvement measures that have been successfully implemented in other Portuguese regions (e.g. Lisbon, Porto), or in the European context, with a high degree of efficiency and social acceptability (e.g. Borrego et al., 2011; Duque et al., 2016; Miranda et al., 2015).

Two of the most common traffic management options in urban areas were selected:

- (i) replacement of 50% of the vehicle fleet below the European emission standards (EURO) 4 (registered until the end of 2004) by electric vehicles (hereinafter referred as ELEC) that produce little local air pollution, and the engines are much more efficient than conventional internal combustion engines;
- (ii) introduction of a Low Emission Zone (LEZ) in the Fernão de Magalhães Avenue (identified in Figure 5.1), with an extension of approximately 830 m, where the circulation of vehicles below EURO 4 and trucks is banned.

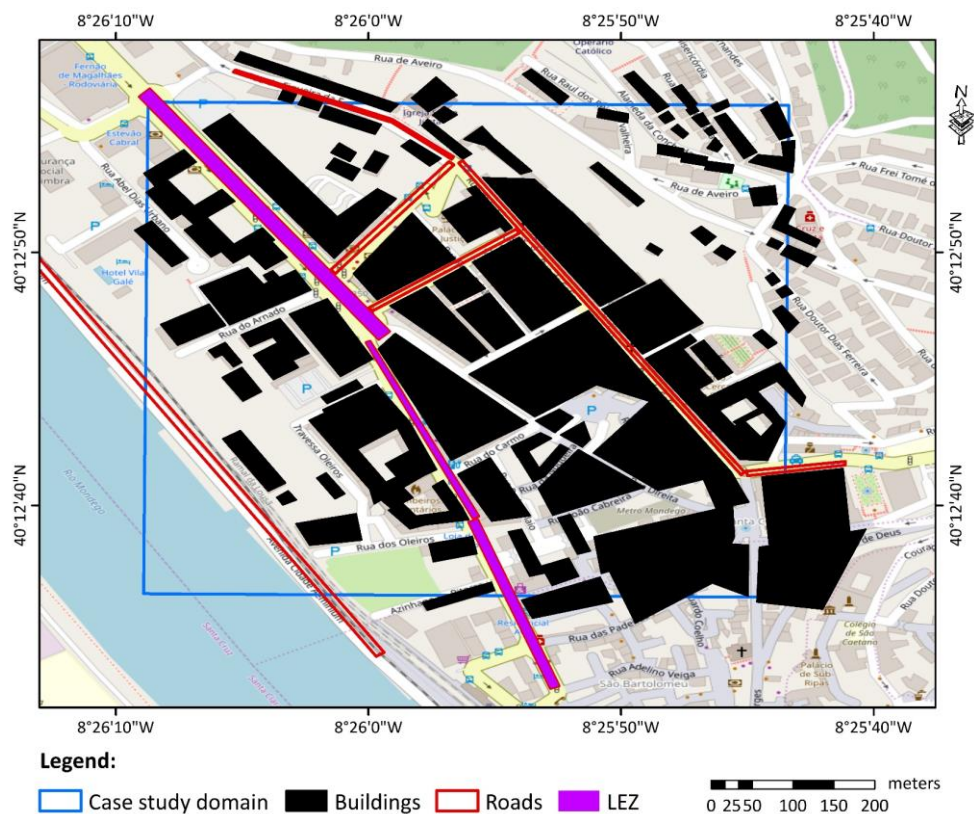


Figure 5.1. Spatial representation of the Fernão de Magalhães Avenue LEZ.

The electric mobility has been expanding rapidly, leading many countries to adopt a variety of measures to encourage the change from conventional to electric vehicles (EV), such as incentives for their acquisition, and strengthening the EV’s charging network and autonomy. In 2018, the global EV fleet exceeded 5.1 million, up 2 million more than in the previous year and almost doubling the number of new EV sales (IEA, 2019).

Regarding the LEZs, their introduction has been regulated in many developed cities of European and Asian countries, restricting the total or partial circulation of vehicles in certain periods of the day. This air pollution management strategy has low implementation and operation costs, and it is often considered as the most effective measure that local entities can take to improve the air quality of their cities (URL15; Wang et al., 2017).

5.2. Evaluation of the chain of impacts

To evaluate the impacts chain resulting from the selected traffic management options, a Scenario Analysis Approach (SAA) was applied to the local case study and simulation periods previously analysed in the base scenario (hereinafter referred as REF), using the methodologies and base modelling setup adopted and presented in Chapter 4. SAA is a

systematic method widely used to estimate the impact of air pollution sources, from changes in emissions to social value impacts (air quality, health, environment, economy) (Miranda et al., 2016; Relvas and Miranda, 2018). The Figure 5.2 illustrates the entire chain of impacts to be evaluated following a SAA.

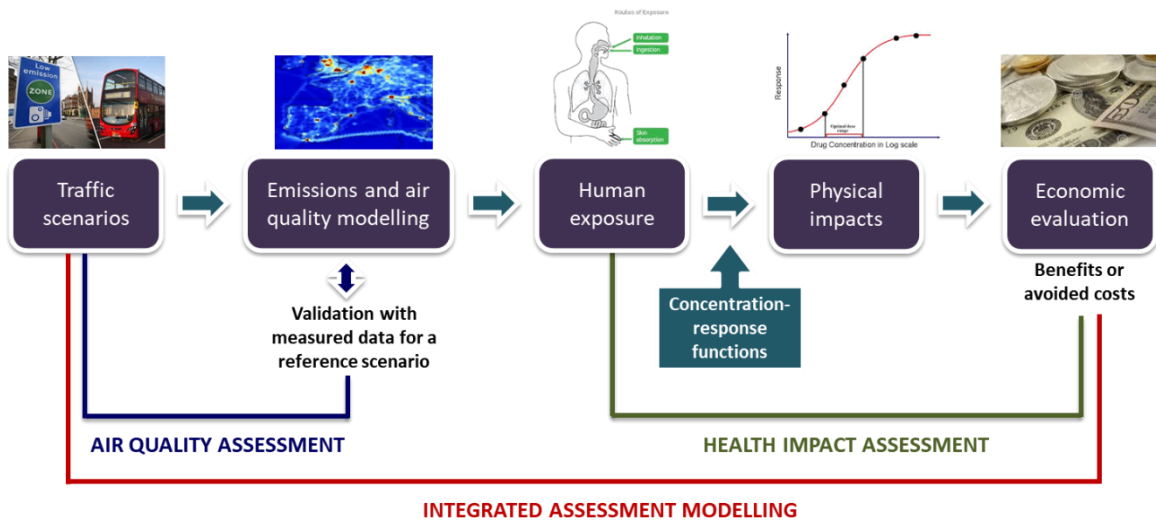


Figure 5.2. Diagram of the chain of impacts associated to the selected traffic management options, to be evaluated following a SAA.

The main SAA steps for the integrated assessment of the impact of traffic scenarios (ELEC and LEZ) can be grouped as follows:

- *Air quality assessment*
 - (i) to compute NO₂ emissions for the traffic management scenarios;
 - (ii) to model how these changes in atmospheric emissions will change spatial and temporal NO₂ concentrations;
- *Health impact assessment*
 - (iii) to assess the human exposure resulting from the NO₂ concentration changes;
 - (iv) to quantify the total avoided physical health impacts with the expected air quality improvement;
 - (v) to value these impacts in monetary terms considering the different cost components (direct, indirect and intangible costs). Such economic evaluation reflects the benefits or avoided costs of the implementation of the traffic scenarios.

The REF scenario results, validated in Section 4.3.2, were used for assessing the impact of the tested scenarios.

5.2.1. Atmospheric emissions

In urban areas, NO₂ emissions are largely related to the local road traffic activity, incisively contributing to worrying air pollution hotspots. To minimize the adverse effects, over the case study and for the chosen traffic management scenarios, NO₂ emissions in each road segment were recalculated using the TREM model and based on the following assumptions:

- in the ELEC scenario, 50% of the fleet composition below EURO 4 was replaced by electric vehicles, impacting all simulated road segments;
- for the LEZ scenario, fleet composition data were only changed in the road segments that correspond to the Fernão de Magalhães Avenue, banning the circulation of vehicles below EURO 4 and trucks.

As expected, larger NO₂ emission reductions were obtained at the Fernão de Magalhães Avenue, due to its strong road traffic activity. For the whole simulation domain, a reduction in NO₂ emissions of 17.8 (50%) and 7.8 kg.d⁻¹ (22%) was estimated for the ELEC and LEZ scenarios, respectively (Appendix D).

Finally, the estimated emissions for the traffic scenarios were automatically disaggregated for each hour (i.e. using adjusted traffic profiles) when running the VADIS CDF model.

5.2.2. Air quality

The local scale air quality model in the multiscale framework was applied to the traffic scenarios to quantify the impact of NO₂ emission changes on the spatio-temporal patterns of NO₂ concentrations.

Figure 5.3 presents the time series with hourly modelled NO₂ concentrations for the scenarios and for both simulation periods considering the COI station location.

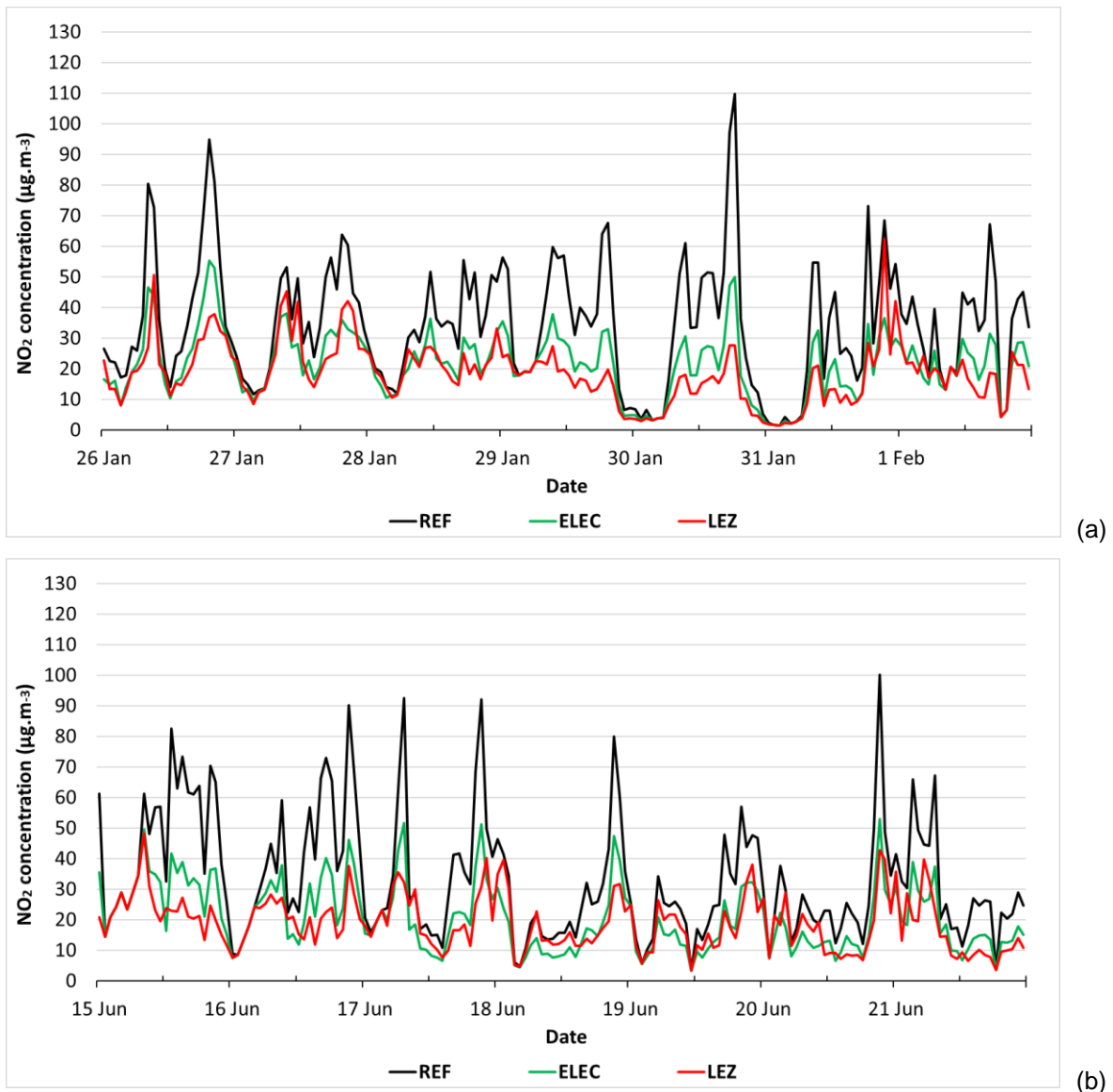


Figure 5.3. Time series of hourly modelled NO_2 concentrations ($\mu\text{g}\cdot\text{m}^{-3}$) in (a) winter and (b) summer periods for the reference and traffic scenarios at the location of the air quality monitoring station COI.

Overall, larger air quality improvements were obtained for the time periods with higher REF NO_2 concentrations, being more evident for the LEZ scenario. In turn, small differences between results of REF and traffic scenarios were found for lower REF NO_2 concentrations, which correspond to the times of the day with low or moderate road traffic activity (noon and night). Therefore, this hourly variability of the modelled NO_2 concentrations is closely related with the traffic emissions and the way these are disaggregated.

Analysing the daily averaged profiles of NO_2 concentrations for the same location and simulation periods (Figure 5.4), local pollution reductions for both traffic scenarios were estimated at all hours, especially in the periods of the day associated to traffic activity peaks.

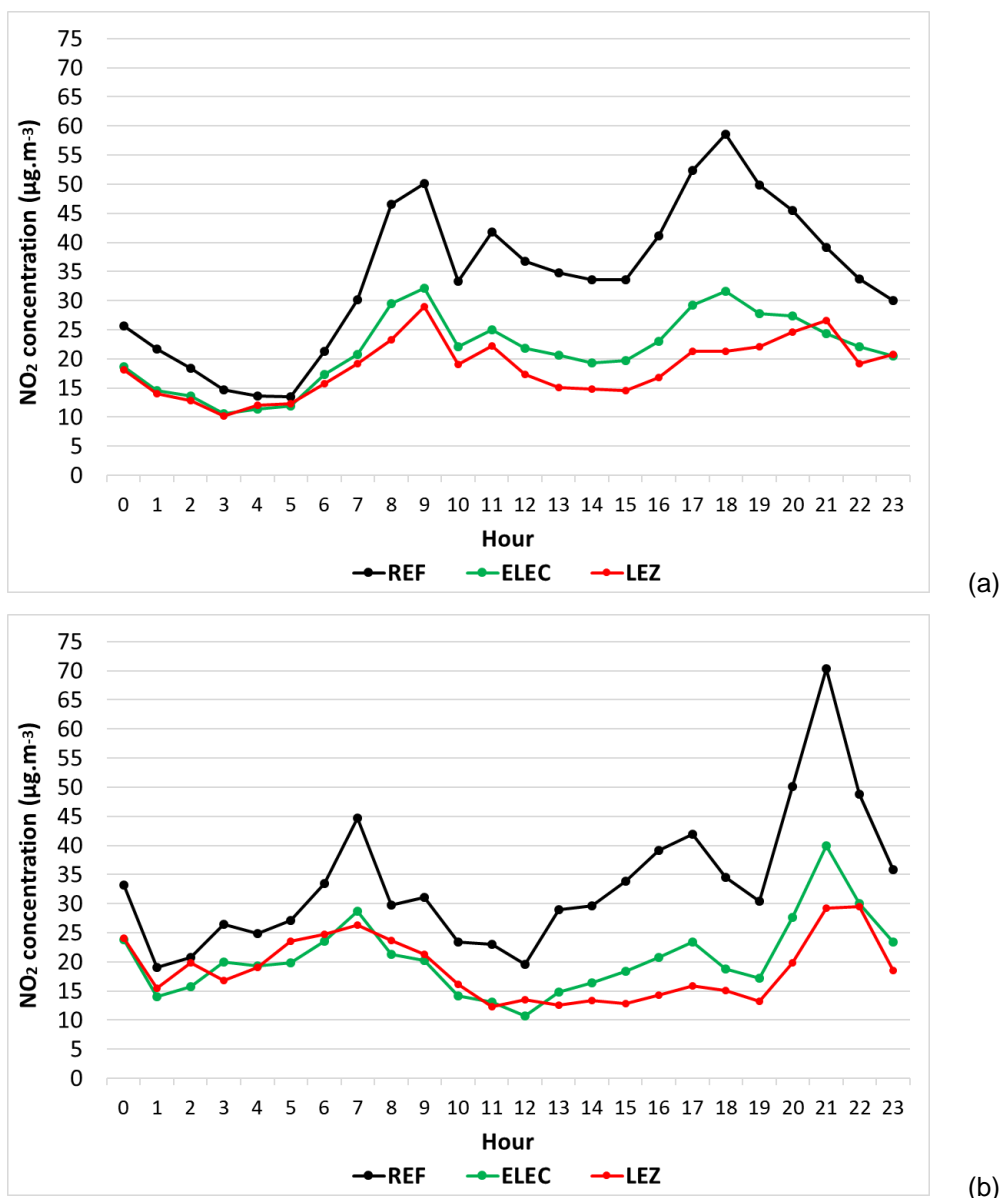


Figure 5.4. Daily averaged profiles of NO₂ concentrations (µg.m⁻³) in (a) winter and (b) summer periods for the reference and traffic scenarios at the location of the air quality monitoring station COI.

For the analysis of the spatial pattern of air quality improvement over the case study, one peak hour for each simulation period was selected (Figure 5.5), taking into account the higher observed NO₂ concentrations and a good agreement between measurements and the REF_adj-based modelled data (Figure 4.21).

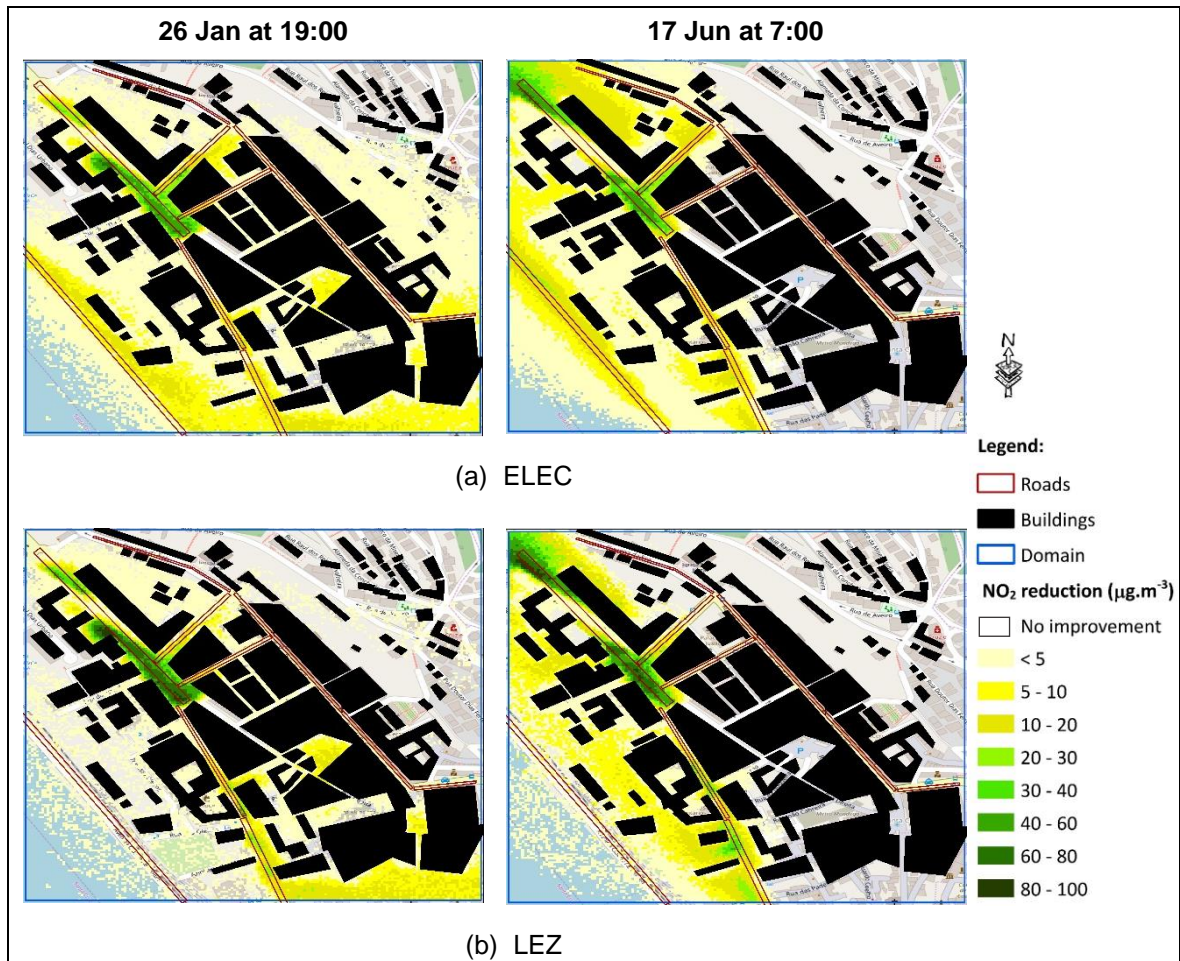


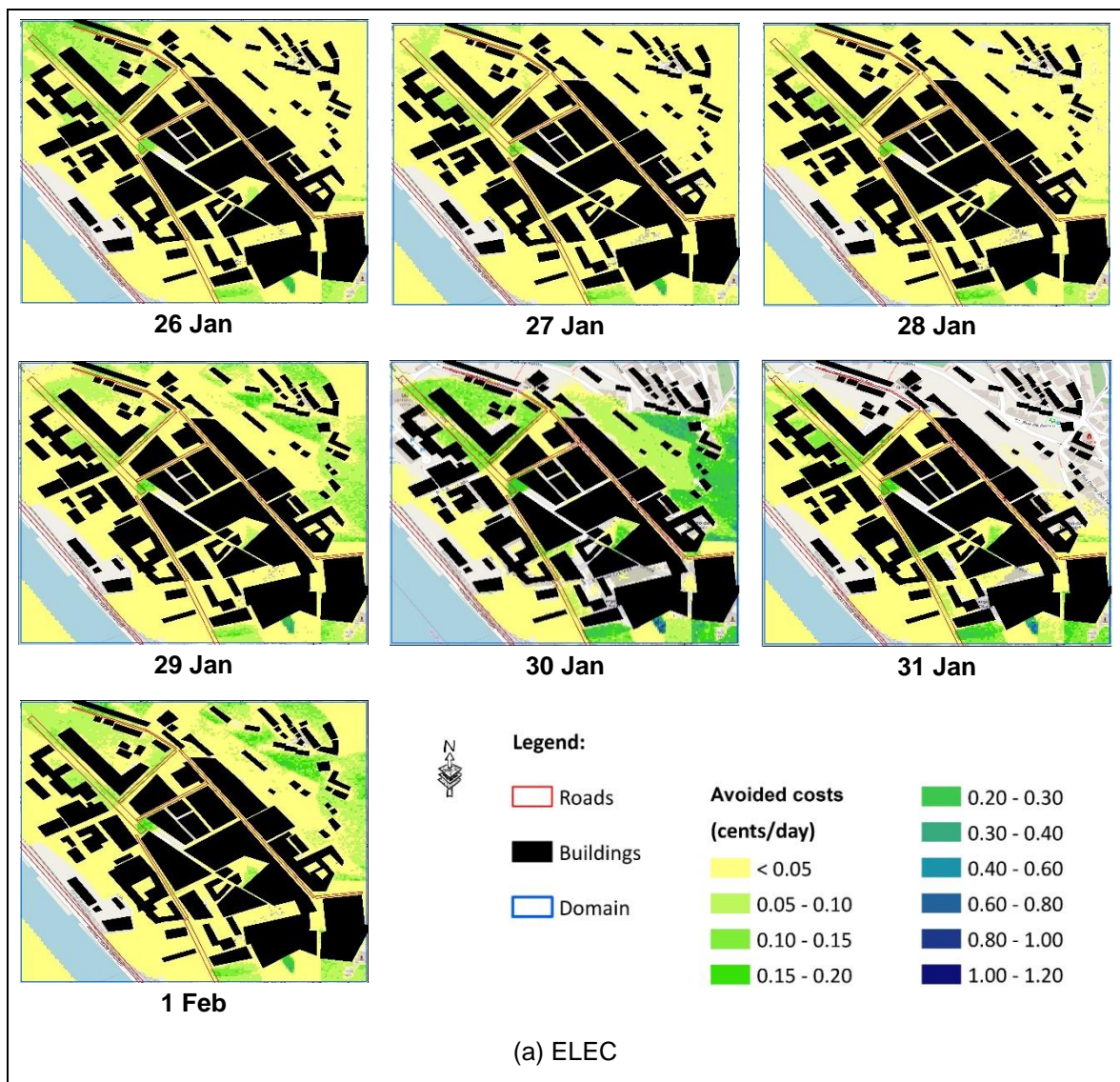
Figure 5.5. Reduction of NO₂ concentrations (μg.m⁻³) (REF minus scenario) on 26th January at 19:00 (on the left) and 17th June at 7:00 (on the right) comparing each tested scenario with the reference: (a) ELEC; and (b) LEZ.

In general, the most relevant air quality improvements in both traffic scenarios were estimated for a part of the Fernão de Magalhães Avenue (up to 100 μg.m⁻³), where REF NO₂ emissions and corresponding reduction for the traffic scenarios were higher (1-3 road segments in Appendix D). Besides the emissions, these air quality estimates were also strongly influenced by the urban geometry (e.g. height and orientation of buildings), which interferes with the accumulation and dispersion patterns of NO₂ concentrations, and by local wind regimes (direction and wind speed) affecting the turbulence. From the point of view of the atmospheric flow, on 26th January at 19:00 and 17th June at 7:00, prevailing winds of northwest and southeast, respectively, and slightly stable conditions according to the Pasquill classification (average wind speed of 1 m.s⁻¹) were recorded.

5.2.3. Human health

Regarding the HIA of the traffic management scenarios for the simulation periods, the non-linear AirQ+ methodology and selected health input metrics were applied to the local case study, in order to quantify the avoided short-term physical health impacts and corresponding monetary savings compared with the reference scenario.

As HIA results, the spatial distribution of potential benefits or avoided costs (REF minus scenario) per day with the implementation of the traffic scenarios is presented in Figures 5.6 and 5.7. For a better understanding of these differences, the health damage costs estimated for the REF are mapped in Appendix E.



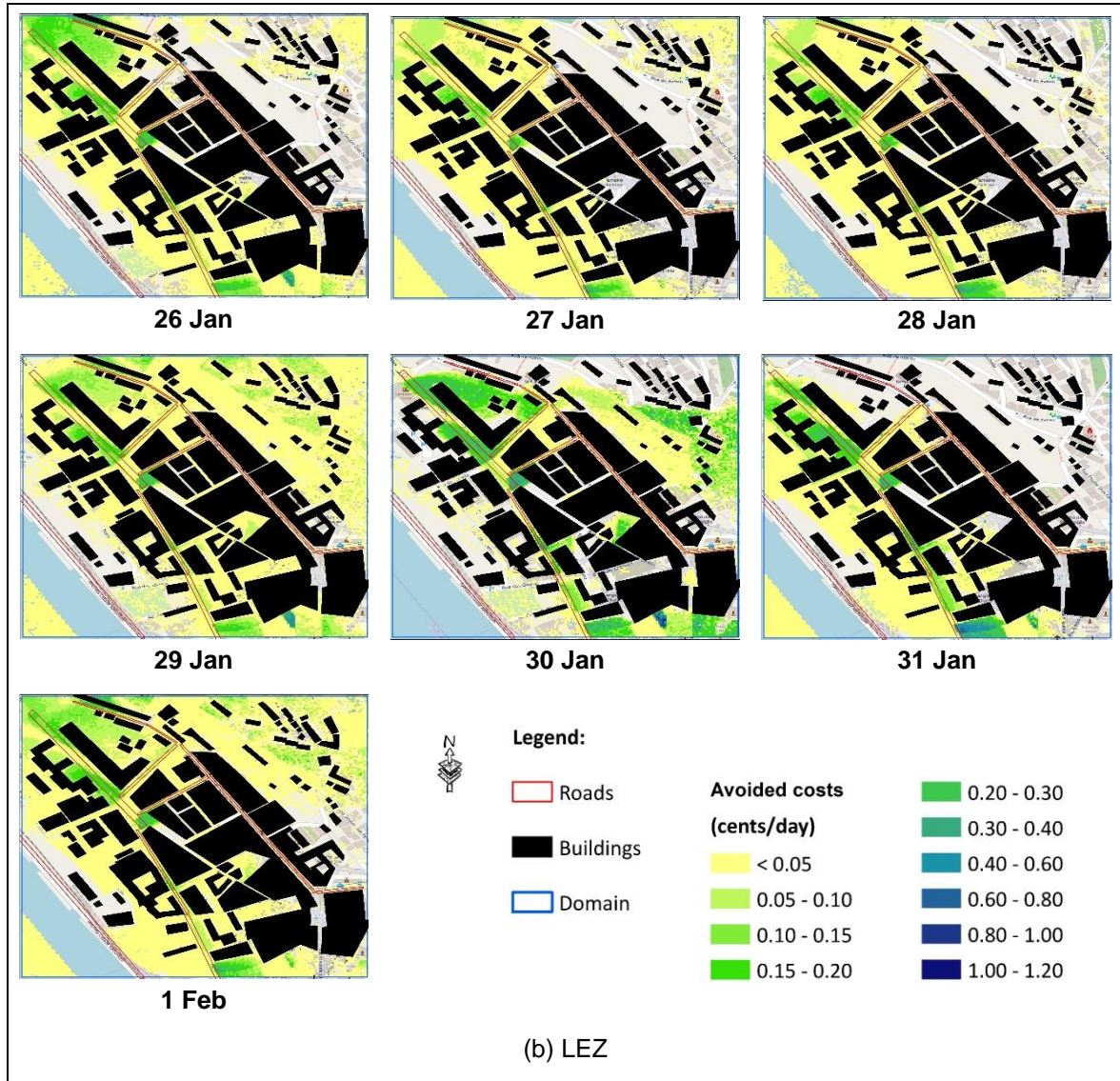
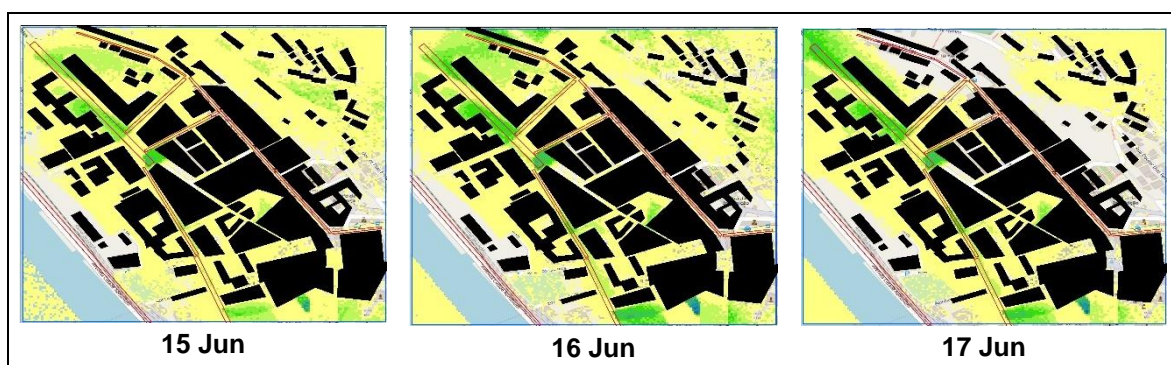
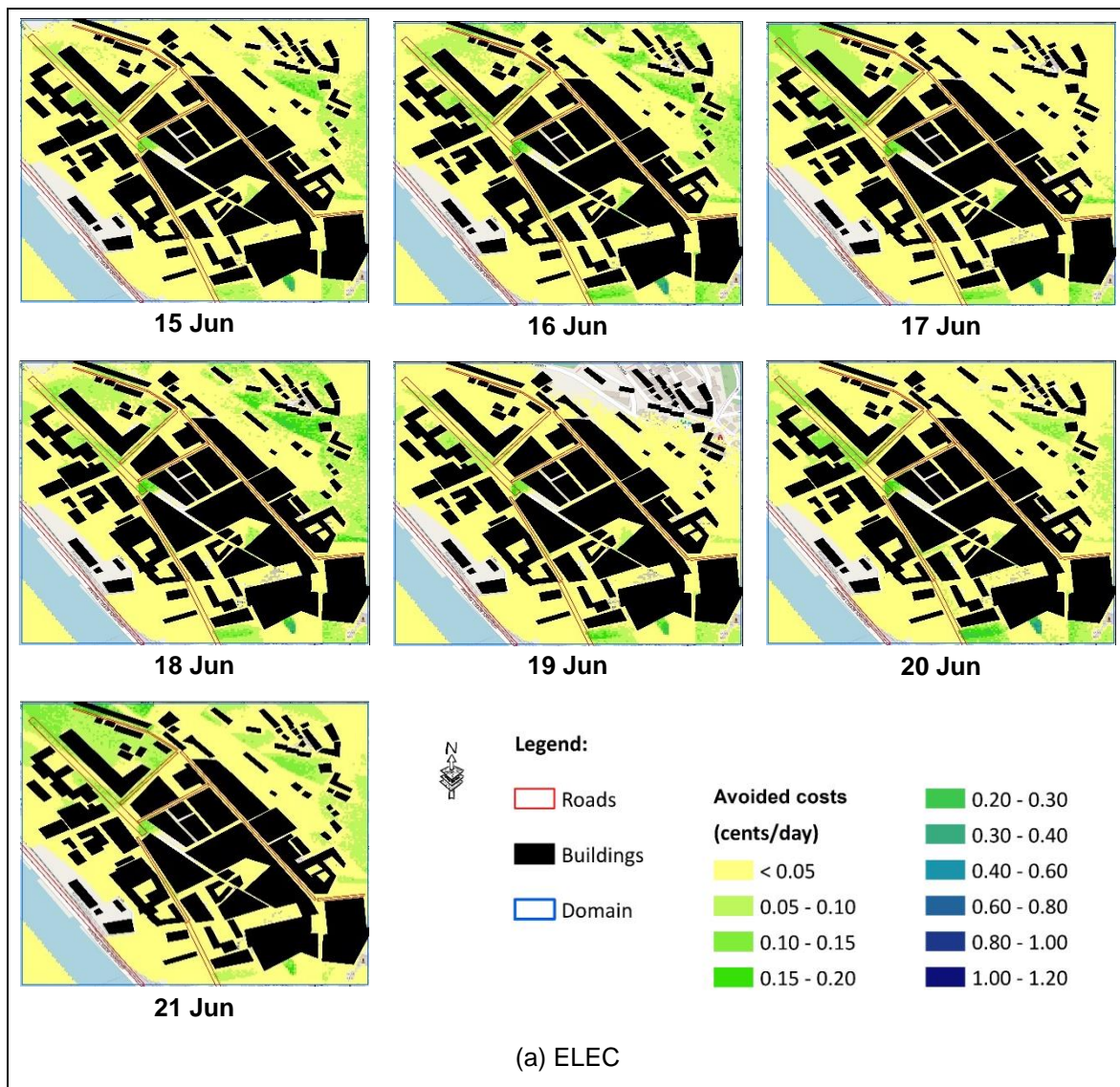


Figure 5.6. Short-term health benefits (cents/day) (REF minus scenario) resulting from the (a) ELEC and (b) LEZ scenarios for the winter period.



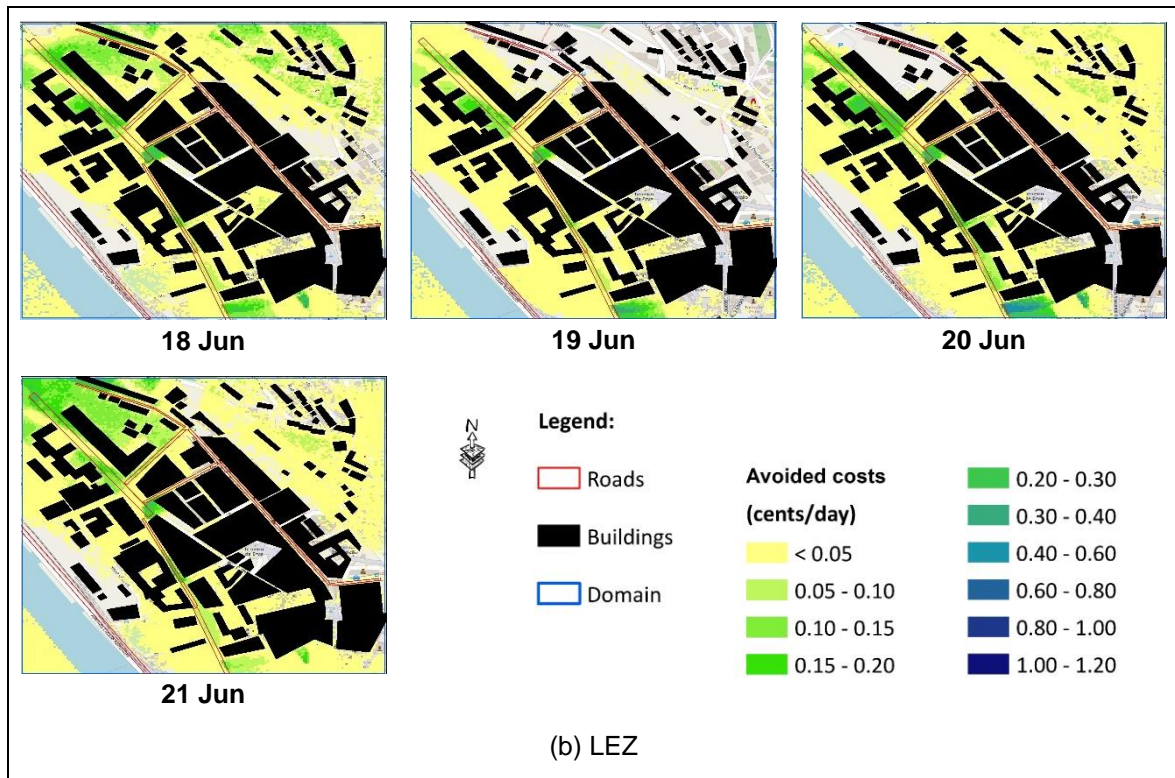
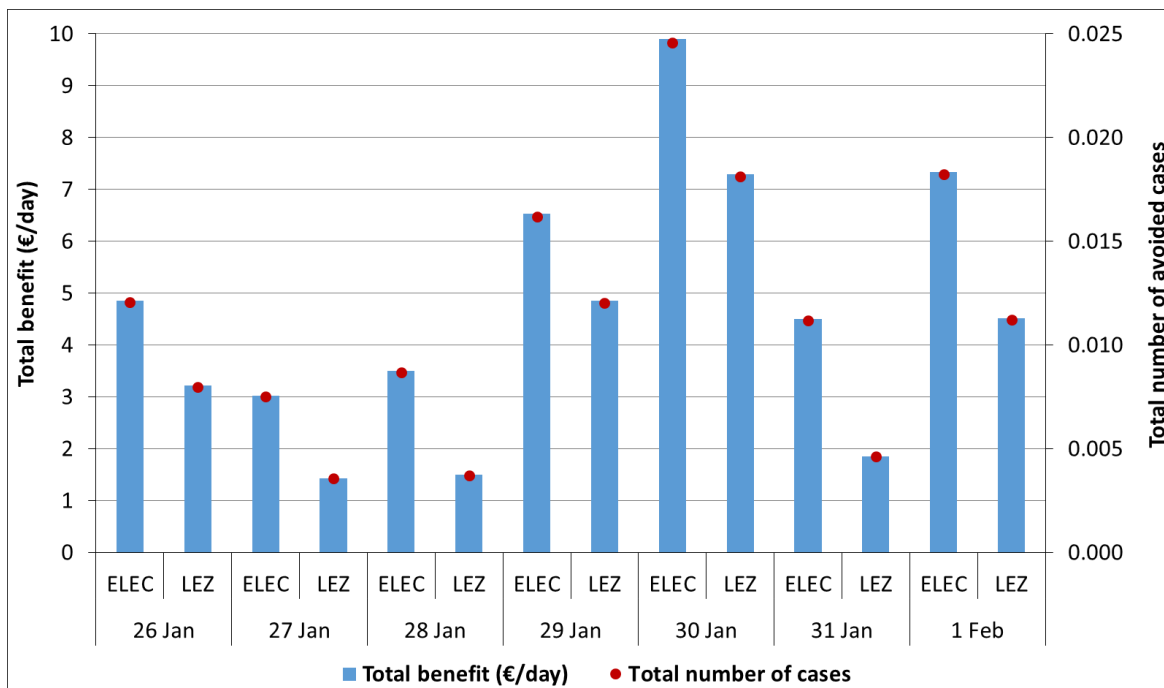


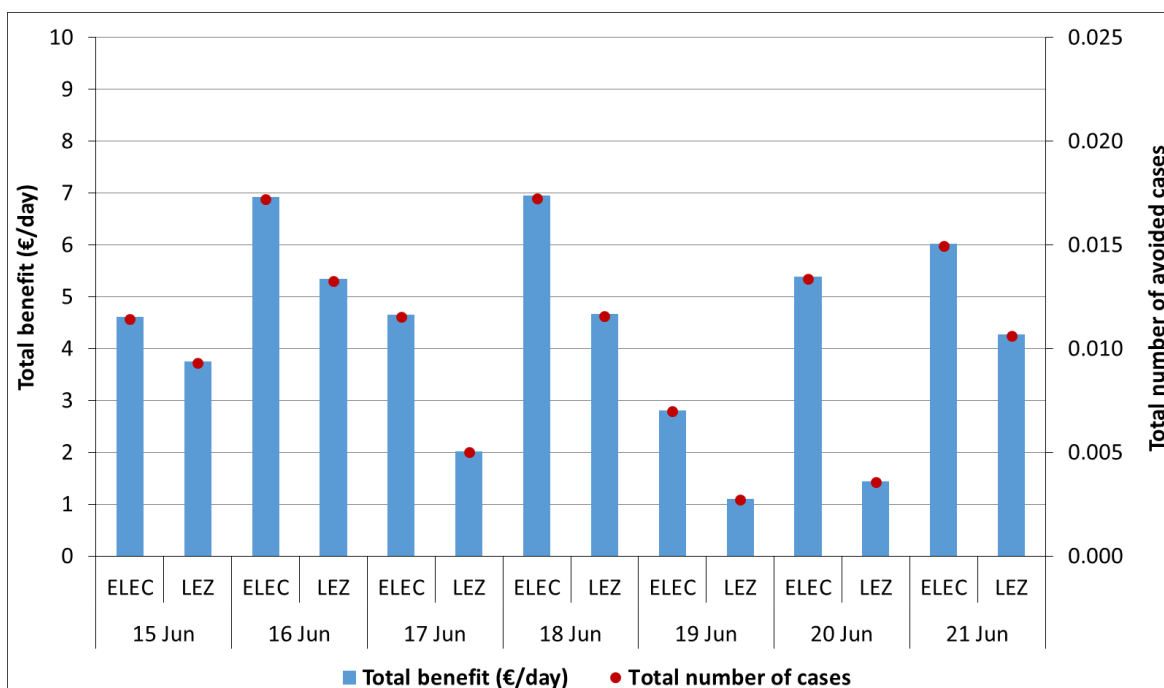
Figure 5.7. Short-term health benefits (cents/day) (REF minus scenario) resulting from the (a) ELEC and (b) LEZ scenarios for the summer period.

This economic evaluation represents the difference of estimated health damage costs between the reference and each traffic scenario, considering the sum of the health indicators impact. Making a comparative analysis of the daily health benefits by scenario, overall, ELEC benefits cover a larger geographic area, because the ELEC scenario resulted in NO₂ emission reductions in all designed road segments. Nevertheless, over the LEZ influence area, higher benefits were estimated, given the wider restrictions for the circulation of road vehicles. These results show the relevance of the NO₂ emission reductions and expected air quality improvement, also influenced by the urban structure and local meteorological fields, in quantifying the daily benefit. However, the air quality improvement, by itself, does not explain the benefit, it has to be combined with population data (Figure 4.24) to get a clear positive impact on the residents' health. Thus, highest health benefits (up to 1.2 cents/day) were estimated in grid cells that combine larger NO₂ improvements and higher population values.

To complement this spatial analysis, Figure 5.8 shows the daily total health impacts avoided in each traffic scenario for the whole domain and simulation periods.



(a)



(b)

Figure 5.8. Daily total avoided health impacts for the (a) winter and (b) summer periods using the ELEC and LEZ scenarios.

Daily estimates indicate a higher total number of avoided cases and associated monetary benefits using the ELEC scenario. Focusing on the simulation periods, in winter, the largest

total benefit in both scenarios was estimated for 30th January, being expected daily health savings of 9.9 € (0.025 avoided cases) and 7.3 € (0.018 avoided cases) for the ELEC and LEZ scenarios, respectively. The lowest impact was calculated for the 27th January, with daily savings around 3 € (ELEC) and 1.4 € (LEZ). In summer, largest monetary benefits were predicted for 16th and 18th June, corresponding to 7 € in the ELEC scenario, and approximately 5 € for the LEZ. Table 5.1 presents total and daily averaged health impacts estimated for the whole simulation domain and for each traffic scenario considering all days of each simulation period – winter and summer.

Table 5.1. Total and daily averaged health impacts estimated in each scenario for the (a) winter and (b) summer periods considering the whole domain.

Scenario	Metric	Winter		Summer	
		Number of avoided cases	Benefit (€)	Number of avoided cases	Benefit (€)
ELEC	Average	0.014	5.7	0.013	5.3
	Sum	0.098	39.7	0.093	37.4
LEZ	Average	0.009	3.5	0.008	3.2
	Sum	0.061	24.7	0.056	22.6

For both metrics, the number of avoided cases and the monetary benefit calculated for the winter period were slightly higher than those estimated for the summer. Comparing the health impacts estimated for the scenarios, the results translate the numbers indicated in Figure 5.8, where the ELEC contributes to larger health benefits.

5.3. Summary

This chapter was designed with two purposes: (i) to evaluate the operability of the developed modair4health system, and (ii) to support the decision-making in selecting the best strategies for urban air quality and health improvement. To that end, using the methodologies and input data recommended in Chapter 4, two traffic management scenarios were selected and tested for the local case study and simulation periods: replacement of 50% of the vehicle fleet below EURO 4 by electric vehicles (ELEC), and introduction of a Low Emission Zone (LEZ). The entire chain of impacts was evaluated based on the REF, reflecting the expected benefits with the implementation of the traffic scenarios.

For streets with known emission, the ELEC positive impact was felt in all simulated road segments, whereas emission reductions for the LEZ were only confined to the segments where the LEZ was designed.

The air quality impact assessment of these emission changes showed air quality improvements in both reduction scenarios and for all simulation hours, but these were more relevant in time periods with higher REF NO₂ concentrations. In turn, these concentration peaks, caused by high road traffic activity and increased emissions, led to a greater effectiveness of the emission reduction scenarios. Spatially, higher air quality improvements were observed near the target streets, but there was also a strong influence of the urban structure and local wind regimes (direction and wind speed).

Translating the air quality improvement in daily avoided health impacts (number of cases and costs), larger benefits were estimated with the ELEC scenario, because NO₂ emission reductions were spatially allocated to all road segments. On the LEZ influence area, the broader restrictions to the road circulation, contributed to higher health benefits.

Chapter 6

Conclusions

6.1. Main research findings

6.2. Future developments

6. CONCLUSIONS

The main purpose of the thesis was to develop and apply an integrated multiscale modelling system that allows to simulate atmospheric concentrations and resulting health impacts in a broad spatial (regional to local scales) and temporal (short and long-term) horizon. The scientific advances and methodological limitations found are analysed in Section 6.1, whereas the future developments, based on these weaknesses, and guidelines for improving integrated assessment modelling synergies, are delineated in Section 6.2.

6.1. Main research findings

In this section, the main research findings related with the development and application of the modair4health system, are analysed and discussed as a response to the formulated research questions and accomplished objectives.

1. What are the most appropriate modelling tools for quantifying multiscale air quality and health impacts? How to connect them?

The review and critical analysis of the state-of-the-art on multiscale air quality and health modelling, together with the proposed guidelines on how to overcome the existing limitations, were decisive to answer to this research question, which served as support for the development of the modair4health system.

For multiscale air quality modelling, two air quality models able to simulate atmospheric concentrations from regional/urban (WRF-Chem) to local (VADIS) scales, were selected. The option for the online mesoscale model WRF-Chem represents an added value in atmospheric modelling, since potential meteorology-chemistry feedbacks are considered. The link to the local scale was done with the CFD model VADIS, in order to accurately reproduce the spatial variability and pollutant dispersion within the urban structure. To cover the multiple spatial scales and resolutions, the models were carefully coupled (offline coupling), ensuring that the background and boundary meteorological and chemical conditions extracted from the WRF-Chem urban domain are properly assimilated by the local scale.

When moving from urban air pollution to health impacts, the linear and non-linear methodologies recommended by the WHO were adopted, because they can be applied to a wide range of environmental conditions and are seen as the most suitable at the city level.

To evaluate the monetary losses with the estimated physical health impacts, national or sub-national statistics should be preferentially used. If not available, the alternative will be to use economic evaluation studies updated for the reference year and geographic region of the case study.

Finally, using programming tools, the different components that integrate the system were operationalized as a whole, promoting some adaptations and improvements in the functioning schemes of the models and methodologies.

2. How do input data and model setup influence the modelling results?

To answer to this research question, different configurations and input data involving the selected modelling tools were tested.

The WRF-Chem model was configured to run three simulation domains in two-way nesting with increasing resolutions (up to 1 km² - target urban domain), in order to: investigate feedbacks of the online meteorology-chemistry coupling; evaluate the influence of LC changes on the air quality; and analyse the variability of pollutant concentrations in the two smallest domains (5 and 1 km² grid resolutions). The feedback results confirm that the aerosol particles have a key role in the atmosphere dynamics, influencing the net radiation budget and underlying meteorological conditions. Thereby, the option for simulations with the aerosol effect turned on, only possible through the use of online atmospheric models, is recommended, either to improve the weather predictions, but also to obtain more accurate air quality estimates, since the potential feedbacks favour the numerical resolution, in very small time steps, of the physical and chemical processes occurring within the atmospheric boundary layer. However, in spite of the current developments in this research area, improving the aerosol estimates and their properties using data assimilation techniques, improving microphysics parametrizations, and increasing the grid spacing and resolution of the input data, are emerging challenges to decrease the modelling uncertainties and to get more reliable forecasts. Regarding the LC, the objective was to evaluate its influence on the air quality when using the new LC classification developed in the scope of the thesis. Its greater spatial discretization by dominant LC categories contributed to enhance urban pollution hotspots, more evident over the smallest domain (1 km² resolution). This analysis highlights the relevance that a detailed LC database and a finer grid spacing may have in mesoscale air quality modelling. In view of these conclusions, the use of the new LC classification and the option for 1 km² resolution outputs to provide background chemical conditions for the local scale modelling are recommended.

In air quality modelling at local scale, the VADIS CFD model was tested using two methodologies to represent the behaviour of the traffic emissions: i) long-term seasonal traffic profiles based on air quality observations recorded in a traffic station located within the simulation domain; and ii) traffic emissions that are automatically disaggregated for each simulation hour, considering a factor resulting from the weighting between traffic station observations and background NO₂ concentrations. Based on obtained NO₂ results, the automated approach is recommended as long as the observations for the local case study and simulation periods are available. However, despite this close relationship between traffic-induced NO₂ emissions and ambient NO₂ concentrations, the influence of other pollution sources or transport from other locations should not be neglected.

To quantify the extent of health impacts related to the urban air pollution, the two WHO methodologies were applied to the local case study and VADIS simulation periods. The non-linear approach presented lower health outcomes (i.e. fewer cases and damage costs), which seem to be better adjusted to the local reality, mainly for higher NO₂ concentrations, whereas the linear model is associated to overestimated health impacts. This conclusion is shared in epidemiological studies combining meta-analyses recorded during air pollution episodes and different types of health results, hence the non-linear methodology is recommended, especially when high pollutant concentrations are expected.

3. What is the impact of the urban structure on the dispersion of air pollutants?

The characteristics of the urban structure strongly influenced the dispersion and accumulation patterns of NO₂ over the local case study. Overall, higher hourly concentration gradients were estimated around the main streets, where the highest traffic emissions were allocated. However, the spatial variability of these air concentrations was also affected by the geometry itself of the urban obstacles (e.g. height, orientation and spacing between buildings), causing relevant changes in the atmospheric flow (direction and wind speed), provided through the WRF-Chem outputs as time-varying boundary conditions to initialize the CFD simulations. These local atmospheric dynamics within the urban canopy (i.e. space between the ground surface and the highest building height) favoured the pollutant dispersion according to the prevailing wind directions. On the other hand, the flow dynamics perturbations induced by the obstacles tended to reduce the wind speed, leading to the formation of local air pollution hotspots.

4. Will a modelling system be able to accurately estimate air concentrations and health impacts in urban areas?

Based on the different performed tests, it was verified the importance of coupling different types of air quality models, showing that the WRF-Chem mesoscale model with nesting capabilities is useful to capture the transboundary pollution and to estimate concentrations on the outskirts of cities, and the CFD model with adjusted traffic profiles allows to accurately reproduce the spatial and temporal variability of air concentrations in busiest road traffic areas.

Given this more comprehensive and accurate framework of the air quality assessment, when quantifying human exposure effects, the uncertainties inherent to the health impacts modelling tend to decrease. With this purpose, having as reference the non-linear WHO methodology, it is necessary to select the most appropriate health input metrics according to the required HIA specificities.

5. How might the modelling system capabilities be useful to support decision-makers and stakeholders in selecting the best strategies for air quality and health management?

The modair4health system showed to be able to comparatively evaluate different air quality improvement scenarios, providing quantified spatial and temporal information of environmental, social and economic value, in order to facilitate the choice of efficient air quality and health management strategies and decisions. Moreover, its operability allows to quickly test other urban air pollution control policies, and it can be easily adapted and applied to other case studies considering local and regional influences.

6.2. Future developments

The development and the applications of the modair4health system were addressed to overcome the gaps identified in the current scientific knowledge. However, despite the innovations and reached outcomes, there is still research work to be done, which can be summarized in the following topics:

(i) Testing other air quality modelling configurations and input data

A set of new applications involving other physical and chemical parametrizations included into the WRF-Chem model (e.g. microphysics schemes, chemical mechanisms,

urban canopy schemes) should be performed. Also, for both air quality models, more detailed input data (e.g. emissions, meteorology, boundary conditions) are needed.

(ii) Detailing emission inventories

For regional-to-urban air quality modelling with dynamic downscaling, it is necessary to improve the EI regarding the spatial resolution and sources characterization, especially at the urban scale. Moreover, whenever air pollution management strategies are required, the nature and the focus of emission reduction measures are mostly oriented towards urban areas and, thus, detailed EI are fundamental for decision support.

(iii) Applying the modair4health system to other air pollutants and health indicators, considering short and long-term human exposures

For the local (case study) and urban domains, the system can be applied to other air pollutants and health indicators. As the case study was focused on one of the busiest road traffic areas of the city of Coimbra (Fernão de Magalhães Avenue), it will make sense to analyse PM₁₀, which is also a problematic contaminant associated to the road traffic. The link with the health, at this spatial level, has to be made only to assess short-term health effects triggered by air pollution episodes, since the computational requirements of the CFD model are a barrier to long-term exposure assessments. These long-term studies that require, at least, 1-year air quality data, could be carried out for the urban domain simulated with the WRF-Chem model. Health input metrics to be used are dependent on the availability of epidemiological evidences (i.e. CRF) relating the pollutant, exposure time and health indicators. Preferentially, national statistics or more specific health data should be used.

(iv) Testing other air pollution management strategies, making a cost-benefit analysis

Based on the sustainable urban mobility plans designed for the Coimbra region and in close collaboration with the local entities, the assessment of the entire chain of impacts should be extended to the urban simulation domain, testing other types of measures that contribute to healthy cities (e.g. promoting the use of public transports, reducing speed limits, expanding the pedestrian and cycling network). To complement this scenario analysis approach, a cost-benefit analysis comparing implementation costs of measures and health benefits (or avoided costs) is a clear added value in the decision-making process.

(v) Quantifying the modelling uncertainties

Regardless of the system performance for any configurations and input data, the modelling uncertainties at all steps of the scenario analysis approach should be investigated. Their quantification, either by sensitivity or probabilistic analyses or using the Monte Carlo method, is important to be communicated, in order to support the stakeholders and decisions-makers in choosing the best urban air pollution control policies.

(vi) Employing techniques of data assimilation and inverse modelling

The application of these techniques within the multiscale air quality modelling component could contribute to produce improved air quality estimates, since observational data are used to refine the modelling outputs (data assimilation). Combining predictions with observations, will also allow to identify the origin and emission rate of the main pollution sources (inverse modelling). Nevertheless, a balance between improved air quality results at different scales and computational efforts will have to be performed.

(vii) Increasing the spatial resolution of the WRF-Chem model

Another way to improve urban air quality estimates and to simultaneously reduce the uncertainties when providing outputs to the local scale, would be the inclusion of a LES approach within WRF-Chem. The WRF-Chem/LES coupling has the turbulence-resolving capability in realistic conditions, involving boundary layers driven by large-scale flows. Thereby, it will be possible to do high-resolution simulations (finer than 1 km²) with surface layer parametrizations that take into account its heterogeneity.

(viii) Including the CFD as a WRF-Chem module

The integration of the VADIS CFD model within the WRF-Chem is other challenging issue, either operationally, with advantages in computational processing, or in terms of the underlying modelling principles, where the turbulence parameterization when crossing different models and scales is seen as one of the most critical aspects in the multiscale atmospheric modelling field.

The two last topics have still to be further worked, using the guidelines of ongoing scientific developments as support.

References

REFERENCES

- APPRAISAL, 2013a. Air quality assessment and planning, including modelling and measurement, Deliverable 2.3, May 2013, FP7-ENV CA 303895.
- APPRAISAL, 2013b. Review and gaps identification in AQ and HIA methodologies at regional and local scale, D2.4 Health Impact Assessment (HIA), July 2013, FP7-ENV CA 303895.
- Archer-Nicholls, S., Lowe, D., Schultz, D.M., McFiggans, G., 2016. Aerosol–radiation–cloud interactions in a regional coupled model: the effects of convective parameterisation and resolution. *Atmos. Chem. Phys.* 16, 5573–5594. <https://doi.org/10.5194/acp-16-5573-2016>
- Baklanov, A., Grimmond, S., Mahura, A., Athanassiadou, M. (Eds.), 2009. *Meteorological and Air Quality Models for Urban Areas*. Springer Berlin Heidelberg, Berlin, Heidelberg. <https://doi.org/10.1007/978-3-642-00298-4>
- Baklanov, A., Hänninen, O., Slørdal, L.H., Kukkonen, J., Bjergene, N., Fay, B., Finardi, S., Hoe, S.C., Jantunen, M., Karppinen, A., Rasmussen, A., Skouloudis, A., Sokhi, R.S., Sørensen, J.H., Ødegaard, V., 2007. Integrated systems for forecasting urban meteorology, air pollution and population exposure. *Atmos. Chem. Phys.* 7, 855–874. <https://doi.org/10.5194/acp-7-855-2007>
- Baklanov, A.A., Nuterman, R.B., 2009. Multi-scale atmospheric environment modelling for urban areas. *Adv. Sci. Res.* 3, 53–57. <https://doi.org/10.5194/asr-3-53-2009>
- Ballester, F., Rodríguez, P., Iñíguez, C., Saez, M., Daponte, A., Galán, I., Taracido, M., Arribas, F., Bellido, J., Cirarda, F.B., Cañada, A., Guillén, J.J., Guillén-Grima, F., López, E., Pérez-Hoyos, S., Lertxundi, A., Toro, S., 2006. Air pollution and cardiovascular admissions association in Spain: Results within the EMECAS project. *J. Epidemiol. Community Health* 60, 328–336. <https://doi.org/10.1136/jech.2005.037978>
- Beevers, S.D., Kitwiroon, N., Williams, M.L., Carslaw, D.C., 2012. One way coupling of CMAQ and a road source dispersion model for fine scale air pollution predictions. *Atmos. Environ.* 59, 47–58. <https://doi.org/10.1016/J.ATMOENV.2012.05.034>
- Belhaj, M., Fridell, E., 2008. *External Costs in the Transport Sector: A Literature Review*. Stockholm.

- Benavides, J., Snyder, M., Guevara, M., Soret, A., Pérez García-Pando, C., Amato, F., Querol, X., Jorba, O., 2019. CALIOPE-Urban v1.0: Coupling R-LINE with a mesoscale air quality modelling system for urban air quality forecasts over Barcelona city (Spain). *Geosci. Model Dev. Discuss.* 1–35. <https://doi.org/10.5194/gmd-2019-48>
- Borrego, C., Carvalho, A., Sa, E., Sousa, S., Coelho, D., Lopes, M., Monteiro, A., Mir, A., 2011. Air Quality Plans for the Northern Region of Portugal: Improving Particulate Matter and Coping with Legislation, in: *Advanced Air Pollution*. InTech. <https://doi.org/10.5772/18842>
- Borrego, C., Tchepel, O., Costa, A.M., Amorim, J.H., Miranda, A.I., 2003. Emission and dispersion modelling of Lisbon air quality at local scale. *Atmos. Environ.* 37, 5197–5205. <https://doi.org/10.1016/J.ATMOSENV.2003.09.004>
- Brandt, J., Silver, J.D., Christensen, J.H., Andersen, M.S., Bønløkke, J.H., Sigsgaard, T., Geels, C., Gross, A., Hansen, A.B., Hansen, K.M., Hedegaard, G.B., Kaas, E., Frohn, L.M., 2013. Contribution from the ten major emission sectors in Europe and Denmark to the health-cost externalities of air pollution using the EVA model system – an integrated modelling approach. *Atmos. Chem. Phys.* 13, 7725–7746. <https://doi.org/10.5194/acp-13-7725-2013>
- Brandt, J., Silver, J.D., Frohn, L.M., Geels, C., Gross, A., Hansen, A.B., Hansen, K.M., Hedegaard, G.B., Skjøth, C.A., Villadsen, H., Zare, A., Christensen, J.H., 2012. An integrated model study for Europe and North America using the Danish Eulerian Hemispheric Model with focus on intercontinental transport of air pollution. *Atmos. Environ.* 53, 156–176. <https://doi.org/10.1016/J.ATMOSENV.2012.01.011>
- Brenk, I. van den, 2018. *The use of Health Impact Assessment tools in European Cities*. Utrecht.
- Briant, R., Tuccella, P., Deroubaix, A., Khvorostyanov, D., Menut, L., Mailler, S., Turquety, S., 2017. Aerosol–radiation interaction modelling using online coupling between the WRF 3.7.1 meteorological model and the CHIMERE 2016 chemistry-transport model, through the OASIS3-MCT coupler. *Geosci. Model Dev.* 10, 927–944. <https://doi.org/10.5194/gmd-10-927-2017>
- Brown, M.J., 2000. *Urban Parameterizations for Mesoscale Meteorological Models, Mesoscale Atmospheric Dispersion*. WIT Press.

- Burnett, R., Chen, H., Szyszkowicz, M., Fann, N., Hubbell, B., Pope, C.A., Apte, J.S., Brauer, M., Cohen, A., Weichenthal, S., Coggins, J., Di, Q., Brunekreef, B., Frostad, J., Lim, S.S., Kan, H., Walker, K.D., Thurston, G.D., Hayes, R.B., Lim, C.C., Turner, M.C., Jerrett, M., Krewski, D., Gapstur, S.M., Diver, W.R., Ostro, B., Goldberg, D., Crouse, D.L., Martin, R. V., Peters, P., Pinault, L., Tjepkema, M., Van Donkelaar, A., Villeneuve, P.J., Miller, A.B., Yin, P., Zhou, M., Wang, L., Janssen, N.A.H., Marra, M., Atkinson, R.W., Tsang, H., Thach, T.Q., Cannon, J.B., Allen, R.T., Hart, J.E., Laden, F., Cesaroni, G., Forastiere, F., Weinmayr, G., Jaensch, A., Nagel, G., Concin, H., Spadaro, J. V., 2018. Global estimates of mortality associated with longterm exposure to outdoor fine particulate matter. *Proc. Natl. Acad. Sci. U. S. A.* 115, 9592–9597. <https://doi.org/10.1073/pnas.1803222115>
- CCDRC, 2010. Plano de Melhoria da Qualidade do Ar na Região Centro. Coimbra.
- Chapman, E.G., Gustafson, W.I., Easter, R.C., Barnard, J.C., Ghan, S.J., Pekour, M.S., Fast, J.D., 2009. Coupling aerosol-cloud-radiative processes in the WRF-Chem model: Investigating the radiative impact of elevated point sources. *Atmos. Chem. Phys.* 9, 945–964. <https://doi.org/10.5194/acp-9-945-2009>
- Chen, D., Liu, Z., Davis, C., Gu, Y., 2017. Dust radiative effects on atmospheric thermodynamics and tropical cyclogenesis over the Atlantic Ocean using WRF-Chem coupled with an AOD data assimilation system. *Atmos. Chem. Phys.* 17, 7917–7939. <https://doi.org/10.5194/acp-17-7917-2017>
- Chen, F., Kusaka, H., Bornstein, R., Ching, J., Grimmond, C.S.B., Grossman-Clarke, S., Loridan, T., Manning, K.W., Martilli, A., Miao, S., Sailor, D., Salamanca, F.P., Taha, H., Tewari, M., Wang, X., Wyszogrodzki, A.A., Zhang, C., 2011. The integrated WRF/urban modelling system: development, evaluation, and applications to urban environmental problems. *Int. J. Climatol.* 31, 273–288. <https://doi.org/10.1002/joc.2158>
- CIM-RC, 2018. Plano de Ação de Mobilidade Urbana Sustentável (PAMUS) na Comunidade Intermunicipal Região de Coimbra. Coimbra.
- CIM-RC, 2016. Plano Intermunicipal de Mobilidade e Transportes da Região de Coimbra. Coimbra.
- Costa, S., Ferreira, J., Silveira, C., Costa, C., Lopes, D., Relvas, H., Borrego, C., Roebeling, P., Miranda, A.I., Paulo Teixeira, J., 2014. Integrating health on air quality assessment - Review report on health risks of two major european outdoor air pollutants: PM and NO₂. *J. Toxicol. Environ. Heal. - Part B Crit. Rev.* 17. <https://doi.org/10.1080/10937404.2014.946164>
- DEFRA, 2019a. Air quality damage cost guidance. London.

- DEFRA, 2019b. Impact pathways approach: Guidance for air quality appraisal. London.
- DGT, 2017. A Land Cover/Use Map of Mainland Portugal for 2010. Directorate-General for the Territorial Development, Lisbon.
- Dias, D., Antunes, A.P., Tchepel, O., 2019. Modelling of Emissions and Energy Use from Biofuel Fuelled Vehicles at Urban Scale. *Sustainability* 11, 2902. <https://doi.org/10.3390/su11102902>
- Dias, D., Tchepel, O., Antunes, A.P., 2016. Integrated modelling approach for the evaluation of low emission zones. *J. Environ. Manage.* 177, 253–263. <https://doi.org/10.1016/j.jenvman.2016.04.031>
- Duque, L., Relvas, H., Silveira, C., Ferreira, J., Monteiro, A., Gama, C., Rafael, S., Freitas, S., Borrego, C., Miranda, A.I., 2016. Evaluating strategies to reduce urban air pollution. *Atmos. Environ.* 127. <https://doi.org/10.1016/j.atmosenv.2015.12.043>
- Duyzer, J., van den Hout, D., Zandveld, P., van Ratingen, S., 2015. Representativeness of air quality monitoring networks. *Atmos. Environ.* 104, 88–101. <https://doi.org/10.1016/j.atmosenv.2014.12.067>
- EC, 2005. ExternE Externalities of Energy - Methodology 2005 Update. European Commission, Luxembourg.
- EEA, 2019. Air quality in Europe — 2019 report. Copenhagen. <https://doi.org/10.2800/822355>
- EEA, 2017. Air quality in Europe — 2017 report. Copenhagen. <https://doi.org/10.2800/850018>
- EHA, 2006. The Stockholm Trial: Effects on air quality and health, report SLB 4:2006. Stockholm.
- Fast, J.D., Gustafson, W.I., Easter, R.C., Zaveri, R.A., Barnard, J.C., Chapman, E.G., Grell, G.A., Peckham, S.E., 2006. Evolution of ozone, particulates, and aerosol direct radiative forcing in the vicinity of Houston using a fully coupled meteorology-chemistry-aerosol model. *J. Geophys. Res.* 111, D21305. <https://doi.org/10.1029/2005JD006721>
- Forkel, R., Balzarini, A., Baró, R., Bianconi, R., Curci, G., Jiménez-Guerrero, P., Hirtl, M., Honzak, L., Lorenz, C., Im, U., Pérez, J.L., Pirovano, G., San José, R., Tuccella, P., Werhahn, J., Žabkar, R., 2015. Analysis of the WRF-Chem contributions to AQMEII phase2 with respect to aerosol radiative feedbacks on meteorology and pollutant distributions. *Atmos. Environ.* 115, 630–645. <https://doi.org/10.1016/j.atmosenv.2014.10.056>

- Forkel, R., Werhahn, J., Hansen, A.B., McKeen, S., Peckham, S., Grell, G., Suppan, P., 2012. Effect of aerosol-radiation feedback on regional air quality – A case study with WRF/Chem. *Atmos. Environ.* 53, 202–211. <https://doi.org/10.1016/j.atmosenv.2011.10.009>
- Franke, J., Hellsten, A., Schlünzen, K.H., Carissimo, B., 2011. The COST 732 Best Practice Guideline for CFD simulation of flows in the urban environment: A summary. *Int. J. Environ. Pollut.* 44, 419–427. <https://doi.org/10.1504/IJEP.2011.038443>
- Gidhagen, L., Johansson, C., Langner, J., Foltescu, V.L., 2005. Urban scale modeling of particle number concentration in Stockholm. *Atmos. Environ.* 39, 1711–1725. <https://doi.org/10.1016/J.ATMOSENV.2004.11.042>
- Grell, G.A., Knoche, R., Peckham, S.E., McKeen, S.A., 2004. Online versus offline air quality modeling on cloud-resolving scales. *Geophys. Res. Lett.* 31, L16117. <https://doi.org/10.1029/2004GL020175>
- Grell, G.A., Peckham, S.E., Schmitz, R., McKeen, S.A., Frost, G., Skamarock, W.C., Eder, B., 2005. Fully coupled “online” chemistry within the WRF model. *Atmos. Environ.* 39, 6957–6975. <https://doi.org/10.1016/J.ATMOSENV.2005.04.027>
- Guenther, A., Karl, T., Harley, P., Wiedinmyer, C., Palmer, P.I., Geron, C., 2006. Estimates of global terrestrial isoprene emissions using MEGAN (Model of Emissions of Gases and Aerosols from Nature). *Atmos. Chem. Phys.* 6, 3181–3210. <https://doi.org/10.5194/acp-6-3181-2006>
- Hammit, J.K., 2005. Methodological Review of WTP and QALY Frameworks for Valuing Environmental Health Risks to Children. Harvard.
- Hanly, P., Timmons, A., Walsh, P.M., Sharp, L., 2012. Breast and prostate cancer productivity costs: A comparison of the human capital approach and the friction cost approach. *Value Heal.* 15, 429–436. <https://doi.org/10.1016/j.jval.2011.12.012>
- Héroux, M.-E., Anderson, H.R., Atkinson, R., Brunekreef, B., Cohen, A., Forastiere, F., Hurley, F., Katsouyanni, K., Krewski, D., Krzyzanowski, M., Künzli, N., Mills, I., Querol, X., Ostro, B., Walton, H., 2015. Quantifying the health impacts of ambient air pollutants: recommendations of a WHO/Europe project. *Int. J. Public Health* 60, 619–627. <https://doi.org/10.1007/s00038-015-0690-y>
- Hofman, J., Lefebvre, W., Janssen, S., Nackaerts, R., Nuyts, S., Mattheyses, L., Samson, R., 2014. Increasing the spatial resolution of air quality assessments in urban areas: A comparison of biomagnetic monitoring and urban scale modelling. *Atmos. Environ.* 92, 130–140. <https://doi.org/10.1016/J.ATMOSENV.2014.04.013>

- Holland, M., Hunt, A., Hurley, F., Navrud, S., Watkiss, P., 2005. Methodology for the Cost-Benefit analysis for CAFE: Volume 1: Overview of Methodology. Didcot.
- Hood, C., MacKenzie, I., Stocker, J., Johnson, K., Carruthers, D., Vieno, M., Doherty, R., 2018. Air quality simulations for London using a coupled regional-to-local modelling system. *Atmos. Chem. Phys.* 18, 11221–11245. <https://doi.org/10.5194/acp-18-11221-2018>
- Hurley, F., Hunt, A., Cowie, H., Holland, M., Miller, B., Pye, S., Watkiss, P., 2005. Methodology for the Cost-Benefit Analysis for CAFE - Volume 2: Health Impact Assessment, AEA Technology Environment. Didcot.
- IEA, 2019. Global EV Outlook 2019 - Scaling-up the transition to electric mobility. Paris.
- Isakov, V., Touma, J.S., Burke, J., Lobdell, D.T., Palma, T., Rosenbaum, A., Ozkaynak, H., 2009. Combining regional- and local-scale air quality models with exposure models for use in environmental health studies. *J. Air Waste Manag. Assoc.* 59, 461–72.
- Jensen, S.S., Ketzler, M., Becker, T., Christensen, J., Brandt, J., Plejdrup, M., Winther, M., Nielsen, O.-K., Hertel, O., Ellermann, T., 2017. High resolution multi-scale air quality modelling for all streets in Denmark. *Transp. Res. Part D Transp. Environ.* 52, 322–339. <https://doi.org/10.1016/J.TRD.2017.02.019>
- Jiménez-Esteve, B., Udina, M., Soler, M.R., Pepin, N., Miró, J.R., 2018. Land use and topography influence in a complex terrain area: A high resolution mesoscale modelling study over the Eastern Pyrenees using the WRF model. *Atmos. Res.* 202, 49–62. <https://doi.org/10.1016/J.ATMOSRES.2017.11.012>
- Jiménez, P., Jorba, O., Parra, R., Baldasano, J.M., 2006. Evaluation of MM5-EMICAT2000-CMAQ performance and sensitivity in complex terrain: High-resolution application to the northeastern Iberian Peninsula. *Atmos. Environ.* 40, 5056–5072. <https://doi.org/10.1016/J.ATMOSENV.2005.12.060>
- Joe, D.K., Zhang, H., DeNero, S.P., Lee, H.-H., Chen, S.-H., McDonald, B.C., Harley, R.A., Kleeman, M.J., 2014. Implementation of a high-resolution Source-Oriented WRF/Chem model at the Port of Oakland. *Atmos. Environ.* 82, 351–363. <https://doi.org/10.1016/J.ATMOSENV.2013.09.055>
- Kay, S.M., 1988. Modern spectral estimation : theory and application. Prentice Hall.
- Kim, Y., Sartelet, K., Raut, J.-C., Chazette, P., 2015. Influence of an urban canopy model and PBL schemes on vertical mixing for air quality modeling over Greater Paris. *Atmos. Environ.* 107, 289–306. <https://doi.org/10.1016/J.ATMOSENV.2015.02.011>

- Kim, Y., Wu, Y., Seigneur, C., Roustan, Y., 2018. Multi-scale modeling of urban air pollution: development and application of a Street-in-Grid model (v1.0) by coupling MUNICH (v1.0) and Polair3D (v1.8.1). *Geosci. Model Dev* 11, 611–629. <https://doi.org/10.5194/gmd-11-611-2018>
- Kong, X., Forkel, R., Sokhi, R.S., Suppan, P., Baklanov, A., Gauss, M., Brunner, D., Barò, R., Balzarini, A., Chemel, C., Curci, G., Jiménez-Guerrero, P., Hirtl, M., Honzak, L., Im, U., Pérez, J.L., Pirovano, G., San Jose, R., Schlünzen, K.H., Tsegas, G., Tuccella, P., Werhahn, J., Žabkar, R., Galmarini, S., 2015. Analysis of meteorology–chemistry interactions during air pollution episodes using online coupled models within AQMEII phase-2. *Atmos. Environ.* 115, 527–540. <https://doi.org/10.1016/j.atmosenv.2014.09.020>
- Koopmanschap, M.A., van Ineveld, B.M., 1992. Towards a new approach for estimating indirect costs of disease. *Soc. Sci. Med.* 34, 1005–1010. [https://doi.org/10.1016/0277-9536\(92\)90131-9](https://doi.org/10.1016/0277-9536(92)90131-9)
- Kuik, F., Lauer, A., Churkina, G., Denier van der Gon, H.A.C., Fenner, D., Mar, K.A., Butler, T.M., 2016. Air quality modelling in the Berlin–Brandenburg region using WRF-Chem v3.7.1: sensitivity to resolution of model grid and input data. *Geosci. Model Dev.* 9, 4339–4363. <https://doi.org/10.5194/gmd-9-4339-2016>
- Kukkonen, J., Olsson, T., Schultz, D.M., Baklanov, A., Klein, T., Miranda, A.I., Monteiro, A., Hirtl, M., Tarvainen, V., Boy, M., Peuch, V.-H., Poupkou, A., Kioutsioukis, I., Finardi, S., Sofiev, M., Sokhi, R., Lehtinen, K.E.J., Karatzas, K., San José, R., Astitha, M., Kallos, G., Schaap, M., Reimer, E., Jakobs, H., Eben, K., 2012. A review of operational, regional-scale, chemical weather forecasting models in Europe. *Atmos. Chem. Phys.* 12, 1–87. <https://doi.org/10.5194/acp-12-1-2012>
- Kwak, K.-H., Baik, J.-J., Ryu, Y.-H., Lee, S.-H., 2015. Urban air quality simulation in a high-rise building area using a CFD model coupled with mesoscale meteorological and chemistry-transport models. *Atmos. Environ.* 100, 167–177. <https://doi.org/10.1016/J.ATMOSENV.2014.10.059>
- Lateb, M., Meroney, R.N., Yataghene, M., Fellouah, H., Saleh, F., Boufadel, M.C., 2016. On the use of numerical modelling for near-field pollutant dispersion in urban environments – A review. *Environ. Pollut.* 208, 271–283. <https://doi.org/10.1016/J.ENVPOL.2015.07.039>

- Likhvar, V.N., Pascal, M., Markakis, K., Colette, A., Hauglustaine, D., Valari, M., Klimont, Z., Medina, S., Kinney, P., 2015. A multi-scale health impact assessment of air pollution over the 21st century. *Sci. Total Environ.* 514, 439–449. <https://doi.org/10.1016/j.scitotenv.2015.02.002>
- Liu, X.-Y., Zhang, Y., Zhang, Q., He, K.-B., 2016. Application of online-coupled WRF/Chem-MADRID in East Asia: Model evaluation and climatic effects of anthropogenic aerosols. *Atmos. Environ.* 124, 321–336. <https://doi.org/10.1016/j.atmosenv.2015.03.052>
- Maibach, M., Schreyer, C., Sutter, D., Essen, H.P., Boon, B.H., Smokers, R., Schrotten, A., Doll, C., Pawlowska, B., Bak, M., 2008. Handbook on estimation of external costs in the transport sector, report produced within the study Internalisation Measures and Policies for All external Cost of Transport (IMPACT), Version 1.1, CE Delft.
- Marques, R.C., Cruz, N.F., Simões, P., Ferreira, S.F., Pereira, M.C., 2013. EIMPack – Economic Impact of the Packaging and Packaging Waste Directive, Task 5 – Environmental Valuation (Literature Review), work programme financed by European Investment Bank, Instituto Superior Técnico. Lisbon.
- Masson, V., 2006. Urban surface modeling and the meso-scale impact of cities. *Theor. Appl. Clim.* 84, 35–45. <https://doi.org/10.1007/s00704-005-0142-3>
- Mechler, R., Amann, M., Schoepp, W., 2002. A methodology to estimate changes in statistical life expectancy due to the control of particulate matter air pollution, Interim Report IR-02-035 on work of the IIASA. IR-02-035, Laxenburg.
- Mensink, C., Colles, A., Janssen, L., Cornelis, J., 2003. Integrated air quality modelling for the assessment of air quality in streets against the council directives. *Atmos. Environ.* 37, 5177–5184. <https://doi.org/10.1016/J.ATMOSENV.2003.07.014>
- Miranda, A., Silveira, C., Ferreira, J., Monteiro, A., Lopes, D., Relvas, H., Borrego, C., Roebeling, P., 2015. Current air quality plans in Europe designed to support air quality management policies. *Atmos. Pollut. Res.* 6, 434–443. <https://doi.org/10.5094/APR.2015.048>
- Miranda, A.I., Ferreira, J., Silveira, C., Relvas, H., Duque, L., Roebeling, P., Lopes, M., Costa, S., Monteiro, A., Gama, C., Sá, E., Borrego, C., Teixeira, J.P., 2016. A cost-efficiency and health benefit approach to improve urban air quality. *Sci. Total Environ.* 569–570. <https://doi.org/10.1016/j.scitotenv.2016.06.102>

- Nasari, M.M., Szyszkowicz, M., Chen, H., Crouse, D., Turner, M.C., Jerrett, M., Pope, C.A., Hubbell, B., Fann, N., Cohen, A., Gapstur, S.M., Diver, W.R., Stieb, D., Forouzanfar, M.H., Kim, S.-Y., Olives, C., Krewski, D., Burnett, R.T., Burnett, R.T., 2016. A class of non-linear exposure-response models suitable for health impact assessment applicable to large cohort studies of ambient air pollution. *Air Qual. Atmos. Heal.* 9, 961–972. <https://doi.org/10.1007/s11869-016-0398-z>
- Ostro, B., 2004. *Outdoor Air Pollution: Assessing the Environmental Burden of Disease at National and Local Levels*, Environmen. ed. Geneva.
- Oxley, T., Dore, A.J., ApSimon, H., Hall, J., Kryza, M., 2013. Modelling future impacts of air pollution using the multi-scale UK Integrated Assessment Model (UKIAM). *Environ. Int.* 61, 17–35. <https://doi.org/10.1016/J.ENVINT.2013.09.009>
- Palacios-Peña, L., Baró, R., Guerrero-Rascado, J.L., Alados-Arboledas, L., Brunner, D., Jiménez-Guerrero, P., 2017. Evaluating the representation of aerosol optical properties using an online coupled model over the Iberian Peninsula. *Atmos. Chem. Phys.* 17, 277–296. <https://doi.org/10.5194/acp-17-277-2017>
- Pay, M.T., Martínez, F., Guevara, M., Baldasano, J.M., 2014. Air quality forecasts on a kilometer-scale grid over complex Spanish terrains. *Geosci. Model Dev.* 7, 1979–1999. <https://doi.org/10.5194/gmd-7-1979-2014>
- Pendlebury, D., Gravel, S., Moran, M.D., Lupu, A., 2018. Impact of chemical lateral boundary conditions in a regional air quality forecast model on surface ozone predictions during stratospheric intrusions. *Atmos. Environ.* 174, 148–170. <https://doi.org/10.1016/j.atmosenv.2017.10.052>
- Pervin, T., Gerdtham, U.-G., Lyttkens, C., 2008. Societal costs of air pollution-related health hazards: A review of methods and results. *Cost Eff. Resour. Alloc.* 6, 19. <https://doi.org/10.1186/1478-7547-6-19>
- Pineda, N., Jorba, O., Jorge, J., Baldasano, J.M., 2004. Using NOAA AVHRR and SPOT VGT data to estimate surface parameters: application to a mesoscale meteorological model. *Int. J. Remote Sens.* 25, 129–143. <https://doi.org/10.1080/0143116031000115201>
- Pizzol, M., Thomsen, M., Frohn, L.M., Andersen, M.S., 2010. External costs of atmospheric Pb emissions: valuation of neurotoxic impacts due to inhalation. *Environ. Heal.* 9, 9. <https://doi.org/10.1186/1476-069X-9-9>
- Ramanathan, V., Feng, Y., 2009. Air pollution, greenhouse gases and climate change: Global and regional perspectives. *Atmos. Environ.* 43, 37–50. <https://doi.org/10.1016/J.ATMOSENV.2008.09.063>

- Relvas, H., Miranda, A.I., 2018. An urban air quality modeling system to support decision-making: design and implementation. *Air Qual. Atmos. Heal.* 11, 815–824. <https://doi.org/10.1007/s11869-018-0587-z>
- Relvas, H., Miranda, A.I., Carnevale, C., Maffei, G., Turrini, E., Volta, M., 2017. Optimal air quality policies and health: a multi-objective nonlinear approach. *Environ. Sci. Pollut. Res.* 24, 13687–13699. <https://doi.org/10.1007/s11356-017-8895-7>
- Rückerl, R., Schneider, A., Breitner, S., Cyrys, J., Peters, A., 2011. Health effects of particulate air pollution: A review of epidemiological evidence. *Inhal. Toxicol.* <https://doi.org/10.3109/08958378.2011.593587>
- Russell, M., Hakami, A., Makar, P.A., Akingunola, A., Zhang, J., Moran, M.D., Zheng, Q., 2019. An evaluation of the efficacy of very high resolution air-quality modelling over the Athabasca oil sands region, Alberta, Canada. *Atmos. Chem. Phys.* 19, 4393–4417. <https://doi.org/10.5194/acp-19-4393-2019>
- Russo, A., Soares, A.O., 2014. Hybrid Model for Urban Air Pollution Forecasting: A Stochastic Spatio-Temporal Approach. *Math. Geosci.* 46, 75–93. <https://doi.org/10.1007/s11004-013-9483-0>
- Russo, M.A., Gama, C., Monteiro, A., 2019. How does upgrading an emissions inventory affect air quality simulations? *Air Qual. Atmos. Heal.* 12, 731–741. <https://doi.org/10.1007/s11869-019-00692-x>
- San José, R., Pérez, J.L., Balzarini, A., Baró, R., Curci, G., Forkel, R., Galmarini, S., Grell, G., Hirtl, M., Honzak, L., Im, U., Jiménez-Guerrero, P., Langer, M., Pirovano, G., Tuccella, P., Werhahn, J., Žabkar, R., 2015. Sensitivity of feedback effects in CBMZ/MOSAIC chemical mechanism. *Atmos. Environ.* 115, 646–656. <https://doi.org/10.1016/J.ATMOSENV.2015.04.030>
- Santiago, J.L., Martilli, A., 2010. A Dynamic Urban Canopy Parameterization for Mesoscale Models Based on Computational Fluid Dynamics Reynolds-Averaged Navier–Stokes Microscale Simulations. *Boundary-Layer Meteorol.* 137, 417–439. <https://doi.org/10.1007/s10546-010-9538-4>
- Schlünzen, K.H., Grawe, D., Bohnenstengel, S.I., Schlüter, I., Koppmann, R., 2011. Joint modelling of obstacle induced and mesoscale changes—Current limits and challenges. *J. Wind Eng. Ind. Aerodyn.* 99, 217–225. <https://doi.org/10.1016/J.JWEIA.2011.01.009>

- Seethaler, R., 1999. Health Costs due to Road Traffic-related Air Pollution: An impact assessment project of Austria, France and Switzerland, Synthesis Report published by Federal Department of Environment, Transport, Energy and Communications. Berne.
- Seethaler, R.K., Künzli, N., Sommer, H., Chanel, O., Herry, M., Masson, S., Vernaud, J.-C., Filliger, P., Horak, F.J., Kaiser, R., Medina, S., Puybonnieux-Texier, V., Quénel, P., Schneider, J., Studnicka, M., Heldstab, J., 2003. Economic costs of air pollution-related health impacts: An impact assessment project of Austria, France and Switzerland. *Clean Air Environ. Qual.* 37, 35–43.
- Silveira, C., Ferreira, J., Miranda, A.I., 2019. The challenges of air quality modelling when crossing multiple spatial scales. *Air Qual. Atmos. Heal.* 12, 1003–1017. <https://doi.org/10.1007/s11869-019-00733-5>
- Silveira, C., Roebeling, P., Lopes, M., Ferreira, J., Costa, S., Teixeira, J.P., Borrego, C., Miranda, A.I., 2016. Assessment of health benefits related to air quality improvement strategies in urban areas: An Impact Pathway Approach. *J. Environ. Manage.* 183, 694–702. <https://doi.org/10.1016/J.JENVMAN.2016.08.079>
- Siour, G., Colette, A., Menut, L., Bessagnet, B., Coll, I., Meleux, F., 2013. Bridging the scales in a eulerian air quality model to assess megacity export of pollution. *Environ. Model. Softw.* 46, 271–282. <https://doi.org/10.1016/J.ENVSOFT.2013.04.001>
- Soriano, C., Jorba, O., Baldasano, J.M., 2004. One-Way Nesting Versus Two-Way Nesting: Does It Really Make a Difference?, in: *Air Pollution Modeling and Its Application XV*. Kluwer Academic Publishers, Boston, pp. 177–185. https://doi.org/10.1007/0-306-47813-7_18
- Sporre, M.K., Blichner, S.M., Karset, I.H.H., Makkonen, R., Berntsen, T.K., 2019. BVOC–aerosol–climate feedbacks investigated using NorESM. *Atmos. Chem. Phys.* 19, 4763–4782. <https://doi.org/10.5194/acp-19-4763-2019>
- Srivastava, A., Rao, B.P.S., 2011. Urban Air Pollution Modeling, in: *Air Quality-Models and Applications*. InTech. <https://doi.org/10.5772/16776>
- Stein, A.F., Isakov, V., Godowitch, J., Draxler, R.R., 2007. A hybrid modeling approach to resolve pollutant concentrations in an urban area. *Atmos. Environ.* 41, 9410–9426. <https://doi.org/10.1016/J.ATMOSENV.2007.09.004>
- Talbot, C., Bou-Zeid, E., Smith, J., Talbot, C., Bou-Zeid, E., Smith, J., 2012. Nested Mesoscale Large-Eddy Simulations with WRF: Performance in Real Test Cases. *J. Hydrometeorol.* 13, 1421–1441. <https://doi.org/10.1175/JHM-D-11-048.1>

- Tang, U.W., Wang, Z.S., 2007. Influences of urban forms on traffic-induced noise and air pollution: Results from a modelling system. *Environ. Model. Softw.* 22, 1750–1764. <https://doi.org/10.1016/J.ENVSOF.2007.02.003>
- Tang, Y., Carmichael, G.R., Thongboonchoo, N., Chai, T., Horowitz, L.W., Pierce, R.B., Al-Saadi, J.A., Pfister, G., Vukovich, J.M., Avery, M.A., Sachse, G.W., Ryerson, T.B., Holloway, J.S., Atlas, E.L., Flocke, F.M., Weber, R.J., Huey, L.G., Dibb, J.E., Streets, D.G., Brune, W.H., 2007. Influence of lateral and top boundary conditions on regional air quality prediction: A multiscale study coupling regional and global chemical transport models. *J. Geophys. Res. Atmos.* 112. <https://doi.org/10.1029/2006JD007515>
- Thatcher, M., Hurley, P., 2010. A customisable downscaling approach for local-scale meteorological and air pollution forecasting: Performance evaluation for a year of urban meteorological forecasts. *Environ. Model. Softw.* 25, 82–92. <https://doi.org/10.1016/J.ENVSOF.2009.07.014>
- Thomas, M.A., Kahnert, M., Andersson, C., Kokkola, H., Hansson, U., Jones, C., Langner, J., Devasthale, A., 2015. Integration of prognostic aerosol–cloud interactions in a chemistry transport model coupled offline to a regional climate model. *Geosci. Model Dev.* 8, 1885–1898. <https://doi.org/10.5194/gmd-8-1885-2015>
- Thunis, P., Miranda, A., Baldasano, J.M., Blond, N., Douros, J., Graff, A., Janssen, S., Juda-Rezler, K., Karvosenoja, N., Maffei, G., Martilli, A., Rasoloharimahefa, M., Real, E., Viaene, P., Volta, M., White, L., 2016. Overview of current regional and local scale air quality modelling practices: Assessment and planning tools in the EU. *Environ. Sci. Policy* 65, 13–21. <https://doi.org/10.1016/J.ENVSCI.2016.03.013>
- Tranmer, J.E., Guerriere, D.N., Ungar, W.J., Coyte, P.C., 2005. Valuing patient and caregiver time: A review of the literature. *Pharmacoeconomics.* <https://doi.org/10.2165/00019053-200523050-00005>
- Tuccella, P., Curci, G., Visconti, G., Bessagnet, B., Menut, L., Park, R.J., 2012. Modeling of gas and aerosol with WRF/Chem over Europe: Evaluation and sensitivity study. *J. Geophys. Res. Atmos.* 117, n/a-n/a. <https://doi.org/10.1029/2011JD016302>
- van Essen, H., Schrotten, A., Otten, M., Sutter, D., Schreyer, C., Zandonella, R., Maibach, M., Doll, C., 2011. External Costs of Transport in Europe, Update Study for 2008.
- Vardoulakis, S., Fisher, B.E., Pericleous, K., Gonzalez-Flesca, N., 2003. Modelling air quality in street canyons: a review. *Atmos. Environ.* 37, 155–182. [https://doi.org/10.1016/S1352-2310\(02\)00857-9](https://doi.org/10.1016/S1352-2310(02)00857-9)

-
- Wang, Y., Song, S., Qiu, S., Lu, L., Ma, Y., Li, X., Hu, Y., 2017. Study on International Practices for Low Emission Zone and Congestion Charging. Beijing.
- Werner, M., Kryza, M., Skjøth, C.A., Wałaszek, K., Dore, A.J., Ojrzyńska, H., Kapłon, J., 2017. Aerosol-Radiation Feedback and PM10 Air Concentrations Over Poland. *Pure Appl. Geophys.* 174, 551–568. <https://doi.org/10.1007/s00024-016-1267-2>
- WHO, 2016a. Ambient Air Pollution: A global assessment of exposure and burden of disease, World Health Organization.
- WHO, 2016b. Health risk assessment of air pollution: General principles. World Health Organization.
- WHO, 2013a. Recommendations for concentration–response functions for cost–benefit analysis of particulate matter, ozone and nitrogen dioxide, Health risks of air pollution in Europe – HRAPIE project. World Health Organization, Copenhagen.
- WHO, 2013b. Health effects of particulate matter: Policy implications for countries in Eastern Europe, Caucasus and central Asia. World Health Organization.
- WHO, 2013c. New emerging risks to health from air pollution – results from the survey of experts, Health risks of air pollution in Europe – HRAPIE project. World Health Organization, Copenhagen.
- WHO, 2008. Economic valuation of transport-related health effects: Review of methods and development of practical approaches, with a special focus on children. World Health Organization.
- WHO, 2002. Guidelines for concentration and exposure-response measurement of fine and ultra fine particulate matter for use in epidemiological studies. World Health Organization.
- WMO, 2016. WMO Statement on the Status of the Global Climate in 2015, WMO-No. 11. ed. World Meteorological Organization.
- Wu, S., Mickley, L.J., Kaplan, J.O., Jacob, D.J., 2012. Impacts of changes in land use and land cover on atmospheric chemistry and air quality over the 21st century. *Atmos. Chem. Phys.* 12, 1597–1609. <https://doi.org/10.5194/acp-12-1597-2012>
- Xu, G., Jiao, L., Zhao, S., Yuan, M., Li, X., Han, Y., Zhang, B., Dong, T., Xu, G., Jiao, L., Zhao, S., Yuan, M., Li, X., Han, Y., Zhang, B., Dong, T., 2016. Examining the Impacts of Land Use on Air Quality from a Spatio-Temporal Perspective in Wuhan, China. *Atmosphere (Basel)*. 7, 62. <https://doi.org/10.3390/atmos7050062>

Zhang, C., Chen, M., Li, R., Ding, Y., Lin, H., 2015. A virtual geographic environment system for multiscale air quality analysis and decision making: A case study of SO₂ concentration simulation. *Appl. Geogr.* 63, 326–336. <https://doi.org/10.1016/J.APGEOG.2015.07.011>

Zhang, Y., 2008. Online-coupled meteorology and chemistry models: history, current status, and outlook. *Atmos. Chem. Phys.* 8, 2895–2932. <https://doi.org/10.5194/acp-8-2895-2008>

Zhang, Y., Karamchandani, P., Glotfelty, T., Streets, D.G., Grell, G., Nenes, A., Yu, F., Bennartz, R., 2012. Development and initial application of the global-through-urban weather research and forecasting model with chemistry (GU-WRF/Chem). *J. Geophys. Res. Atmos.* 117. <https://doi.org/10.1029/2012JD017966>

URL1. AirQ+: software tool for health risk assessment of air pollution. Available at: <http://www.euro.who.int/en/health-topics/environment-and-health/air-quality/activities/airq-software-tool-for-health-risk-assessment-of-air-pollution>. [Last access: November 2019]

URL2. Global Health Observatory data repository (GHO). Available at: <http://apps.who.int/gho/data/node.home>. [Last access: September 2019]

URL3. European Health for All database (HFA-DB). Available at: <https://gateway.euro.who.int/en/datasets/european-health-for-all-database>. [Last access: September 2019]

URL4. WPS Static Data. Available at: <https://dtcenter.org/tutorial/data-containers/wps-static-data>. [Last access: May 2018]

URL5. ERA Interim, Daily. Available at: <https://www.ecmwf.int/en/forecasts/datasets/reanalysis-datasets/era-interim>. [Last access: April 2017]

URL6. WRF-Chem Tools for the Community. Available at: <https://www2.aom.ucar.edu/wrf-chem/wrf-chem-tools-community>. [Last access: June 2017]

URL7. Grid emissions in 0.1°x0.1° long-lat resolution. Available at: https://www.ceip.at/new_emep-grid/01_grid_data. [Last access: September 2019]

URL8. COPERT - The industry standard emissions calculator. Available at: <https://www.emisia.com/utilities/copert>. [Last access: November 2018]

URL9. Estatísticas. Available at: <https://www.acap.pt/pt/estatisticas>. [Last access: November 2018]

URL10. Statistics Portugal. Available at: <https://www.ine.pt>. [Last access: November 2018]

URL11. Open Transport Map. Available at: <http://opentransportmap.info>. [Last access: November 2018]

URL12. Normais Climatológicas – 1971-2000. Available at: <https://www.ipma.pt/pt/oclima/normais.clima/1971-2000/#107>. [Last access: June 2017]

URL13. Coimbra topographic map. Available at: <https://en-in.topographic-map.com/maps/gauc/Coimbra>. [Last access: November 2018]

URL14. QualAr – Rede de Medição da Qualidade do Ar. Available at: <https://qualar1.apambiente.pt/qualar/index.php?page=2>. [Last access: November 2018]

URL15. Urban Access Regulations in Europe. Available at: <https://urbanaccessregulations.eu>. [Last access: March 2019]

Appendixes

APPENDIX A - Reclassification scheme of the new land cover classification

APPENDIX B - User options for application of the modair4health system

APPENDIX C - Characterization of the Portuguese air quality monitoring network

APPENDIX D - Estimation of road traffic-induced NO₂ emissions for the case study considering the reference and traffic management scenarios

APPENDIX E - Short-term health damage costs estimated for the reference scenario

APPENDIX A - Reclassification scheme of the new land cover classification

Corine and Portugal-specific LC categories	33-classes USGS LC categories
Non-irrigated arable land Pastures	2 - Dryland cropland and pasture
Permanently irrigated land Rice fields Greenhouses and nurseries Vineyards Fruit trees and berry plantations Olive groves Annual crops associated with permanent crops Complex cultivation patterns Land principally occupied by agriculture, with significant areas of natural vegetation Agro-forestry areas	3 - Irrigated cropland and pasture 6 - Cropland/woodland mosaic
Natural grasslands	7 - Grassland
Shrubland	8 - Shrubland
Moors and heathland Sclerophyllous vegetation Transitional woodland-shrub	9 - Mixed shrubland/grassland
Deciduous broadleaf forest	11 - Deciduous broadleaf forest
Evergreen broadleaf forest	13 - Evergreen broadleaf forest
Coniferous forest	14 - Evergreen needleleaf forest
Mixed forest	15 - Mixed forest
Water courses Water bodies Coastal and inland lagoons Estuaries Sea and ocean	16 - Water bodies
Inland marshes Peat bogs Salt marshes Salines Intertidal flats	17 - Herbaceous wetland
Beaches, dunes and sands Bare rocks Sparsely vegetated areas Burnt areas Deforestation	19 - Barren or sparsely vegetated
Glaciers and perpetual snow	24 - Snow or ice
Discontinuous urban fabric Green urban areas Sport and leisure facilities	31 - Low intensity residential
Continuous urban fabric Industrial or commercial units Road and rail networks and associated land Port areas Airports	32 - High intensity residential
Mineral extraction sites Dump sites Construction sites Infrastructures for energy production and water treatment	33 - Industrial or commercial

APPENDIX B - User options for application of the modair4health system**- GENERAL OPTIONS**

(i) *Select the air pollutant to analyse:*

(PM2.5; PM10; NO₂; O₃; CO)

pollutant = NO₂

(ii) *Consider Integrated Assessment Modelling (IAM):*

(0 - No; 1 - Yes; 2 - Skip to the postprocessing)

IAM = 1

(iii) *Select the component to run when no IAM is required:*

(1 - air quality; 2 - health)

component = 1

(iv) *Select the application scales to run air quality and/or health:*

(1 - regional to urban; 2 - local; 3 - multiscale)

scales = 2

(v) *Consider air quality and health management (AQHM):*

(0 - No; 1 - Yes)

AQHM = 1

If AQHM is required, select the scenario to analyse:

(ELEC; LEZ)

scenario = ELEC

- CONFIGURATIONS TO RUN AIR QUALITY

(vi) *Select the simulation periods:*

WRF-Chem (regional to urban scale; run up to an entire year; format - yyyy/mm/dd)

WRF_inidate = 2015/01/26

WRF_enddate = 2015/02/01

VADIS (local scale; run air pollution episodes; format - yyyy/mm/dd_hh:00)

VADIS_inidate = 2015/01/26_00:00

VADIS_enddate = 2015/02/01_00:00

(vii) *Select the traffic emission profile to run local scale air quality:*

(1 - user-defined; 2 - seasonal; 3 - adjusted)

emis_profile = 3

For the option 3, select the air quality monitoring station inside/near the local domain:

station = COI

- **CONFIGURATIONS TO RUN HEALTH**

(viii) *Air pollution exposure time to analyse:*

(1 - short-term; 2 - long-term)

health_effects = 1

(ix) *Select the time period to quantify health effects (format: yyyy/mm/dd):*

health_inidate = 2015/01/26

health_enddate = 2015/02/01

(x) *Select the AirQ+ methodology to use:*

(1 - linear; 2 - non-linear)

health_method = 2

- **POSTPROCESSING OPTIONS**

(xi) *Include postprocessing:*

(0 - No; 1 - Yes)

post_proc = 1

(xii) *Select the scale(s) and domain(s) to analyse:*

WRF-Chem (1 - regional to urban; domains - d01, d02, d03)

VADIS (2 - local; domain - d04)

post_scale = 2

WRF_dom = d03

VADIS_dom = d04

(xiii) *Select the time periods:*

date (format: yyyy/mm/dd)

hour (format: hh; must be in 00..24)

post_inidate = 2015/01/26

post_enddate = 2015/02/01

post_inihour = 08

post_endhour = 20

(xiv) *Spatial analysis:*

(0 - No; 1 - Yes, only modelled data; 2 - Yes, overlap modelled and observed data)
metrics (average; minimum; maximum)

spat_dist = 2

spat_metric = average

(xv) *Model evaluation:*

(0 - No; 1 - Yes)

model_eval = 1

If model evaluation is required, select an air quality station or typology:

(i) insert station acronym; (ii) Allstations; (iii) Background (Rural, Suburban, Urban);
(iv) Rural; (v) Suburban; (vi) Urban; (vii) Traffic

post_station = COI

Note: for the local scale, it is necessary to set the VADIS cell that corresponds to the geographic location of the monitoring station.

Validation:

Statistical metrics (observed and modelled mean, correlation, BIAS, RMSE)

(0 - No; 1 - Yes)

validation = 1

Time series:

(0 - No; 1 - Yes)

time_series = 1

Daily profiles:

(0 - No; 1 - Yes)

daily_prof = 1

APPENDIX C - Characterization of the Portuguese air quality monitoring network

Code	Station	Acronym	Environment	Influence	Latitude (decimal degrees)	Longitude (decimal degrees)	Altitude (m)	Municipality	Zone	Measured pollutants	Start of activity
1047	Minho-Lima	MIN	Rural	Background	41.800	-8.700	777	Viana do Castelo	Norte Litoral	PM2.5, PM10, NO _x , NO, NO ₂ , O ₃	11/03/2005
1048	Douro Norte	DRN	Rural	Background	41.370	-7.789	1086	Vila Real	Norte Interior	PM2.5, PM10, NO _x , NO, NO ₂ , O ₃ , SO ₂	03/02/2004
2020	Fundão	FUN	Rural	Background	40.232	-7.300	473	Fundão	Centro Interior	PM2.5, PM10, NO _x , NO, NO ₂ , O ₃ , SO ₂	01/06/2003
2021	Fornelo do Monte	FRN	Rural	Background	40.640	-8.100	741	Vouzela	Centro Interior	PM10, NO _x , NO, NO ₂ , O ₃	23/09/2005
2019	Ervedeira	ERV	Rural	Background	39.922	-8.893	60	Leiria	Centro Litoral	PM2.5, PM10, NO _x , NO, NO ₂ , O ₃ , SO ₂	01/01/2003
2022	Montemor-o-Velho	MOV	Rural	Background	40.183	-8.677	96	Montemor-o-Velho	Centro Litoral	PM10, NO _x , NO, NO ₂ , O ₃	06/09/2007
3096	Chamusca	CHA	Rural	Background	39.353	-8.468	143	Chamusca	Vale do Tejo e Oeste	PM2.5, PM10, NO _x , NO, NO ₂ , O ₃ , SO ₂	01/11/2002
3102	Lourinhã	LNH	Rural	Background	39.278	-9.246	143	Lourinhã	Vale do Tejo e Oeste	PM2.5, PM10, NO _x , NO, NO ₂ , O ₃	01/12/2008
3099	Fernando Pó	FPO	Rural	Background	38.636	-8.691	57	Palmela	Península de Setúbal / Alcácer do Sal	PM2.5, PM10, NO _x , NO, NO ₂ , O ₃ , SO ₂	18/04/2007
4002	Monte Velho	MVE	Rural	Background	38.076	-8.799	53	Santiago do Cacém	Alentejo Litoral	PM2.5, PM10, NO _x , NO, NO ₂ , O ₃ , SO ₂ , heavy metals	01/01/1976

Appendix C

Code	Station	Acronym	Environment	Influence	Latitude (decimal degrees)	Longitude (decimal degrees)	Altitude (m)	Municipality	Zone	Measured pollutants	Start of activity
4006	Terena	TER	Rural	Background	38.616	-7.398	187	Alandroal	Alentejo Interior	PM2.5, PM10, NOx, NO, NO ₂ , O ₃ , SO ₂	15/02/2005
5012	Cerro	CER	Rural	Background	37.312	-7.68	300	Alcoutim	Algarve	PM2.5, PM10, NOx, NO, NO ₂ , O ₃ , SO ₂	15/10/2004
1042	Frossos-Braga	FRO	Suburban	Background	41.566	-8.454	51	Braga	Entre Douro e Minho	PM10, NOx, NO, NO ₂ , O ₃	10/03/2004
1054	Anta-Espinho	ESP	Suburban	Background	41.006	-8.643		Espinho	Porto Litoral	PM10, NOx, NO, NO ₂ , O ₃	25/02/2011
1031	VNTelha-Maia	VNT	Suburban	Background	41.259	-8.662	88	Maia	Porto Litoral	PM10, NOx, NO, NO ₂ , O ₃	01/01/1999
1021	Custóias-Matosinhos	CUS	Suburban	Background	41.201	-8.645	100	Matosinhos	Porto Litoral	PM10, NOx, NO, NO ₂ , O ₃	01/01/1999
1034	Leça do Balio-Matosinhos	LEC	Suburban	Background	41.220	-8.630	40	Matosinhos	Porto Litoral	PM10, O ₃	01/01/2000
1051	Mindelo-Vila do Conde	VCO	Suburban	Background	41.345	-8.736	25	Vila do Conde	Porto Litoral	PM10, NOx, NO, NO ₂ , O ₃	22/12/2009
2004	Estarreja	EST	Suburban	Background	40.750	-8.583	15	Estarreja	Litoral Noroeste do Baixo Vouga	PM2.5, PM10, NOx, NO, NO ₂ , O ₃ , SO ₂	01/05/1990
2018	Ílhavo	ILH	Suburban	Background	40.588	-8.672	32	Ílhavo	Aveiro / Ílhavo	PM10, NOx, NO, NO ₂ , O ₃ , SO ₂	27/03/2003
1044	Paços de Ferreira	PFE	Urban	Background	41.274	-8.376	300	Paços de Ferreira	Entre Douro e Minho	PM2.5, PM10, NOx, NO, NO ₂ , O ₃	20/02/2004
1052	Burgães-Santo Tirso	STR	Urban	Background	41.346	-8.477	47	Santo Tirso	Entre Douro e Minho	PM10, NOx, NO, NO ₂ , O ₃	17/12/2009

Code	Station	Acronym	Environment	Influence	Latitude (decimal degrees)	Longitude (decimal degrees)	Altitude (m)	Municipality	Zone	Measured pollutants	Start of activity
1053	Avintes	AVI	Urban	Background	41.097	-8.556	88	Gaia	Porto Litoral	PM10, NOx, NO, NO ₂ , O ₃	12/07/2010
1050	Sobreiras-Lordelo do Ouro	SOB	Urban	Background	41.148	-8.659	17	Porto	Porto Litoral	PM2.5, PM10, NOx, NO, NO ₂ , O ₃	01/12/2007
1023	Ermesinde-Valongo	ERM	Urban	Background	41.217	-8.551	140	Valongo	Porto Litoral	PM10, NOx, NO, NO ₂ , O ₃	01/01/1999
2016	Instituto Geofísico de Coimbra	IGE	Urban	Background	40.206	-8.412	145	Coimbra	Coimbra	PM10, NOx, NO, NO ₂ , O ₃	01/01/2003
3082	Alfragide/Amadora	ALF	Urban	Background	38.738	-9.208	109	Amadora	AML Norte	PM2.5, PM10, NOx, NO, NO ₂ , O ₃ , SO ₂ , heavy metals	06/01/1998
3084	Reboleira	REB	Urban	Background	38.753	-9.232	132	Amadora	AML Norte	PM10, NOx, NO, NO ₂ , O ₃	06/02/2001
3070	Beato	BEA	Urban	Background	38.733	-9.114	56	Lisboa	AML Norte	NOx, NO, NO ₂ , O ₃ , C ₆ H ₆	01/11/1992
3071	Olivais	OLI	Urban	Background	38.768	-9.109	32	Lisboa	AML Norte	PM2.5, PM10, NOx, NO, NO ₂ , O ₃ , SO ₂ , CO	01/03/1992
3087	Restelo	RES	Urban	Background	38.705	-9.210	143	Lisboa	AML Norte	PM10, NOx, NO, NO ₂ , O ₃	20/02/2002
3085	Loures-Centro	LOU	Urban	Background	38.828	-9.166	10	Loures	AML Norte	PM10, NOx, NO, NO ₂ , O ₃	01/06/2001
3091	Quinta do Marquês	QMA	Urban	Background	38.697	-9.324	48	Oeiras	AML Norte	PM10, NOx, NO, NO ₂ , O ₃	01/09/2002
3089	Mem Martins	MEM	Urban	Background	38.784	-9.348	173	Sintra	AML Norte	PM2.5, PM10, NOx, NO, NO ₂ , O ₃ , SO ₂	19/10/2002

Appendix C

Code	Station	Acronym	Environment	Influence	Latitude (decimal degrees)	Longitude (decimal degrees)	Altitude (m)	Municipality	Zone	Measured pollutants	Start of activity
3101	Alverca	ALV	Urban	Background	38.896	-9.040	22	Vila Franca de Xira	AML Norte	PM10, NOx, NO, NO ₂ , O ₃ , SO ₂	31/12/2008
3083	Laranjeiro	LAR	Urban	Background	38.663	-9.159	63	Almada	AML Sul	PM2.5, PM10, NOx, NO, NO ₂ , O ₃ , CO	12/01/2001
3103	Fidalguinhos	FID	Urban	Background	38.650	-9.049	24	Barreiro	AML Sul	PM10, NOx, NO, NO ₂ , SO ₂	23/12/2009
3093	Arcos	ARC	Urban	Background	38.529	-8.894	2	Setúbal	Setúbal	PM10, NOx, NO, NO ₂ , O ₃ , CO	05/04/2002
5008	Malpique	MAL	Urban	Background	37.091	-8.251	45	Albufeira	Aglomeraco Sul	PM10, NOx, NO, NO ₂ , O ₃ , SO ₂	04/09/2004
5007	Joaquim Magalhes	JMG	Urban	Background	37.014	-7.928	4	Faro	Aglomeraco Sul	PM2.5, PM10, NOx, NO, NO ₂ , O ₃ , SO ₂	11/08/2004
1041	Fr Bartolomeu Mrtires-S.Vitor	FRB	Urban	Traffic	41.550	-8.406	175	Braga	Entre Douro e Minho	PM10, NOx, NO, NO ₂	09/03/2004
1046	Cnego Dr. Manuel Faria-Azurm	AZU	Urban	Traffic	41.449	-8.296	185	Guimares	Entre Douro e Minho	PM10, NOx, NO, NO ₂ , benzene derivatives	07/04/2004
1043	Pe Moreira Neves-Casteles de Cepeda	PMN	Urban	Traffic	41.205	-8.338	184	Paredes	Entre Douro e Minho	PM10, NOx, NO, NO ₂	07/01/2004
1024	D.Manuel II-Vermoim	VER	Urban	Traffic	41.237	-8.618	90	Maia	Porto Litoral	PM2.5, PM10, NOx, NO, NO ₂	01/11/1999
1030	Joo Gomes Laranjo-S.Hora	SRH	Urban	Traffic	41.184	-8.662	72	Matosinhos	Porto Litoral	PM10, NOx, NO, NO ₂ , CO	01/09/2001

Code	Station	Acronym	Environment	Influence	Latitude (decimal degrees)	Longitude (decimal degrees)	Altitude (m)	Municipality	Zone	Measured pollutants	Start of activity
1028	Francisco Sá Carneiro-Campanha	FSC	Urban	Traffic	41.164	-8.590	146	Porto	Porto Litoral	PM10, NOx, NO, NO ₂ , CO	01/10/2000
2017	Aveiro	AVE	Urban	Traffic	40.636	-8.647	20	Aveiro	Aveiro / Ílhavo	PM10, NOx, NO, NO ₂ , CO	15/01/2003
2006	Coimbra/ Avenida Fernão Magalhães	COI	Urban	Traffic	40.216	-8.434	26	Coimbra	Coimbra	PM10, NOx, NO, NO ₂ , CO	08/07/2008
3072	Entrecampos	ENT	Urban	Traffic	38.747	-9.151	86	Lisboa	AML Norte	PM2.5, PM10, NOx, NO, NO ₂ , SO ₂ , O ₃ , benzene	01/03/1992
3075	Avenida da Liberdade	AVL	Urban	Traffic	38.719	-9.148	44	Lisboa	AML Norte	PM10, NOx, NO, NO ₂ , CO	01/01/1994
3100	Santa Cruz de Benfica	BEN	Urban	Traffic	38.750	-9.205	76	Lisboa	AML Norte	PM10, NO, NO ₂ , CO	16/12/2008
3097	Odivelas-Ramada	ODI	Urban	Traffic	38.801	-9.183	124	Odivelas	AML Norte	PM10, NOx, NO, NO ₂ , CO	01/12/2003
3094	Quebedo	QUE	Urban	Traffic	38.524	-8.887	16	Setúbal	Setúbal	PM10, NOx, NO, NO ₂ , SO ₂ , CO, benzene	01/05/2002
5011	David Neto	DVN	Urban	Traffic	37.138	-8.543	6	Portimão	Aglomeracão Sul	PM10, NOx, NO, NO ₂ , CO, benzene	30/06/2004

APPENDIX D - Estimation of road traffic-induced NO₂ emissions for the case study considering the reference and traffic management scenarios

Road segment	Length (m)	Location	Road traffic NO ₂ emission (kg/day)			NO ₂ emission reduction (kg/day)	
			REF	ELEC	LEZ	REF-ELEC	REF-LEZ
1	241	Fernão de Magalhães Avenue	3.150	1.575	1.543	1.575	1.607
2	241	Fernão de Magalhães Avenue	3.150	1.575	1.543	1.575	1.607
3	241	Fernão de Magalhães Avenue	3.150	1.575	1.543	1.575	1.607
4	108	Fernão de Magalhães Avenue	1.420	0.708	0.693	0.712	0.727
5	108	Fernão de Magalhães Avenue	1.420	0.708	0.693	0.712	0.727
6	118	Fernão de Magalhães Avenue	1.540	0.772	0.757	0.768	0.783
7	118	Fernão de Magalhães Avenue	1.540	0.772	0.757	0.768	0.783
8	100	Cidade Aeminium Avenue	1.027	0.513	1.027	0.513	0.000
9	100	Cidade Aeminium Avenue	1.027	0.513	1.027	0.513	0.000
10	100	Cidade Aeminium Avenue	1.027	0.513	1.027	0.513	0.000
11	100	Cidade Aeminium Avenue	1.027	0.513	1.027	0.513	0.000
12	100	Cidade Aeminium Avenue	1.027	0.513	1.027	0.513	0.000
13	100	Cidade Aeminium Avenue	1.027	0.513	1.027	0.513	0.000
14	39	Figueira da Foz Street	0.405	0.202	0.405	0.203	0.000
15	39	Figueira da Foz Street	0.405	0.202	0.405	0.203	0.000
16	39	Figueira da Foz Street	0.405	0.202	0.405	0.203	0.000
17	39	Figueira da Foz Street	0.405	0.202	0.405	0.203	0.000
18	24	Figueira da Foz Street	0.248	0.124	0.248	0.124	0.000
19	24	Figueira da Foz Street	0.248	0.124	0.248	0.124	0.000
20	24	Figueira da Foz Street	0.248	0.124	0.248	0.124	0.000
21	86	João Machado Street	1.127	0.564	1.127	0.564	0.000
22	86	João Machado Street	1.127	0.564	1.127	0.564	0.000
23	77	Sofia Street	1.009	0.505	1.009	0.505	0.000
24	77	Sofia Street	1.009	0.505	1.009	0.505	0.000
25	77	Sofia Street	1.009	0.505	1.009	0.505	0.000
26	77	Sofia Street	1.009	0.505	1.009	0.505	0.000
27	77	Sofia Street	1.009	0.505	1.009	0.505	0.000
28	77	Sofia Street	1.009	0.505	1.009	0.505	0.000
29	42	Doutor Manuel Rodrigues Street	0.548	0.274	0.548	0.274	0.000
30	42	Doutor Manuel Rodrigues Street	0.548	0.274	0.548	0.274	0.000
31	42	Doutor Manuel Rodrigues Street	0.548	0.274	0.548	0.274	0.000
32	42	Doutor Manuel Rodrigues Street	0.548	0.274	0.548	0.274	0.000
33	46	Olímpio Nicolau Rui Fernandes Street	0.606	0.303	0.606	0.303	0.000
34	46	Olímpio Nicolau Rui Fernandes Street	0.606	0.303	0.606	0.303	0.000

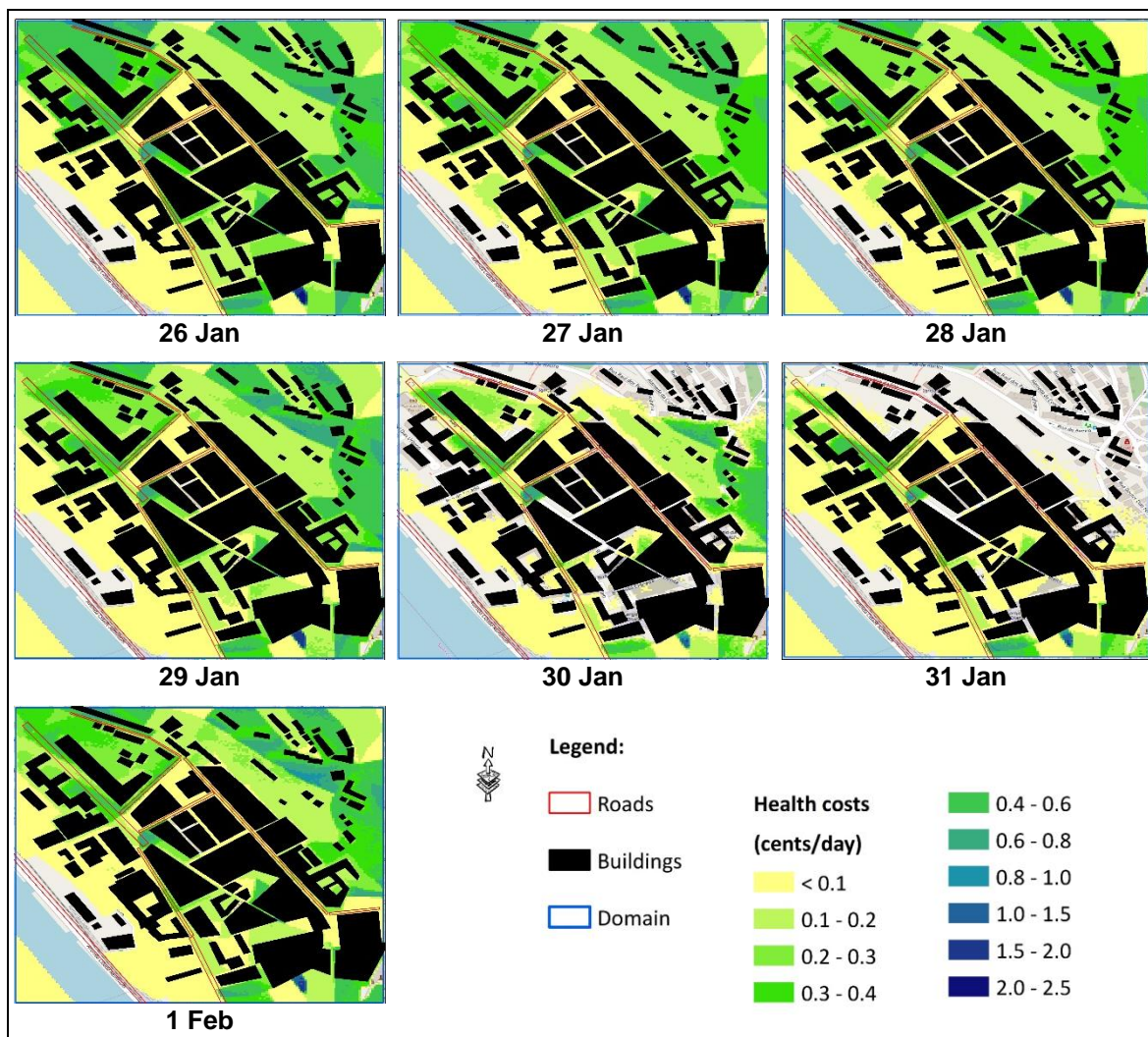
APPENDIX E - Short-term health damage costs estimated for the reference scenario

Figure E.1. Short-term health damage costs (cents/day) estimated for the REF scenario in the winter period.

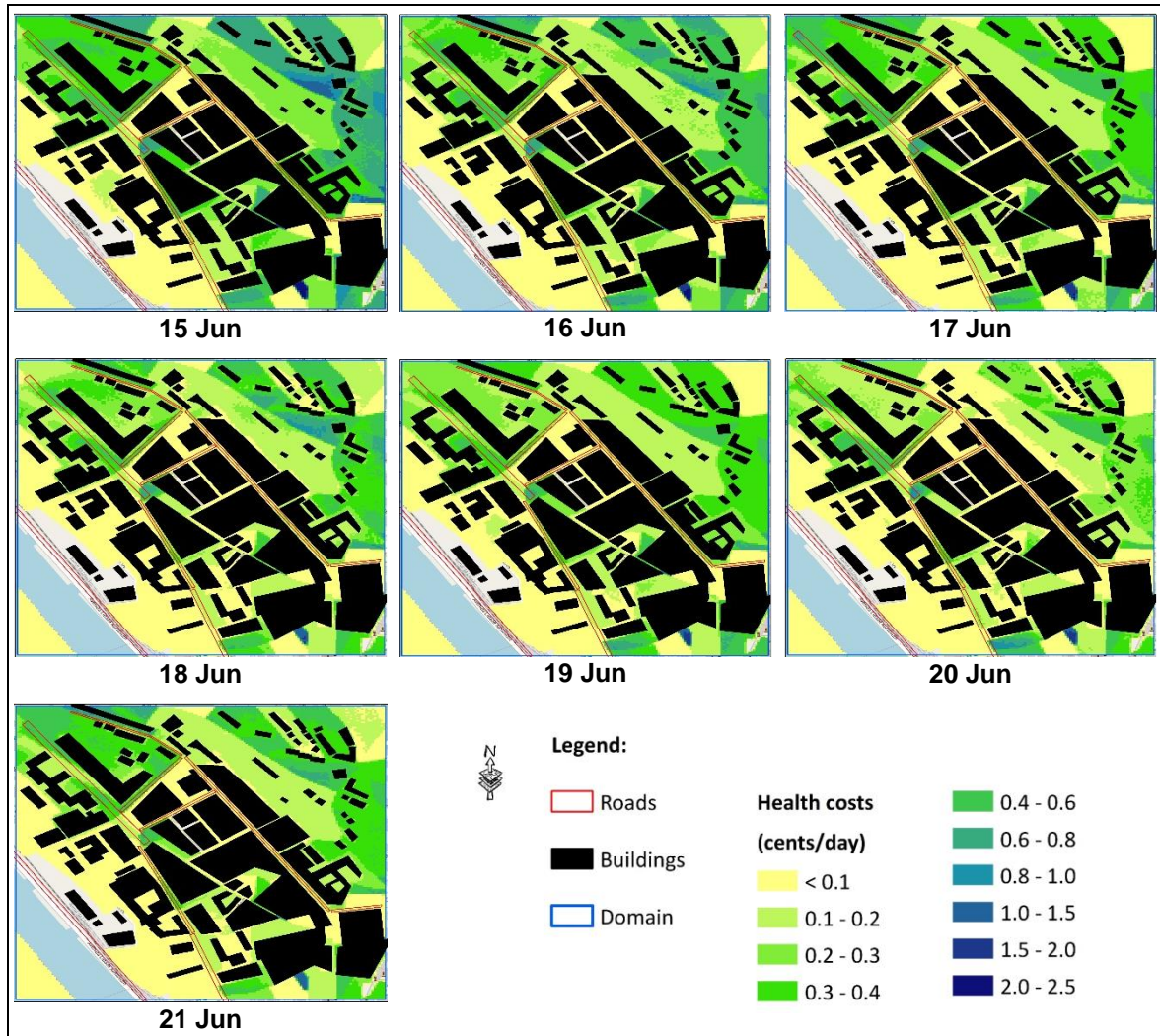


Figure E.2. Short-term health damage costs (cents/day) estimated for the REF scenario in the summer period.